Development of a Biosensor-Guided Evolution Platform for Engineering Synthetic Methylotrophic Escherichia coli Towards L-Lactate Bioproduction

Auteur : Hellich, Agathe
Promoteur(s) : Genva, Manon
Faculté : Gembloux Agro-Bio Tech (GxABT)
Diplôme : Master en bioingénieur : chimie et bioindustries, à finalité spécialisée
Année académique : 2024-2025
URI/URL : http://hdl.handle.net/2268.2/23168

Development of a Biosensor-Guided Evolution Platform for Engineering Synthetic Methylotrophic *Escherichia coli* Towards L-Lactate Bioproduction

AGATHE HELLICH

TRAVAIL DE FIN D'ÉTUDES PRÉSENTÉ EN VUE DE L'OBTENTION DU DIPLÔME DE MASTER BIOINGÉNIEUR EN CHIMIE ET BIOINDUSTRIES

ANNÉE ACADÉMIQUE 2025-2026

(CO)-PROMOTEUR(S: MANON GENVA, JULIANO SABEDOTTI, JAMES LIAO, LIANG-YU NIEH

LIÈGE université
Gembloux
Agro-Bio Tech

Bioceb
European Master in Biological and Chemical Engineering for a Sustainable Bioeconomy

Development of a Biosensor-Guided Evolution Platform for Engineering Synthetic Methylotrophic *Escherichia coli* Towards L-Lactate Bioproduction

AGATHE HELLICH

TRAVAIL DE FIN D'ÉTUDES PRÉSENTÉ EN VUE DE L'OBTENTION DU DIPLÔME DE

MASTER BIOINGÉNIEUR EN CHIMIE ET BIOINDUSTRIES

ANNÉE ACADÉMIQUE 2025-2026

(CO)-PROMOTEUR(S: MANON GENVA, JULIANO SABEDOTTI, JAMES LIAO, LIANG-YU NIEH

Internship conducted at Academia Sinica, Taiwan,
Institute of Biological Chemistry
Laboratory of Dr. James C. Liao

from January to July 2025

I would like to express my sincere gratitude to my supervisors at my host institutions, Professor James C. Liao and Liang-Yu Nieh, for their invaluable guidance and support.

I am deeply thankful to all members of the lab for their warm welcome, their scientific mentorship, and friendly help inside and outside the lab.

I also wish to heartfully thank my academic supervisors, Dr. Manon Genva from ULiège and Dr. Juliano Sabedotti from Taltech for their constructive feedback and dedication.

My thanks extend as well to the Bioceb coordination team, whose efforts made this international academic journey possible and enriching.

ABSTRACT(S)

Current strategies for microbial evolution aimed at enhancing bioproduction remain limited, primarily relying on growth-coupled selection methods. These approaches often fail to identify strains with high production potential. Decoupling growth from product formation using biosensors offers a promising alternative to effectively screen for high-performing production strains. This project aims to develop a methodological standard for biosensor-guided evolutionary platform, specifically based on genetically encoded biosensors consisting of a fluorescent protein linked to a ligand-binding domain. The proof of concept is focused on engineering synthetic methylotrophic Escherichia coli strains for efficient L-lactate production from methanol.

The experimental approach integrates three main modules: methanol assimilation in industrially relevant M9 medium, chromosome-based L-lactate biosynthesis, and intracellular lactate detection using single-fluorescent protein based biosensors. Key results of this work include the identification and genomic integration of an effective heterologous L-lactate dehydrogenase, resulting in stable, plasmid-free production; the functional validation of biosensors responsiveness within engineered strains; and critical insights into genetic stability, redox balance, and modular expression systems. More work remains to bring together the progress achieved in different streams – improving growth rate, producing L-lactate, tuning detection – and ultimately derive a reproducible cell factory development methodology, applicable to broader metabolite portfolios, leveraging the modularity of single fluorescent protein based biosensors. Ultimately, this work bridges biosensing, synthetic biology, and evolution engineering.

Les stratégies actuelles d'évolution microbienne visant à améliorer la bioproduction restent limitées, reposant principalement sur des méthodes de sélection couplées à la croissance. Ces approches peinent souvent à identifier des souches à fort potentiel productif. Le découplage entre croissance cellulaire et production métabolique, via l'utilisation de biosenseurs, représente une alternative prometteuse pour cribler efficacement les souches les plus performantes. Ce travail propose de développer une méthodologie standardisée pour une plateforme évolutive guidée par biosenseurs, fondée sur des biosenseurs génétiquement encodés combinant une protéine fluorescente et un domaine de liaison au ligand. La preuve de concept s'appuie sur l'ingénierie de souches synthétiques d'Escherichia coli méthylotrophes, optimisées pour la production de L-lactate à partir de méthanol. L'approche expérimentale repose sur trois modules intégrés : l'assimilation du méthanol dans un milieu M9 à pertinence industrielle, la biosynthèse de L-lactate via intégration chromosomique, et la détection intracellulaire du lactate par des biosenseurs à fluorophore unique.

Parmi les résultats majeurs, on note l'identification et l'intégration génomique d'une L-lactate déshydrogénase hétérologue efficace, permettant une production stable sans plasmide ; la validation fonctionnelle de la réponse des biosenseurs dans les souches modifiées ; ainsi que des réflexions critiques sur la stabilité génétique, l'équilibre redox et l'expression modulaire des voies métaboliques. Des efforts supplémentaires sont nécessaires pour intégrer ces différents volets – amélioration de la croissance, production de L-lactate, calibration des capteurs – en une méthode de développement de souches usines généralisable et applicable à un éventail plus large de métabolites grâce à la modularité des biosenseurs à protéine fluorescente. Ce travail s'inscrit à l'interface du domane des biosenseurs, de la biologie synthétique et de l'ingénierie évolutive.

CONTENTS

1. INTRODUCTION

Cell factories are microorganisms engineered via metabolic engineering, synthetic biology, and systems biology, in order to produce valuable compounds (Davy, Kildegaard and Andersen, 2017; Aguilar, Twardowski and Wohlgemuth, 2019). Cell factories could be key to "close the loop" of the circular economy, as they can be optimised to convert renewable feedstocks - such as sugars, methanol, CO_2, or waste biomass - into higher-value products - such as fuels, chemicals, pharmaceuticals, and biomaterials (Yan *et al.*, 2024; Carter, 2025). Cell factories fit naturally into the bioeconomy paradigm, as they may enable sustainable, circular, and resource-efficient production systems (Matsuo *et al.*, 2024). In the face of climate change, cell factories can contribute to mitigation by enabling the bioconversion of greenhouse gases and their derivatives into valuable products. Similarly, in the face of resource depletion, they may play a pivotal role in valorising waste streams into higher-value chemicals and materials. Thus, cell factories represent a promising route to addressing the intertwined challenges of climate and resource crises simultaneously, by reducing reliance on petrochemical feedstocks for the manufacturing of bulk and fine chemicals.

As a matter of fact, cell factories are often greener than their equivalent "chemical factories", because they employ enzymes as biocatalysts, whereas traditional synthetic chemistry often relies on non-recyclable catalysts that require rare and/or toxic metals. Enzymes operate under mild conditions (e.g. ambient temperatures and pressures, neutral pH, aqueous media) (Pandey *et al.*, 2024). They are very efficient catalysts, biodegradable, compatible with each other (allowing cascades and equilibrium shifts), not restricted to their natural role (potentially exploiting a wider scope of substrates). They encompass a broad spectrum of reactions, and are potentially chemo-, regio-, enantio-selective (meanwhile racemic mixtures obtained by chemical synthesis result in major wastage) (Faber, 2018). By contrast to biomanufacturing, chemical manufacturing remains heavily reliant on petrochemical resources, harsh reaction conditions, organic solvents, and tends to generate significant greenhouse gas emissions, toxic by-products, and waste. The relative benefit of biological pathways for the environment can and must be confirmed by Life Cycle Analysis (LCA) (Juodeikiene *et al.*, 2015; Fu *et al.*, 2023).

In designing cell factories, rational genetic engineering allows to introduce and tune bacterial pathways towards a target product based on existing knowledge of enzymes and cell metabolism. However, these interventions often cause imbalances in cellular homeostasis, metabolic burden, and growth inhibition (Williams, Pretorius and Paulsen, 2016; Teng *et al.*, 2022). To overcome these limitations, adaptative laboratory evolution (ALE) is an empirical approach that allows cells to adapt and adjust to the modifications, in systemic ways that could not have been anticipated by rational design. Over successive generations, mutants are selected that mitigate growth defects and restore metabolic balance through naturally occurring genetic variations (Godara and Kao, 2020; Wu *et al.*, 2022). Nonetheless, while through ALE it is relatively simple to select for traits such as improved growth rate or stress tolerance, it is much more complicated to select for enhanced production of a desired product (Sandberg *et al.*, 2019). Such selection necessitates time-consuming downstream analyses of production levels implying extraction, purification, and chromatography (e.g., HPLC), which limit throughput and slow down strain development cycles (Shepelin *et al.*, 2018).

Genetically encoded biosensors come in to circumvent this bottleneck. Not only do they allow to visualize whether cells produce the compound of interest, but also measure its quantity. The real-time monitoring of intracellular metabolite concentrations or fluxes opens significant opportunities to accelerate the development of cell factories (Liu, Liu and Wang, 2017; Teng *et al.*, 2022). Once rational design is completed, applying all state-of-the-art biochemical knowledge available, following-up with biosensor-guided evolution could allow simultaneous optimization of both growth and production phenotypes (Williams, Pretorius and Paulsen, 2016). Accordingly, this thesis explores the synergistic combination of rational design, ALE, and biosensor technologies to provide an accelerated and robust platform for the evolution of microbial strains with enhanced production capabilities, facilitating the translation of metabolic engineering innovations into scalable bioprocesses (Ren *et al.*, 2025). The

overarching aim is to establish a method for cell-factory development applicable to diverse substrates and products; methanol and L-lactate have been respectively chosen for the proof of concept. Converting methanol to L-lactate exemplifies the transformation of a simple C1 compound into a value-added C3 metabolite—a key objective in the development of next-generation cell factories.

L-lactate is the target product for the proof of concept cell factory, for the iLACCO series of biosensors, developed by Dr. Nasu's group (Academia Sinica, Taiwan) will be applied. His team set the methodological standard for the design of genetically encoded single protein-based intensiometric fluorescent biosensors (Nasu *et al.*, 2021). They proved the effectiveness of their development pipeline in developing the iLACCO series, tailored to detect intracellular L-lactate (Hario *et al.*, 2024). So far, they have taken advantage of these biosensors to image real-time fluctuations in L-lactate during glycolysis, transport inhibition, and metabolic oscillations in mammalian cells. The biosensors could track L-lactate in *Drosophila* brains, paving the way for *in vivo* studies. The authors however envision potential for these tools in applied biotechnology for strain optimization and metabolic engineering. This avenue is explored in this thesis by leveraging the biosensors to screen lactate-producing strains.

Methanol is the target substrate for the proof of concept cell factory, for the synthetic methylotrophic strains developed by Dr. Liao's group (Academia Sinica, Taiwan) will be leveraged. His team enabled *E. coli* to grow on methanol as sole-carbon source by introducing the RuMP pathway and enhancing formaldehyde tolerance mechanisms (Chen *et al.*, 2020; Nieh *et al.*, 2024). Juggling adaptative laboratory evolution (ALE) with an innovative ddp-BAC system for dynamic gene copy number tuning, they achieved a doubling time of 3.5 hours in MOPS methanol minimal medium, against about 9 hours in M9 methanol minimal medium. MOPS medium offers more stable pH buffering and support for some fastidious strains, but involve higher reagent costs and complexity, which limits their scalability. M9 medium is more industrially relevant than MOPS. Composed of inexpensive inorganic salts, M9 aligns with bioprocessing constraints - such as cost-efficiency and simplicity - for high-throughput screening and scale-up workflows (Santos and Stephanopoulos, 2008; LaCroix, Palsson and Feist, 2017). Therefore, one objective of this study is to enhance growth of the cell factory in M9 methanol minimal medium.

In a nutshell, this thesis builds on the work of Dr. Nasu's and Dr. Liao's research groups, to develop an *Escherichia coli* cell factory able to transform methanol into lactate, and to establish an evolutionary engineering process to optimise its performance based on fluorescent biosensors. In order to bridge the *E. coli* methylotrophs to the L-lactate biosensors, *E. coli* had to be engineered to produce L-lactate, which it does not naturally. This required targeted genome modifications, including the expression of heterologous L-lactate dehydrogenase gene(s) and of the lactate biosensor module. Chromosomal incorporation are preferred to plasmid-based systems, for the latter are not as stable, and ill-suited for industrial applications. The majority of the experimental work presented in this thesis was dedicated to this genetic engineering effort, and the results reported herein primarily reflect these objectives.

The experimental approach hopes to bring together rational metabolic engineering, adaptive laboratory evolution (ALE), and single-protein based biosensors. The material and methods section is therefore organised around these three branches. Throughout the experimental workflow, two development streams were pursued independently at first: methanol assimilation on the one hand, and lactate production/detection in the other hand. This separation is reflected in the structure of the forthcoming state-of-the-art section. Nevertheless, the intent is to converge these functionalities eventually, to reach a robust methanol-to-lactate cell factory wherein biosensor-guided adaptive evolution could be applied to rapidly enhance production performance.

2. STATE OF THE ART

2.1. METHANOL CONSUMPTION

2.1.1. Why E. coli rather than a native methylotroph ?

Some microbes, such as *Methylobacterium extorquens, Bacillus methanolicus,* and *Pichia pastoris* are native methylotrophs (Singh *et al.*, 2022). That is, they have the natural capacity to utilize single-carbon (C1) compounds such as methanol. Methylotrophs have been extensively studied since the mid-20th century. These organisms possess specialized and well-characterized pathways for methanol assimilation, including the ribulose monophosphate (RuMP) cycle and the serine cycle (Chistoserdova, Kalyuzhnaya and Lidstrom, 2009; Zhu *et al.*, 2020). These natural methylotrophs have been deployed industrially for the production of amino acids, vitamins, and single-cell proteins. Notwithstanding, their application as microbial cell factories is constrained by limitations in genetic traceability, metabolic engineering toolkits, and industrial scalability (Bennett *et al.*, 2018).

By contrast, *Escherichia coli* (*E. coli*) has long been recognized as a cornerstone chassis for synthetic biology and industrial biotechnology. It owes its popularity as cell factory to biological, engineering, and practical advantages. To start with, extensive genetic and molecular toolkits exist for *E. coli*; *E. coli* has in fact the largest collection of computational design programs, biobricks (promoters, RBSs, terminators), and DNA delivery protocols (Adams, 2016). Second, *E. coli* is easy to cultivate and grows fast. Its doubling time under one hour and its low nutritional requirements enable cost-effective experimentation and industrial-scale fermentation (Faber, 2018). From a both research management and scale-up point of view, *E. coli* is sometime privileged thanks to its safety and regulatory familiarity. Non-pathogenic lab strains (e.g., K-12 derivatives) are classified as Biosafety Level 1 (BSL-1) and have a proven industrial safety record, streamlining regulatory approval (Baba *et al.*, 2006). *E. coli* is also privileged for its metabolic flexibility and engineerability. Not only does *E. coli* synthesize a wide diversity of metabolites, but it also supports well metabolic rewiring, allowing efficient redirection of carbon flux .

All in all, *E. coli* provides faster strain development cycles, lower bioprocess costs, and easier translation from lab to industry. These attributes have made *E. coli* the preferred organism for synthetic biology innovation and industrial applications. For the same reasons, it was chosen for the present study. The *E. coli* strains used (full list in Annex 2) were already engineered by the members of Dr. Liao's group to grow on methanol upon commencement of this thesis work, and the experiments presented here build upon it.

2.1.2. Why methanol as feedstock?

From a biotechnological perspective, methanol has several key advantages over other renewable feedstocks such as lignocellulosic biomass. First, its chemical simplicity and process compatibility: methanol is indeed water-soluble, homogenous and liquid at ambient conditions, enabling easy transport, storage, and integration into existing industrial infrastructure (Cowan *et al.*, 2023). Its water-solubility facilitates assimilation by microorganisms, whereas gaseous single-carbon compounds are hindered by diffusion barriers. Second, methanol has high carbon and energy efficiency. It is highly reduced, i.e. electron-rich, which could theoretically lead to higher yields of reduced chemicals and fuels, minimizing carbon loss as CO_2 (compared to fermentation pathways based on comparatively oxidised sugars) (Kelso *et al.*, 2022). To this day, the vast majority of methanol is utilized as a building block for the production of key chemicals and fuels, e.g. formaldehyde, acetic acid, and methyl tert-butyl ether (MTBE) (Bertau *et al.*, no date; Tabibian and Sharifzadeh, 2023; Hosseinpour, Shayesteh and Es'haghi, 2025), via chemical rather than biochemical processes.

Historically, methanol has been obtained from fossil resources. More than 90% of global methanol is derived from natural gas through steam reforming or from coal gasification (Srirangan *et al.*, 2012).

However, methanol can also be produced from renewable sources: from captured CO_2, from biogas, or from biomass gasification (Mishra *et al.*, 2022; Dell'Aversano *et al.*, 2024). Carbon dioxide can be hydrogenated into methanol using green hydrogen (from renewable-powered electrolysis) and $Cu/ZnO/Al_2O_3$-based catalysts (Chen and Lin, 2018; Dalena *et al.*, 2018). Biogas from waste methanization (anaerobic digestion of organic waste) mainly consists of methane (CH_4) and CO_2; the methane can undergo catalytic partial oxidation (CPO) or steam reforming, converting it into synthesis gas (syngas), a mixture of CO, H_2, and CO_2; this latter syngas is then fed into a methanol synthesis reactor under pressure and temperature, typically using the same types of catalysts (Chen and Lin, 2018; Borgogna *et al.*, 2019). Finally, solid biomass (wood, agricultural residues, municipal solid waste) can be thermochemically converted into syngas at high temperatures (700–1000°C) and in the presence of controlled amounts of oxygen, steam, or air (Eisavi *et al.*, 2022). The resulting syngas (CO, H_2, CO_2, CH_4) is cleaned of impurities. This involves multistep gas cleaning processes, including cyclonic separation and filtration to remove particulates, scrubbing or wet gas cleaning for tar and ammonia removal, and adsorption methods (e.g., activated carbon, zinc oxide beds) to eliminate sulphur compounds (Sun and Tang, 2023). At last, the cleaned syngas entering a methanol synthesis loop.

Last but not least, cell factories metabolising methanol are a strategic stepping stone toward the methane valorisation. Methane, an abundant and potent greenhouse gas, poses formidable obstacles to bioavailability, due its low solubility and mass transfer limitations (E. Bjorck, D. Dobson and Pandhal, 2018). Moreover, engineering the intricate methane-activation enzymatic systems into non-native hosts is arduous: for instance, methane monooxygenase (MMO) is membrane-bound and difficult to express heterologously (Park, Cha and Hahn, 2024). Thus, synthetic methylotrophy - coined in this study as the ability to metabolise methanol - in microbial hosts like *E. coli* or *Pichia pastoris*, represents a critical springboard before tackling the more complex challenge of methane utilization (Singh *et al.*, 2022). From a process engineering perspective as well, methanol-based processes allow for more straightforward process scale-up, control, and optimization, serving as an industrial gateway to future methane-to-chemical processes (Bennett *et al.*, 2018). The latter could in fact rely on co-culture systems or two-step processes combining methane oxidation to methanol, followed by microbial conversion of methanol to the desired products.

The past 20 years have witnessed great advancements in synthetic methylotrophy, masterfully reviewed by Bennett et al. (2018). It is now time to elevate methanol-based bioproduction beyond biomass growth. Indeed, most studies so far have prioritized establishing growth on methanol, while little work explores the production of chemicals (e.g., organic acids, bio-based materials) from methanol (Irla and Wendisch, 2022), with the notable exception of Reiter et al., (2024). In the current work, the ultimate goal is to obtain lactate from methanol, as a proof of concept. From a broader view, leveraging unconventional feedstocks like C1 compounds to produce more complex molecules shall demonstrate the feasibility of integrating carbon recycling and sustainable biomanufacturing via synthetic biology, all the while addressing emerging markets for CO_2-derived chemicals (Ruales-Salcedo *et al.*, 2022).

2.1.3. Turning *E. coli* into a methylotroph

2.1.3.1. Enabling growth of E. coli on methanol as carbon-source

Synthetic methylotrophy, i.e. the engineering of non-methylotrophic hosts like *E. coli* or *S. cerevisiae* to metabolise methanol, has only gained significant attention over the past decade, but is a rapidly evolving field (Wegat, Fabarius and Sieber, 2022). Early work attempted to reconstruct methanol assimilation pathways in bacteria and yeast. In 2015, Whitaker and colleagues demonstrated RuMP cycle reconstruction in E. coli, albeit with minimal methanol-dependent growth (Whitaker *et al.*, 2015). Meyer et al. (2018) refined these approaches, achieving methanol-dependent but still modest growth in E. coli (Meyer *et al.*, 2018). Chen and colleagues were the first to enable growth of E. coli on methanol as sole carbon-source (Chen *et al.*, 2020). Before their success, only heterotrophs feeding on methanol

together with sugars had been developed (Garg *et al.*, 2018; Meyer *et al.*, 2018; Tuyishime and Sinumvayo, 2020).

Chen et alia first expressed in E. coli BW25113 the 3 genes of the RuMP cycle which differ from the typical sugar metabolism of E. coli - *medh*, *hps* and *phi* - as well as a recombinant *tkt* and *tal* (see metabolic map, Figure 2), arranged in two synthetic operons. Then, they initiated laboratory evolution (Figure 1). They obtained an auxotrophic strain unable to grow either on methanol nor on xylose alone. Xylose remained essential to supply Ru5P, which reacts in formaldehyde conversion (see Figure 2). The authors turned to Ensemble Modeling Robustness Analysis (EMRA) to identify and de-bottleneck kinetic traps. EMRA, a computational tool that simulates metabolic flux distributions under parameter variability and predicts which enzymes require up- or down-regulation to improve pathway efficiency (Lee, Lafontaine Rivera and Liao, 2014). In light of the results, they reduced the expression of two enzymes which were diverting carbon flux away from the RuMP cycle, allowing ALE to resume. They then implemented a nutrient weaning ALE strategy, gradually replacing the rich Hi-Def Azur (HDA) medium with MOPS minimal medium containing only methanol as C-source. They obtained a strain capable of autonomous growth on methanol, SM1.

In a nutshell, enabling *E. coli* to feed on methanol implied overcoming major metabolic, regulatory, and toxicity challenges. First, methanol and formaldehyde are inherently toxic to non-native hosts. Second, an increased methanol concentration often decreases the carbon efficiency and growth rates. Third, the methanol assimilation bottlenecks are still incompletely understood, especially in E. coli and yeasts (Wang *et al.*, 2020; Wegat, Fabarius and Sieber, 2022). Fourth, there lacks high-throughput evolution strategies for fitness and production optimization under methanol fermentation conditions (Kelso *et al.*, 2022). The work presented in this thesis continues the synthetic methylotrophy efforts initiated by Dr. Liao's group (Chen *et al.*, 2020; Nieh *et al.*, 2024). They overcame the first, second, and partly third challenges cited above, the present thesis attempts to addresses the fourth challenge.

Figure 1: Strategies deployed by Chen et al. (2020) (above) and Nieh et al. (2024) (bottom) to enable WT *E. coli* to grow on methanol as sole carbon source as fast as native methylotrophs

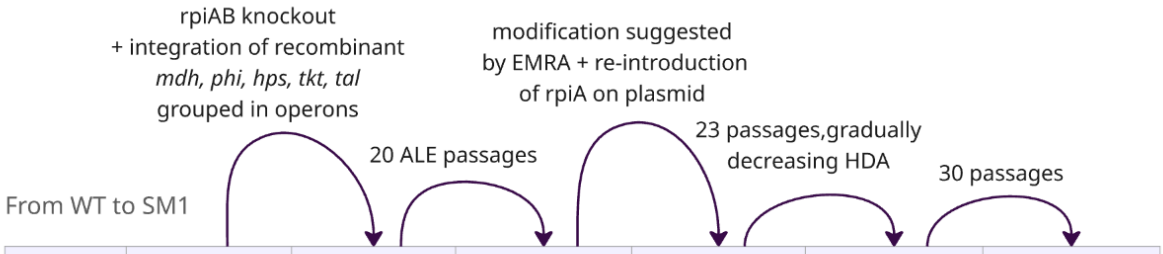

Strain	K12 *E. coli*	CFC381.0	CFC381.20	CFC526.0	CFC526.23	SM1 (CFC 526.53)
Doubling time (h)	0.5 h		OD 0.1 to 1 in 48h		22 h	41 h to saturation
Medium	Glucose minimal medium (min. med.)	min. med. with 400mM MeOH and 20mM xylose	min. med. with 400mM MeOH and 20mM xylose	HDA 100% MeOH	HDA 0%, MOPS, 400mM MeOH, with Nitrate	MOPS, 400mM meOH, with nitrate
Notable mutations		Intentional ΔpfkA, and ΔgapA::gapC	inactivation of frmA, fdoG, gnd (formaldehyde detoxification pathways)			IS flanked a 70 kb tandem repeat region containing a synthetic operon

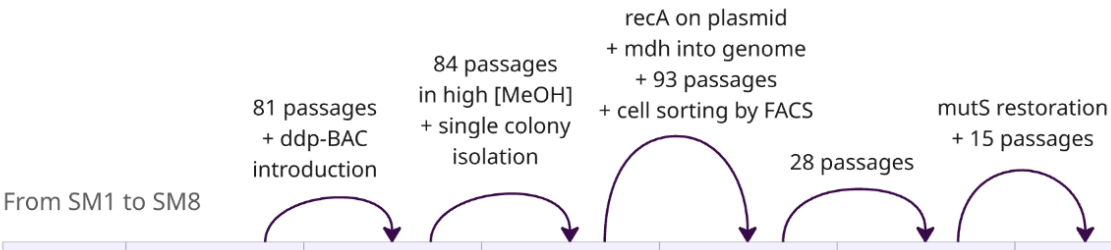

Strain	SM1	SM1p pLY147	CFC841	SM6	SM7	SM8
Doubling time (h)	8.5 h	25 h	10.2 h	4.0 h	3.5 h	3.5 h
Medium	MOPS, 400mM meOH, with nitrate	MOPS MeOH 1000 mM	MOPS MeOH 1200mM	MOPS MeOH 400mM	MOPS MeOH 400mM	MOPS MeOH 400mM
Notable mutations		Copy number variations of ddp-BAC::RHTTP	70kb shrank to 46kb recA knocked out	Partial or full disabling of gltA and rhlB	recA plasmid removed mutS knocked out	

2.1.3.2. Overcoming DNA-protein cross-linking (DPC)

The main challenge in further engineering *E. coli* into a methylotroph was to overcome DNA-protein cross-linking, henceforth referred to as DPC. Methanol is oxidised by medh as soon as it is absorbed. An imbalance between this first reaction and downstream steps causes formaldehyde to accumulate. It then reacts intracellularly, forming DNA-protein crosslinks (DPCs). These crosslinks impair DNA replication, transcription, translation, and protein function (Stingele, Bellelli and Boulton, 2017). DNA and proteins aggregating can lead to self-destruction, or formaldehyde can leach into the medium, poisoning other cells. DPC manifested in experimental observations: After extended time in stationary phase, cells failed to regrow upon passage or had concerningly long lag phases. Flow cytometry revealed an important proportion of dead cells; DPC products were visualised via extraction, staining, and transmission electron microscopy (TEM); and quantitative proteomics confirmed that hundreds of proteins crosslinked with DNA.

The higher the methanol concentration, the more severe the DPC issue. Moreover, it intensifies as exponential phase growth slows (mRNA transcripts levels and qRT-PCR revealed that the cell down-regulated genes regenerating Ru5P through the RuMP cycle more than it down-regulated *mdh*, see Figure 2). In other words, even when the cells were able to grow in methanol, DPC killed the cells in stationary phase. DPC thus made laboratory evolution close to impossible, because the cellular functions would be affected by DPC before the cell can exhibit beneficial mutation to circumvent it. If mutation occurred, they decreased the formaldehyde production (affecting *medh*) rather than increased formaldehyde consumption. Given that DPC is an issue on the global proteome level, the sole solution is to strike a fine balance between formaldehyde generation and consumption fluxes.

Native methylotrophs have complex mechanisms to avoid severe DPC (Collins and Kalyuzhnaya, 2018), however, these regulatory mechanisms defeat the objective of synthetic methylotrophy, i.e. channelling the carbons of methanol into central metabolism. Increasing activities and/or expression levels in downstream pathways is logically preferable to limiting methanol assimilation. For such gain of activity mutation downstream of formaldehyde, several methods were available. The authors focussed on adjusting expression levels of the enzymes utilizing formaldehyde in the RuMP cycle via copy number variations (CNV). For such purpose, traditional plasmid systems are easy to handle but cannot tune the copy number to the/an optimal solution. CNV mediated by transposons are random and limited in the range of copies achievable. In order to find, among a wide range, the best number of gene copies, Nieh and colleagues invented a bacterial artificial chromosome (BAC) system featuring the ddp operon (Nieh *et al.*, 2024).

Genes on this *ddp* operon are duplicated and homologously recombined dynamically. In other words, in a population of cells, a binomial distribution of copy numbers of the said genes will be observed, providing a library of candidates for finding optimal expression levels. As the number of concatemers of the genes constantly vary, this allows the colonies to adjust it to each environment but also to each growth phase. This ability provided a tentative fix, alleviating the DPC problem, time for the cells to find more permanent solution(s). In other words, this novel approach, varying copy numbers dynamically thanks to the ddp operon on a BAC, allowed to bypass the formaldehyde-induced DPC, letting the cells not merely survive but also pursue their natural evolution process, and eventually mutate in such ways that the ddp-BAC system was no longer necessary for them to thrive in methanol medium.

This extended ALE experiment, schematized in Figure 1, resulted in SM7 and SM8 strains. SM7 and SM8 strains are used in this study, as well as SM1 (stage between full methylotrophy and ddp-BAC introduction). The latest strains double under 4 hours in optimal conditions, as fast as native methylotrophs, yet there is still some margin for improvement in conditions approaching industrial fermentation contexts. For instance, M9 medium is less expensive and more common at large scale than MOPS medium, in which the SM strains have been improved so far. Perhaps similar and/or dissimilar mutations would appear if optimising the engineered E. coli in M9 methanol minimal medium: this is undertaken in the present project.

2.2. LACTATE PRODUCTION AND DETECTION

2.2.1. Why L-lactate as target product?

Lactic acid (2-hydroxypropionic acid) is a chiral alpha-hydroxy acid, characterized on the one hand by a hydroxyl group adjacent to the carboxylic acid group, on the other hand by a chiral centre at the second carbon, giving rise to L- and D-enantiomers. Mammalian cells produce and metabolize L-lactate almost exclusively (Manandhar and Shah, 2023). In contrast, bacteria can produce both L- and D-lactate, yet *Escherichia coli* specifically synthesizes solely D-lactate under fermentative conditions (Zhou *et al.*, 2016). At physiological pH (around 7.0–7.4), lactic acid is fully deprotonated lactic acid and exists in its dissociated form, lactate anion, in cells, blood, and extracellular fluids (Papadimitriou *et al.*, 2016). In cellular metabolism, lactate is produced from pyruvate (see Figure2). This reaction regenerates NAD^+ and in so doing helps maintain the redox balance during glycolysis, especially in anaerobic fermentation, muscle cells in effort, and cancer cells (Warburg effect) (Pessione, 2012). Nonetheless, lactate is not merely a metabolic by-product but a multifunctional molecule in cell biology, involved in energy metabolism, redox balance, ecological interactions, and signalling (Teusink, Bachmann and Molenaar, 2011). As a matter of fact, lactate plays roles in host-microbe interactions, serving as a metabolite that shapes microbial communities, modulates immune responses, and influences host metabolism (Pessione, 2012).

Lactic acid's key properties include hydrophilicity (due to the alcohol and carboxyl moieties), mild acidity (pKa ~3.86), biodegradability and non-toxicity. These properties underpin its functional versatility in industry. For instance, its acidity allows it to act as a preservative, acidulant, and buffering agent. It comes into play in the production of food additives, pharmaceuticals, detergents (Bilal, Niu and Wang, 2024; Chong *et al.*, 2024). Furthermore, its chirality makes it a monomer for polylactic acid (PLA). Indeed, the enantiomeric form of lactic acid influences the crystallinity, mechanical properties, and degradation rate of PLA, which is used as a biodegradable plastics in packaging, agriculture, and biomedical fields (Manandhar and Shah, 2023). In addition, it is subject of esterification, which makes it a green solvent precursor. Ethyl lactate, for instance, is a biodegradable and low-toxicity solvent widely used in electronics cleaning, coatings, and pharmaceuticals (Chong *et al.*, 2024). Finally, its reactive hydroxyl and carboxyl functionalities allow it to act as platform chemical. It can be converted to a wide range of C3 derivatives, including propylene glycol, acrylic acid, and lactide, expanding its scope of applications (Bilal, Niu and Wang, 2024; Chong *et al.*, 2024).

Lactic acid can be produced either by chemical synthesis or via microbial fermentation, each with distinct implications in terms of cost, purity, scalability, and sustainability. 90-95% of L-lactic acid production is biomanufacturing; the small percentage which is synthesized is destined to DL-lactate mixtures (Becker *et al.*, 2015; Di Lorenzo *et al.*, 2022). If synthesized chemically, acetaldehyde reacts with hydrogen cyanide, resulting in lactonitrile, which is then hydrolysed. While this method is cost-effective at scale and does not require biomass feedstocks, it results in a racemic mixture of D- and L-lactic acid. Moreover, this process involves toxic precursors and generates environmentally hazardous by-products (Juodeikiene *et al.*, 2015). If produced biochemically, lactic acid bacteria (LAB) or engineered microbial platforms (e.g., *E. coli*, *Bacillus*, *Rhizopus*) are employed to selectively produce enantiopure L-lactic acid via anaerobic fermentation at optimized pH (~5-6) and temperature (30–45 °C). After fermentation, L-lactic acid is recovered by filtration, precipitation (e.g., with calcium carbonate), and further purified through acidification and distillation or electrodialysis. Feedstocks commonly include glucose, starch, and increasingly lignocellulosic biomass and waste substrates (Fei *et al.*, 2020). Techno-Economic Analysis (TEA) reveal that feedstock cost accounts for up to 70% of the total cost (Grasa *et al.*, 2021). Second-generation biorefineries using lignocellulose or food waste show potential to reduce operating costs and GHG emissions, but require more complex pre-treatment and enzyme strategies (Gezae Daful and Görgens, 2017).

Bioproduction processes can be scaled to industrial fermentation levels (10,000–100,000+ L), with low-pH fermentation and integrated downstream purification systems developed to reduce costs and avoid base neutralization (Vanapalli *et al.*, 2023). All major manufacturers - Corbion, NatureWorks, TotalEnergies Corbion, and Cargill - use GMO strains (Béal *et al.*, 2023). TEAs indicate that microbial production becomes preferable when strain productivity exceeds 90 g/L with high yield (>0.9 g/g). In parallel, multiple LCAs confirm that biochemical production significantly outperforms chemical synthesis in terms of carbon footprint, toxicity, and overall sustainability (Ioannidou *et al.*, 2022; Wang, Zhang and Bao, 2025). From a market perspective, the global lactic acid market is projected to exceed USD 6 billion by 2028, driven by the expansion of bio-based packaging, cosmetics, and pharmaceuticals (Mordor Intelligence, 2025).

All of the above considered, lactate constitutes both a scientifically interesting and commercially attractive target product. L-lactate was selected as the target molecule in this study primarily because the biosensors employed have been engineered for intracellular L-lactate (more details in Section 2.2.4.2.). Nevertheless, it is sensical, for a proof of concept, to choose a target product which is already produced at industrial scale by microbial cell factories—albeit typically not by *Escherichia coli*. This choice permits leveraging a well-established body of literature, facilitates benchmarking against other engineered strains (e.g. comparing yields), and allows the exploration of scalability considerations.

2.2.2. Lactate metabolism in E. coli

Figure 2: Simplified metabolic map of the methanol-to-lactate cell-factory.

For the sake of clarity, solely genes mentioned in the text are labelled.

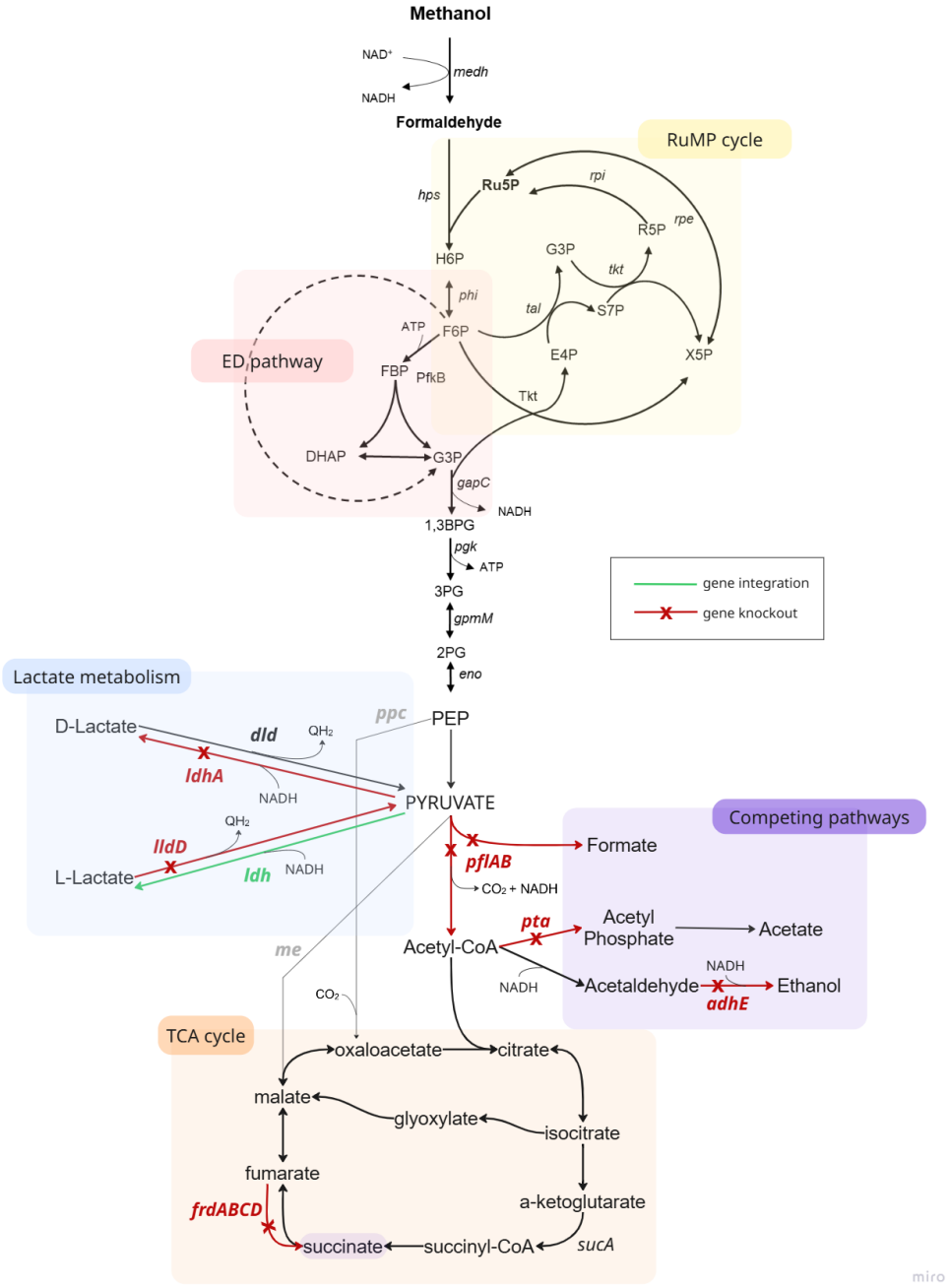

Pathways & Cycles: RuMP cycle, Ribulose monophosphate cycle**;** TCA cycle, tricarboxylic acid cycle; ED pathway, Entner–Doudoroff pathway. **Metabolites:** MeOH, methanol; Ru5P, ribulose-5-phosphate; R5P, ribose-5-phosphate; S7P, sedoheptulose-7-phosphate; G3P, glyceraldehyde-3-phosphate; G6P, glucose-6-phosphate; F6P, fructose-6-phosphate; FBP, fructose-1,6-bisphosphate; DHAP, dihydroxyacetone phosphate; 1,3BPG, 1,3-bisphosphoglycerate; 3PG, 3-phosphoglycerate; 2PG, 2-phosphoglycerate; PEP, phosphoenolpyruvate; E4P, erythrose-4-phosphate; Acetyl-CoA, acetyl coenzyme A; α-Ketoglutarate, alpha-ketoglutarate; CO_2, carbon dioxide; NAD^+/NADH, nicotinamide adenine dinucleotide (oxidized/reduced form); QH_2, reduced quinone (quinol). **Enzymes / Genes:** medh, methanol dehydrogenase; hps, 3-hexulose-6-phosphate synthase; phi, 6-phospho-3-hexuloisomerase; rpi, ribose-5-phosphate isomerase; tkt, transketolase; tal, transaldolase; gapC, glyceraldehyde-3-phosphate dehydrogenase; pgk, phosphoglycerate kinase; gpmM, phosphoglycerate mutase; eno, enolase; ppc, phosphoenolpyruvate carboxylase; ldhA, D-lactate dehydrogenase; lldD, L-lactate dehydrogenase (quinone); ldh, recombinant L-lactate dehydrogenase; dld, D-lactate dehydrogenase (quinone); pta, phosphotransacetylase; adhE, alcohol dehydrogenase E; pflAB, pyruvate formate-lyase complex; frdABCD, fumarate reductase complex; sucA, 2-oxoglutarate dehydrogenase E1 component.

2.2.2.1. Native production and consumption of lactate isomers

E. coli can both produce and utilize lactate, with distinct enzymatic pathways functioning under aerobic and anaerobic regimes. The interplay between these pathways plays an important role in energy generation, redox balancing, and metabolic cross-feeding depending on the oxygen availability.

Under anaerobic conditions, *E. coli* produces D-lactate via the enzyme lactate dehydrogenase A (LdhA). LdhA reduces pyruvate to L-lactate, meanwhile oxidizing NADH to NAD^+. It thus maintains intracellular redox balance, essential for continued glycolytic flux in the absence of respiration (Zhao *et al.*, 2016). Expression of the ldhA gene is tightly regulated by global transcription factors including FNR and ArcA, which are responsive to anaerobic conditions and cellular redox state (Unden, Steinmetz and Degreif-Dünnwald, 2014; Zhao *et al.*, 2019). Metabolic profiling has shown that ldhA knockout on the one hand influences fitness in fluctuating oxygen environments - underscoring the importance of lactate production as a redox sink -, and the other hand can redirect metabolic flux toward alternative reduced end-products such as other C3 acids and alcohols (Kim *et al.*, 2013; Lin *et al.*, 2018).

Under aerobic conditions, *E. coli* utilizes both L-lactate and D-lactate as carbon sources. The oxidation of L-lactate is mediated by the *lld* operon (Aguilera *et al.*, 2008), which includes:

- LldP, a proton/lactate symporter.
- LldR, a transcriptional repressor which controls expression of the operon in response to intracellular lactate levels.
- LldD, a flavin mononucleotide (FMN)-dependent L-lactate dehydrogenase (D stems from the gene numbering, it acts on L-lactate). LldD catalyzes the oxidation of L-lactate to pyruvate, feeding directly into central carbon metabolism; this reaction is integrated with the electron transport chain.

In parallel, the D-lactate dehydrogenase (Dld) enzyme oxidizes D-lactate. Dld is membrane-bound and functions through electron transfer to quinones in the respiratory chain. Dld is complementary to LldD in enabling *E. coli* to fully exploit lactate isomers as energy sources (Unden, Steinmetz and Degreif-Dünnwald, 2014).

All in all, lactate metabolism in *Escherichia coli* is well-characterized and its regulation reflects *E. coli*'s need to finely balance energy production and redox homeostasis. The switch between LdhA-driven fermentation and LldD/Dld-mediated respiration is regulated by the redox-responsive ArcAB two-component system and the transcription factor FNR, already coined above. Both sense intracellular NADH/NAD^+ ratios and the redox state of the quinone pool in order to toggle between fermentative and oxidative pathways (Unden, Steinmetz and Degreif-Dünnwald, 2014).

In contrast, transport mechanisms for lactate in *E. coli* are surprisingly under-characterized. The system differs for L-lactate and D-lactate:

- Regarding L-lactate uptake, the LldP transporter is encoded within the lldPRD operon (*cf* bullet point above). It transports a proton together with L-lactate into the cell, it is specific for L-lactate, and it is active under aerobic conditions (Aguilera *et al.*, 2008).
- Regarding D-lactate uptake, no specific transporter gene has been conclusively identified in *E. coli* (Núñez *et al.*, 2002). Perhaps, since Dld is membrane-bound, it may access D-lactate from the periplasm directly or use non-specific transporters for cytoplasmic flux. Some literature hypothesises that non-specific porins or monocarboxylate permeases may facilitate D-lactate uptake (Núñez *et al.*, 2002).
- Regarding D-lactate export, there is no known dedicated D-lactate exporter in *E. coli.* The D-lactate produced via LdhA accumulates intracellularly, and then may exit the cell via passive diffusion (especially at low pH where lactate is protonated), or via unknown or non-specific monocarboxylate transporters, possibly shared with pyruvate, acetate, or other organic acids

(for instance FocA has been implicated in formate transport and may non-specifically transport other small acids).

- Regarding L-lactate export, since wild-type *E. coli* does not produce L-lactate, no dedicated L-lactate exporter exists.

Tying the above to the specifics of my experiments, to make *E. coli* produce enantiomerically pure L-lactate, at least 3 genetic modifications must be conducted. ldhA shall be knocked out, a recombinant L-ldh shall be knocked-in, LldD shall be knocked out. The latter is chosen over lldR or lldP because intracellular re-consumption is possible: indeed, if L-lactate builds up internally, E. coli may re-oxidize it via LldD (especially under aerobic conditions), thus reducing net yields. Transport dynamics of the L-lactate are expected to be a challenging aspect of this metabolic engineering. Once those three essential modifications are completed, the last step(s) of rational engineering could be to knockout pathways competing for pyruvate, for instance those leading to acetate, succinate, ethanol, formate (Figure 2).

2.2.2.2. Genetic engineering for L-lactate bioproduction

In order to produce L-lactate as fermentation end-product instead of the D-enantiomer, interventions on the *E. coli* genome are necessary. These include:

- introducing heterologous enzymes, typically from Gram-positive lactic acid bacteria,
- redirecting flux toward L-lactate, both carbon flux and redox equivalents,
- improving redox balancing ($NADH/NAD^+$ ratio), as L-ldh requires NADH as cofactor
- improving transport, for instance cloning in recombinant L-lactate transporters.

In order to choose which recombinant L-lactate dehydrogenase(s) to integrate in *E. coli*. The relatively recent review by Liu et al. (2022) features instructive tables: one is an inventory of microbial strains producing L-LA, another records the research status of L-LA production by genetically engineered strains, with 2 occurrences of *E. coli*. Preferences should be given to an L-ldh with high catalytic efficiency (kcat/Km), high substrate specificity, high thermal stability, a coenzyme preference for NADH rather than NADPH, good pH and salt tolerance, and expression potential in a host strain. Diving deeper in this latter factor, Table 1 lists the previous attempts at heterologous expression of L-ldh in E. coli. Based on this table, three candidates L-ldh were selected: from *Bacillus coagulans,* from *Streptococcus bovis* and from *Lactobacillus Casei*.

Steps in engineering *E. coli* for L-lactate production resonate with each other across publications, and resonate with the ones envisioned in the conclusion of the previous sub-section. The order differs from paper to paper, but the steps remain consistent:

- Deleting *ldhA* to block D-lactate formation. To avoid even minimal D-lactate formation and toxicity, Mazumdar et al. (2013) knocked out *mgsA* as well, so as to block the methylglyoxal bypass pathway (not represented on Figure 2).
- Deleting *lldD* to block the undesired utilization of the L-lactate product.
- Expressing an L-lactate dehydrogenase (L-Ldh) to convert pyruvate to L-lactate. In regards to the locus, Niu et al. (2014) expressed it in the middle of the chromosomal lldD gene, under the control of the *ldhA* promoter; Mazundar et al. (2013) replaced the *ldhA*.
- Decreasing the activity pathways depleting pyruvate and/or NADH: for instance, disrupting *pta*, towards acetate, *adhE*, towards ethanol, *frdABCD*, towards succinate, *pflB*, towards acetyl-CoA and formate (see Figure 2). By knocking them all out, Zhou and colleagues ensured that lactate was the sole NADH oxidation route - thus coupling (anaerobic) growth to production – and they achieved high titres (Zhou *et al.*, 2006a).
- Metabolic rewiring: not specific to L-lactate production, it consists in altering endogenous pathways - e.g. enzymes activity or regulatory elements - to stir carbon, energy and cofactors toward the metabolite of interest (Nielsen and Keasling, 2016).

Table 1: Recombinant L-lactate dehydrogenases expressed in *E. coli* for L-lactate bioproduction

ldh Origin	E. coli Strain	Yield / Titer / Productivity	Media Type	Carbon Source	Reference
Lactobacillus acetotolerans (Plasmid)	DH5α	13.4-27.6% glucose to LA 0.59 g/L L-LA	Complex	Glucose (2%)	(Goto *et al.*, 2018)
Bacillus coagulans (chromosomal)	B0013-070 (Δ*ldhA* Δ*lldD)*	73% yield 25.59 g/l	Amended Minimal	Glucose	(Niu *et al.*, 2014)
Lactobacillus casei (chromosomal)	B0013-070 (Δ*ldhA* Δ*lldD)*	58% yield 20.16 g/l	Minimal	Glucose	(Niu *et al.*, 2014)
Streptococcus bovis (chromosomal)	B0013-070 (Δ*ldhA* Δ*lldD)*	46% yield 16.19 g/l	Minimal	Glucose	(Niu *et al.*, 2014)
Streptococcus bovis (chromosomal)	LA01 (Δ*pflB*Δ*frdA*), LA02 (Δ*pta* Δ*adhE*Δ*frdA*)	0.90 g/g glycerol 50 g/L L-lactate 1.3 g/L/h	Minimal	Glycerol (60 g/L)	(Mazumdar *et al.*, 2013)
Enterococcus faecalis KK1 (plasmid)	SZ85 (pBAD-ldh)	0.62 g/g fructose 0.62 g/L 0.026 g/L/h	Complex	Fructose (1 g/L)	(Mulok *et al.*, 2009)
Streptococcus bovis (plasmid)	B or K12 derivatives	0.49-0.55 g/g 57.1 g/L	Amended complex	Glucose, Xylose, or mixture	(Dien, Nichols and Bothast, 2001, 2002)
Lactobacillus casei (plasmid)	RR1 (ΔldhA)	0.7 g/glucose 45 g/L 0.67 g/liter/h	Complex	Glucose	(Chang *et al.*, 1999)
Clostridium acetobutylicum (plasmid)	*acd* mutant *ldh pfl* mutant	51 mM (≈4.6 g/L)	Minimal	Glucose	(Contag, Williams and Rogers, 1990)

Some recombinant L-ldhs have been introduced in *E. coli* to improve D-lactate production as well, for instance (Bernard *et al.*, 1991) cloned into *E. coli* a ldh from *Lactobacillus delbrueckii*, or the same year (Taguchi and Ohta, 1991) cloned into *E. coli* a ldh *from Lactobacillus plantarum*.

Inspired by successful engineering detailed in this section, the strategy in this thesis work was to couple knockouts and knockins, and the one hand replacing ldhA by a recombinant L-ldh, on the other hand replacing lldD by the biosensor protein.

2.2.3. Laboratory evolution to complement rational genetic engineering

Adaptive Laboratory Evolution (ALE) is a powerful experimental approach that harnesses the principles of natural selection: generating genetic diversity then reducing it through environmental pressure. Over successive generations, ALE facilitates the natural enrichment of cells with spontaneous mutations which confer them a fitness advantage under the applied selective regime (Sandberg *et al.*, 2019). No such regime is needed to enhance growth rates in minimal/non-native media, but for more specific purposes the selective pressure may consist in increasing stress (e.g., heat, pH, solvents) or increasing co-substrate utilization (as Chen et al. (2020) did to shift from xylose/HDA to methanol, see Figure 1). Common methodologies involve serial passaging in batch culture, continuous cultivation (e.g., chemostats), or automated platforms capable of in-line monitoring and feedback-controlled passaging (Dragosits and Mattanovich, 2013; Wu *et al.*, 2022).

ALE is distinct from directed evolution: while ALE operates at the whole-organism level under natural mutagenesis, directed evolution typically targets a specific gene or protein and employs artificial

diversification techniques (e.g., error-prone PCR, DNA shuffling), and initiates the next iteration with the best (few) variant(s) (Yuan *et al.*, 2005; Wang *et al.*, 2021). ALE may be slower, due to selection occurring only after extended culture rather than at each passage, but it can capture broader physiological and regulatory adaptations which arise across the entire genome. In other words, the key strength of biosensor-assisted ALE lies in its capacity to uncover beneficial mutations beyond what rational metabolic engineering or targeted mutagenesis might predict. In a number of cases, biosensor-driven ALE optimized carbon partitioning between growth and production, sometimes in genes seemingly unrelated to the pathway at stake (LaCroix, Palsson and Feist, 2017; Sandberg *et al.*, 2019; Hirasawa and Maeda, 2023).

In this project, ALE will foremost be applied to enhance the growth of synthetic methylotrophic (SM) strains on M9 methanol minimal medium. When the genetic modifications cited in the previous section are completed, the lactate-producing and -sensing strains will also undergo ALE to mitigate fitness costs associated with engineering and result in a resilient cell factory thriving under the target conditions.

2.2.4. Biosensors

2.2.4.1. Fluorescent biosensors

The core functionality of a biosensor hinges on two components: (1) the *bioreceptor*, which selectively interacts with the target (may be a biological recognition element e.g., enzymes, antibodies, nucleic acids, or whole cells), and (2) the *transducer*, which converts the biological response into a quantifiable signal (Turner, 2013; Suma and Adarakatti, 2024). Biosensors are usually categorized by their transduction mechanism, as depicted in Figure 3. More details, as well as precise references, are provided in Table 1 in Annex 4. Among optical biosensors, fluorescent biosensors themselves have subtypes:

Small-molecule dyes (e.g., Ca^{2+} indicators like *Fura-2* or *Indo-1*): synthetic dyes need to be micro-injected, and they change fluorescence intensity and/or wavelength upon analyte binding. They are appreciated for their strong (bright) and fast response, but the loading and equilibration/diffusion is cumbersome (Dean and Palmer, 2014).

FRET-based sensors (e.g. *Cameleon*): Förster Resonance Energy Transfer (FRET) involve two fluorescent proteins (FPs) or dyes acting as a donor-acceptor pair (e.g., CFP-YFP). This pair flanks a recognition domain, and when the domain binds, the conformational change alters the distance/orientation between the pair, changing the acceptor/donor emission ratio. Their ratiometric readout makes them self-calibrating and therefore well-suited for dynamic in vivo imaging, though they suffer from limited dynamic range and spectral overlap (Thorn, 2017).

Genetically encoded fluorescent (e.g *LacI-GFP, AraC-GFP*, *TetR-GFP, or GCaMP, IGluSnFr, Perceval*): their main advantage is specified in their name, they are expressed by the cells themselves, so no invasive delivery is necessary, moreover it allows organ- or organelle-specific targeting (Palmer & Tsien, 2006; Dean & Palmer, 2014). A plentiful palette of fluorescent proteins has been developed (e.g., *mCherry*, *mTurquoise2*), hence this type of biosensors is ideal for multiplex imaging.

Figure 3: Taxonomy of biosensor technologies and positioning of the iLACCO series within it.

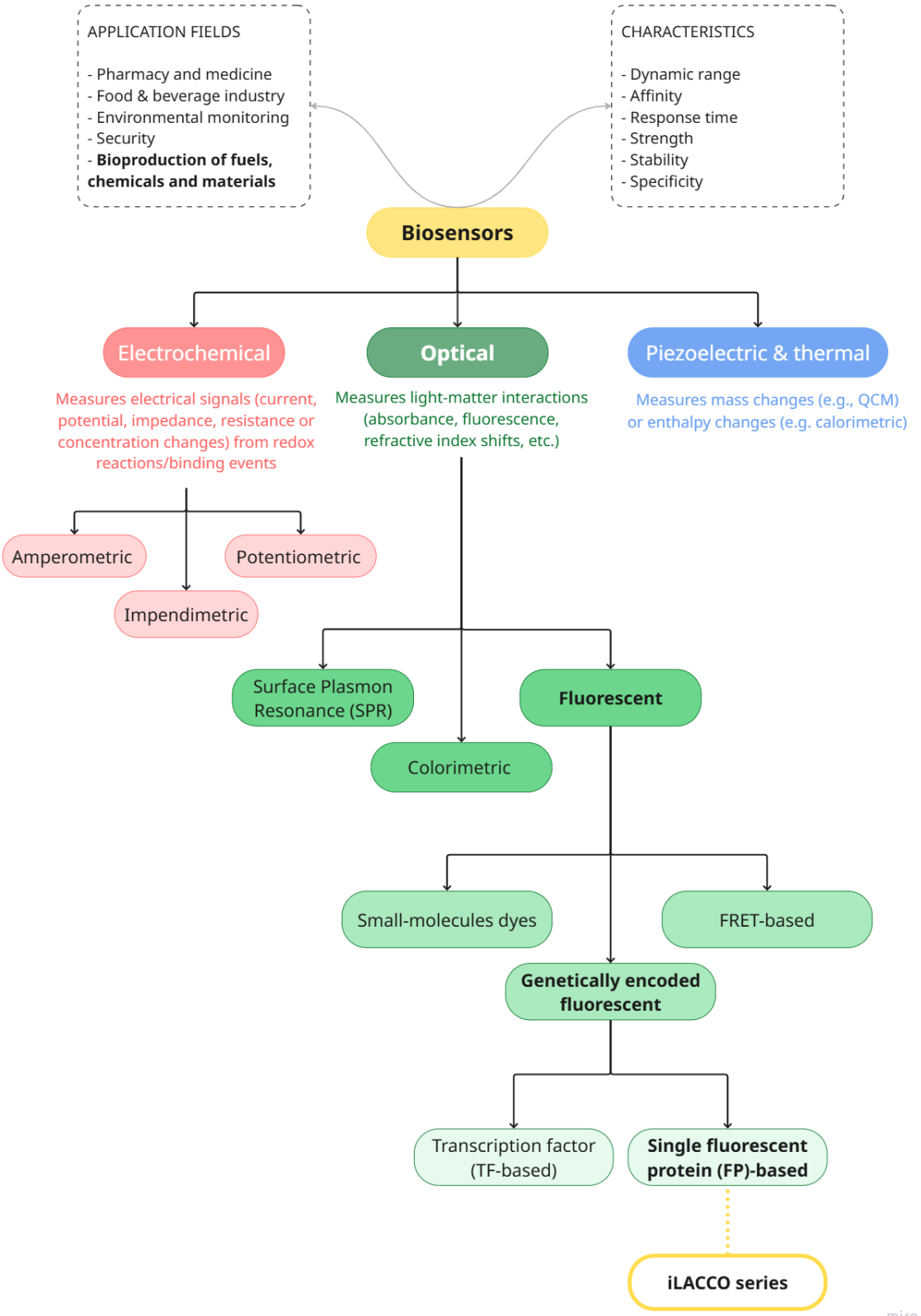

Within genetically encoded fluorescent biosensor, they are two main categories:

- Transcription-factor (TF) based biosensors work by binding of the metabolite to a transcription factor, which activates or represses a promoter controlling expression of reporter, typically a fluorescent protein (Cheng, Tang and Kardashliev, 2018; Ding, Zhou and Deng, 2021a; Li *et al.*, 2022; Tellechea-Luzardo, Stiebritz and Carbonell, 2023)
- Otherwise, the FP is directly attached to a ligand-binding domain. This second type functions through allostery, either through chromophore environment changes, mechanical distortion, oligomerization, or solvent quenching. The iLACCO biosensors used in this thesis project are of the latter type.

As illustrated by afore-mentioned examples, the main advantages of fluorescent biosensors are:

- their sensitivity; even low-abundance analytes (e.g., nitric oxide) can be tracked by single-photon detection (Cook, Walterspiel and Deo, 2023)
- their spatiotemporal resolution; subcellular localization (e.g., mitochondrial Ca^{2+}) can be scrutinized with confocal/multiphoton microscopy.
- their versatility: assays can be conducted *in vitro* - e.g. in microplates - as well as *in vivo* - from tissues to whole-animal imaging.
- their potential for multiplexing: simultaneous detection of multiple targets is possible thanks to spectral unmixing.

The present thesis project leverages all four of these advantages. Playing with the sensitivity (affinity) may assist in detecting larger and larger production levels; the resolution allows to select best single-colonies or even cells for evolution (via manually picking or flow-cytometry), versatility allows controls (e.g. lactate assays, see Materials and Methods) as the method is developed, and multiplexing is crucial in normalising for GFP-biosensor expression level thanks to a co-expressed RFP.

2.2.4.2. Biosensors for intracellular L-lactate

Among single fluorescent-protein (FP) based biosensors, the most impactful have been the GCaMP variants, in which Ca^{2+} binding to a calmodulin domain changes the conformation of the circularly permutated GFP (cpGFP); they revolutionized neuroscience by enabling molecular imaging in vivo (Tian *et al.*, 2009). Other examples include *HyPer*, which senses oxidative stress (H_2O_2) thanks to a redox-sensitive YFP (Kostyuk *et al.*, 2018) and *pHluorin* and *pHuji*, which are pH-dependent FP variants (Germond *et al.*, 2016; Li *et al.*, 2024). Nasu et alia reviewed in depth the structure and mechanism of GCaMP-like systems and inferred best practices for the design of such biosensors (Nasu *et al.*, 2021).

Typically, the sensors consist of one FP fused with linkers to a sensing domain. When this sensing domain binds to the ligand of interest, it induces a conformational change, conveyed to the GFP via the linkers. Examining the structure closely, the FP exhibits a “bulge”, i.e. a protuberance towards the centre of a β-barrel, which allows the chromophore to reside within it (without it, the radius would be slightly too small fit it in the chromophore) (Nasu *et al.*, 2021). This region is in fact where the chromophore is nearest to the β-barrel shell which shields it from the environment. Inserting a sensing domain at this spot widens that gap. The phenol(ate) moiety of the chromophore finds itself exposed. As a consequence, the pKa of the equilibrium between it phenol and phenolate forms shifts. The phenolate form is the brighter fluorescence state, while the phenol form is dimmer. These pKa changes, presumably combined with changing quantum yield and extinction coefficient, explain the fluorescence response. An unfortunate effect of this pKa dependence is that single-FP based biosensors are sensitive to pH changes, which is their major disadvantage.

Furthermore, since the bulge protrudes from the β-barrel so that the chromophore can fit in, it implies that the very regular hydrogen bonding pattern of the β-barrel is disrupted. Coincidently, this allows the bulge region to tolerate insertions or fusions. It is in fact one of the rare location where new termini can be introduced without impeding the ability of the FP to fluoresce. Either the GFP or the

sensing domain can be circularised. In an ideal case, neither is: the termini of the sensing domain are directly linked to the "gateposts residues" framing the bulge region. All in all, both are folded from a single and continuous amino-acid chain. The next step consists in optimizing the linkers. Linkers should be as short as possible - insofar as steric clashes, improper folding or precipitation are avoided - or the conformational change will be attenuated by bond rotations in linker residues. Therefore, initial linkers may be copied from high-performance biosensors, after which each of the amino acids should be deleted to find the minimal linkers, then individual or pairs of residues should be randomized to all possible amino acids, starting from the gate post positions towards the sensing domain. Finally, rounds of directed evolution with random mutagenesis of the entire gene shall give rise to large improvements in response range and folding efficiency.

Nasu and colleagues applied their own published step-by-step guidelines (Nasu *et al.*, 2021) in engineering the iLACCO series (Hario *et al.*, 2024). In terms of arrangement, they fused a cpGFP into the sensing domain, rather than vice versa. In other words, they joined the original termini of the GFP protein, and they linked the gate-post residues (on either side of the bulge) into a loop of an L-lactate binding domain. The GFP was from *Aequorea* and the binding domain from *E. coli* LldR transcriptional regulator protein. The site they chose to connect the two was permissive and conformationally mobile. They used minimal polypeptide linkers, optimising their length and composition as prescribed above. After sequentially randomization to perfect the linkers, eleven rounds of directed evolution on the whole gene led to their final variant, iLACCO1.0. They proceeded with *in vitro* characterization of the photophysical and biochemical properties of the purified biosensor. Its ΔF/F ratio is over 20, absorbance peaks are at 400 and 493 nm, excitation maximum is at 493nm, the emission maximum is at 510nm, the response is negligible for structurally similar molecules and common metabolites, expect for D-lactate, to which it responds with 40x lower affinity than to L-lactate. They followed with *in vivo* characterization of the iLACCO1 variants in mammalian cells, and *ex-vivo* imaging in fly tissue. They could observe intracellular oscillations of L-Lactate levels in mammalian cells starved with glucose. Their findings where consistent with previous studies and models, proving the utility and performance of their biosensors and their development method.

In this thesis work, single protein-based fluorescent biosensors are used, specifically the iLACCO series, tailored to sensing intracellular L-lactate. Dr. Nasu and colleagues have developed iLACCO variants with different affinities (listed under Materials) to accommodate concentrations in different cell types and physiological conditions. As discussed in this section, the rational and modular design of these biosensors was very systematic, and therefore reproducible for other target products. In consequence, establishing a bioproduction platform using these sensors would provide a generalizable strategy for other metabolites/targets. This is the central ambition of this thesis.

2.2.5. Use of biosensors in biomanufacturing

Biosensors have revolutionized screening in metabolic engineering. Conventional screening techniques such as HPLC, GC-MS or capillary electrophoresis impede throughput by their complexity, time-consuming procedures, requirement of high-end instruments, and operational capabilities (Vigneshvar *et al.*, 2016). These complications makes the "test" step a bottleneck in the Design Build-Test-Learn cycle of synthetic biology (Rogers and Church, 2016; Rogers, Taylor and Church, 2016). By contrast, biosensors offer a growth-independent, intracellular readout of product titres, enabling the rapid screening of mutant libraries, for example thanks to automated systems like fluorescence-activated cell sorting (FACS) (Pham *et al.*, 2022). iLACCO biosensors hold the promise of plate-based replating of "brightest" colonies to enrich high producers, bypassing even the need for FACS.

Henceforth, iLACCO-like will refer to sensors relying on engineered ligand-binding domains fused to a (circularly permuted or native) fluorescent scaffold, where metabolite binding directly alters fluorescence signal. FRET and TF-based biosensors have been described under Fluorescent biosensors. There is a clear disparity in how different classes of biosensors have been deployed in ALE for strain improvement. TF-based biosensors have been used extensively, while FRET-based biosensors have been

scarcely applied, and iLACCO-like biosensors virtually never. Indeed, several studies underscore the potential of iLACCO-like biosensors for applications in adaptive laboratory evolution (ALE) and high-throughput strain optimization (Ibraheem and Campbell, 2010; Tamura and Hamachi, 2014; Della Corte *et al.*, 2020; Kim *et al.*, 2021; Liang *et al.*, 2022; Chai *et al.*, 2023), yet their actual deployment in such contexts remains largely unrealized. The current gap between biosensor development and application thus represents an untapped frontier in metabolic engineering.

Now elucidating why TF-based biosensors are used much more than iLACCO-like biosensors in E. coli strain improvement and ALE pipelines, it is not only because they have been used since the 1970s whereas iLACCO-like biosensors are just emerging in the field. TF-biosensors do benefit from historical inertia and tool availability: there are dozens of TF biosensors available in toolkits like SEVA, Addgene, and SynBioHub (Tellechea-Luzardo, Stiebritz and Carbonell, 2023), meanwhile fewer cpGFP-based sensors are openly-accessible, validated in E. coli, and so easily tuneable or customizable. Indeed, another advantage of TF-based based biosensor is their ease of implementation: they are built from a known TF, a promoter responsive to that TF, and a reporter (FP). iLACCO-like biosensors require engineering the fusion between a ligand-binding domain and a FP, as disclosed in the Biosensors for intracellular L-lactate section. In brief, TFs are "plug-and-play" (modular, robust, and low-burden), while cpFPs are protein engineering projects. Moreover, the TF-based architecture implies that the fluorescent output is transcriptionally amplified — often resulting in 100× to 1000× signal change. In contrast, iLACCO-like biosensors yield modest changes (1.5–5× fluorescence), which can be drowned out by noise in high-throughput or noisy evolutionary conditions (Li, Zhang and Ai, 2021). In addition, TF systems are genetically more stable over generations. By contrast, iLACCO-like sensors rely on precise protein folding and chromophore orientation, which can be easily disrupted by spontaneous mutations in long-term cultures (witnessed in Results). Finally, it is worth highlighting that in a number of schemes, the TF-based sensors have been wired to survival genes (antibiotic resistance, toxin-antitoxin systems, auxotrophy complementation) so as to couple growth and selection, which is ideal for adaptive laboratory evolution (ALE) (LaCroix, Palsson and Feist, 2017; Ding, Zhou and Deng, 2021b; Tellechea-Luzardo, Stiebritz and Carbonell, 2023). iLACCO-like sensors only report the state of the metabolite and need external mechanisms (e.g. colony picking on plate or FACS) for selection.

For all the reasons outlined above, TF-based biosensors remain the most practical and field-tested option for strain evolution, especially when using automated, fitness-linked or FACS selection (Zhang *et al.*, 2022). Nonetheless, iLACCO-like biosensors may be best suited for flux tracking and library screening. First, they offer a real-time, reversible readout; the signal is instantaneous, non-integrated fluorescence changes, which is optimal for monitoring dynamic metabolic flux, oscillations, or temporally responsive systems (Li, Zhang and Ai, 2021; Hario *et al.*, 2024). Second, iLACCO-like sensors provide a graded output, unlike many TF circuits result in a binary (on/off) signal because of TF saturation and promoter threshold effects. This is paramount for high-resolution sorting of enzyme libraries — for example, distinguishing enzyme variants that yield 10% vs. 30% more product (Koberstein *et al.*, 2021). Finally, iLACCO-like biosensors do not perturb host circuits or interfere with host regulation like TF-based systems do. This is particularly helpful during library screening of fragile or tightly controlled genetic backgrounds, especially in synthetic or minimized hosts (Eason *et al.*, 2020). All in all, iLACCO-like sensors are best suited for fine-grained discrimination in analysing, ranking, and optimizing variants in screening workflows.

In iteration with strain screening, FP-based biosensors in ALE are used for metabolic discovery, which in turn can inform rational design. They can uncover unknown pathway regulations or reveal connections between metabolites and regulatory systems. For example, biosensors for small-molecule effectors have been used to probe metabolite transport, compartmentalization, and redox status, offering insights that point to relevant mutation targets (Li *et al.*, 2020; Li, Chen and Huo, 2024). In other words, biosensors bypass the limitations of purely rational design by forcing evolution toward metabolite overproduction, and in so doing uncover unsuspected genes involved. The resulting genotypes frequently harbour mutations that downregulate competing pathways, enhance global

regulatory efficiency, and balance carbon flux between growth and production (Ding, Zhou and Deng, 2021b; Seok *et al.*, 2021; Jiang *et al.*, 2023; Mao *et al.*, 2023). Beyond strain screening, biosensors have found applications in real-time bioprocess control. Fluorescent biosensors can be multiplexed (compiling spectrally distinct reporters) to monitor several metabolites simultaneously, providing detailed insights into cell physiology during fermentation (Zhang *et al.*, 2023). Such capabilities are especially valuable in dynamic environments where nutrient availability or by-product accumulation can compromise productivity.

In conclusion, metabolite-responsive biosensors can guide the selection of superior strains in adaptive laboratory evolution (ALE). They do however serve other (compatible) purposes in cell factory development, such as knowledge expansion for rational design, or dynamic pathway control. TF-based fluorescent biosensors have so far been far more widely used than iLACCO-like sensors in strain engineering and ALE workflows—and on valid grounds. However, iLACCO-like biosensors exhibit a set of complementary strengths, for instance allowing colony screening on plates. In developing an evolution platform based on them, this project does not aim to replicate or compete with TF-based platforms, but to enable different modes of selection and monitoring. Due to the recent emergence of (cp)FP biosensors and their limited application in bioproduction contexts (as opposed to physiological sensing), there is currently no standard workflow or widely adopted framework for their use. This thesis aims to establish such a methodological approach —one that would be replicable and generalizable to other structurally similar biosensors and metabolite targets.

3. OBJECTIVES

The overarching objective of this research is to develop a biosensor-guided evolution platform for the engineering of synthetic methylotrophic *Escherichia coli* strains toward efficient L-lactate bioproduction. This entails establishing and integrating three essential modules: methanol assimilation, L-lactate biosynthesis, and real-time intracellular lactate detection, ultimately enabling adaptive laboratory evolution (ALE) strategies guided by metabolite-responsive biosensors.

This goal is broken down into the following specific objectives, schematized in Figure 4:

1. To enhance growth performance of synthetic methylotrophic *E. coli* strains in industrially relevant minimal media (M9) via Adaptative Laboratory Evolution (ALE).

2. To engineer *E. coli* for enantiopure L-lactate production, via chromosomal modifications via CRISPR-Cas9 or Lambda-Red systems.

3. To incorporate genetically encoded fluorescent biosensors specific for L-lactate into the engineered *E. coli* strains and ensure their performance *in vivo*.

4. To apply biosensor-guided adaptive laboratory evolution to simultaneously optimize growth and production phenotypes.

5. To establish a modular and generalizable workflow for biosensor-assisted strain development.

While methanol and L-lactate serve as a proof-of-concept pair, the platform is designed to be applicable to other (C1) substrates and value-added products. The long-term vision is to contribute a reusable methodology to the synthetic biology toolbox for circular bioeconomy applications.

Figure 4: High-level diagram of the experimental goals

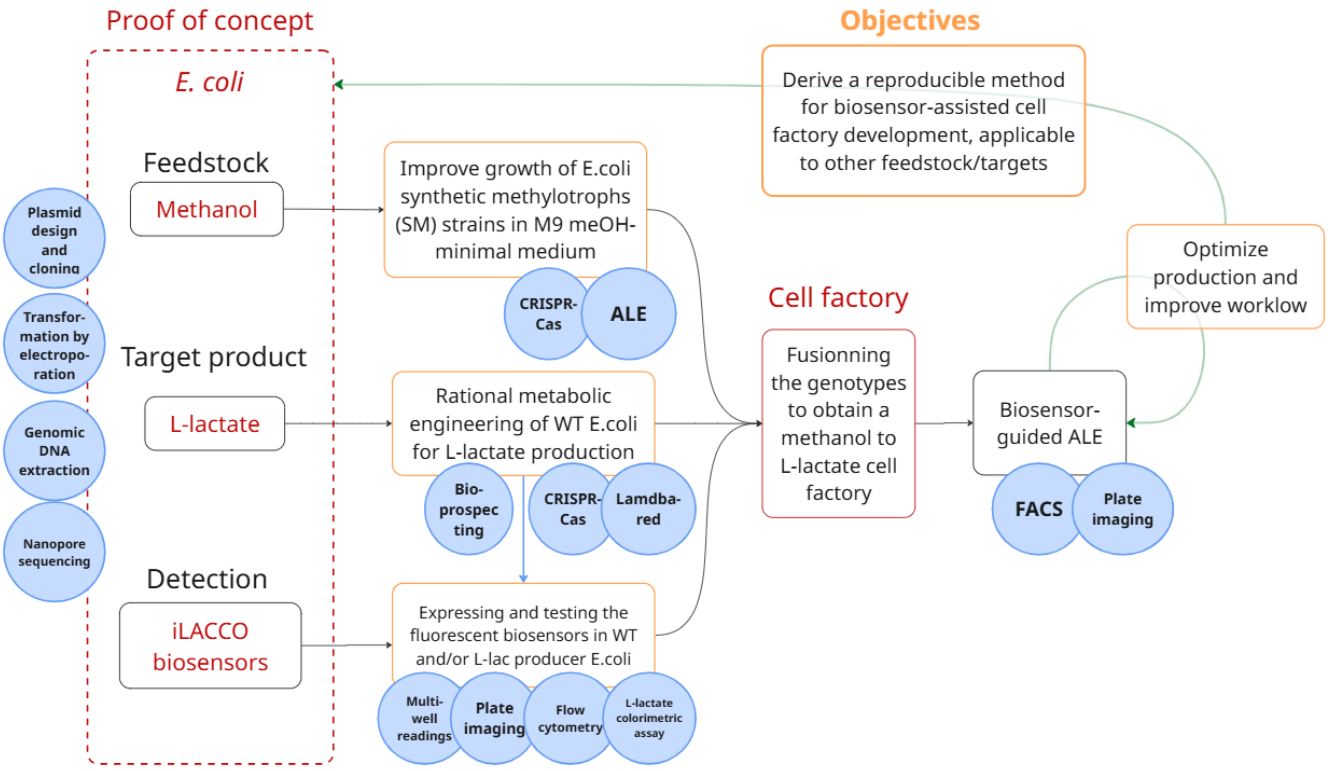

4. MATERIALS AND METHODS

4.1. RATIONAL GENETIC ENGINEERING

4.1.1. Plasmid and strains construction

Escherichia coli K-12 BW25113 was used as the model organism throughout this study. Details can be found in Annex 2 Table 1. The strains employed were:

Wild-type (WT): a Keio collection derivative originally lacking dosP, which was restored meanwhile the Kan^R cassette was excised, leaving it without resistance marker.

Δpta mutant: another Keio collection strain (Baba *et al.*, 2006), deficient in *pta*, the gene encoding phosphate acetyltransferase. The Δpta strain was used in parallel with the WT strain during genome editing to increase the likelihood of successful integration events. This particular deletion was selected to redirect pyruvate flux away from the acetate pathway and toward lactate production (see Figure 2), bearing in mind the intended future use in synthetic methylotrophic strains, known to secrete high levels of acetate (Nieh *et al.*, 2024).

Synthetic methylotrophic strains SM1, SM7 and SM8: genotypic and phenotypic descriptions have been provided in Section 2.2.3. (Chen *et al.*, 2020; Nieh *et al.*, 2024).

DH5α: Wild-type used for plasmid construction (Hanahan, Jessee and Bloom, 1995), provided as competent cells (ECOS) which can be transformed by heat shock.

Unless otherwise specified, cells were grown in 3 mL polypropylene tubes with sealed caps at 37 °C and 250 rpm using a New Brunswick Scientific Innova 44 shaker. Luria-Bertani (LB) medium (Becton Dickinson) was used for general cloning and as the standard rich medium. When required, antibiotics were added at the following final concentrations: carbenicillin (100 mg/L), kanamycin (30 mg/L), chloramphenicol (50 mg/L), and spectinomycin (250 mg/L).

For plasmid construction, all PCR amplifications were carried out using KOD One® polymerase (TOYOBO). PCR products were verified by agarose gel electrophoresis and purified using either the NucleoSpin™ Gel and PCR Clean-up Kit (Macherey-Nagel), MagPure PCR Clean-up Beads, or EasyMag Gel DNA Extraction Kit (ABP Biosciences). Amplified fragments were treated with DpnI (New England Biolabs) to remove template DNA prior to assembly. Plasmids were assembled by Gibson cloning using NEBuilder® HiFi DNA Assembly Master Mix (NEB). In one instance, QuikChange Lightning Multi Site-Directed Mutagenesis Kit (Agilent) was employed, followed by ligation.

Constructed plasmids were transformed into *E. coli* DH5α (NEB) for propagation. Cultures were grown in LB or Terrific Broth (TB) supplemented with the appropriate antibiotics. Plasmid DNA was isolated using the QIAprep Spin Miniprep Kit (Qiagen). Genomic DNA was extracted using the Taco™ mini magnetic bead system (GeneReach, Taiwan). DNA concentrations were quantified with a Qubit fluorometer (Thermo Fisher Scientific). Sequencing of PCR products and genomic DNA was performed via Nanopore sequencing, and all variant calling and annotation were conducted using Geneious Prime software.

DNA transformations were performed by electroporation. 1 mL of overnight culture was harvested, chilled, centrifuged and washed twice with ice-cold 10% glycerol, then resuspended in 100µL of the same solution and transferred to an ice-cold electroporation cuvette. DNA (50–100 ng) was added, and cells were electroporated at 1.8 kV. Recovery was performed in non-selective medium for 1–3 hours before plating on LB agar with appropriate antibiotics.

4.1.2. Techniques for gene editing

This study employed two complementary genome editing strategies for the rational engineering of *Escherichia coli* strains: CRISPR-Cas-mediated editing and λ-Red recombineering. Both techniques enable chromosomal modifications at precise loci and are implemented using plasmid-based systems. The main difference between the two approaches in practice lies in that CRISPR-Cas permits iterative editing without accumulating antibiotic resistance cassettes, whereas λ-Red requires a new antibiotic marker for each genomic insertion.

4.1.2.1. CRIPSR-Cas system

The CRISPR-Cas9 method utilizes a two-plasmid system adapted from (Shukal *et al.*, 2022; Chai *et al.*, 2024). One plasmid – pCas (Kan^R or $Carb^R$) - encodes the Cas9 endonuclease. The second plasmid – pTarget ($Spec^R$) - carries both the guide RNA (gRNA) for site-specific cleavage and a donor DNA template with homology repair the intended genetic insert in between homology regions (500bp each). The pCas plasmid remains in the strain while different pTargets can be transformed in and cured out in turn to perform a series of edits, at the end of which the pCas plasmid is also cured.

The procedure starts with the *E. coli* host strain transformed with pCas and cultivated at 30 °C to maintain plasmid stability (pCas bears a temperature-sensitive origin of replication). To induce expression of the CRISPR-Cas9 machinery, the strains is reinoculated at an initial OD of 0.2 and grown in LB with 100mM arabinose. Once the strain reaches OD 0.8-1.2, the pTarget plasmid is introduced by electroporation (procedure described below). The cells are allowed to recover for 1h in LB before being plated on LB-agar containing Carb (for pCas), Spec (for pTarget), arabinose (for continued induction), other markers that the strain harbours, and 400mM methanol for SM strains. Genome editing events are confirmed via PCR with primers on the chromosome on either side, or one on the insert and the other on the chromosome. Following successful integration, the pTarget plasmid is removed via IPTG-induced plasmid curing. This enabled subsequent transformations with new pTarget variants for additional modifications. Once all desired edits are completed, pCas is eliminated by culturing at 42 °C, exploiting its temperature-sensitive replication.

4.1.2.2. λ-Red Recombineering

λ-Red recombineering relies on homologous recombination between linear DNA fragments and the host chromosome, mediated by the Red recombinase system (Exo, Beta, Gam) (Datsenko and Wanner, 2000) . The procedure is very similar to the CRISPR-Cas system, except that a linear PCR product is transformed in rather *in lieu of* a pTarget plasmid. The workflow could start as above with the host strain containing the pCas plasmid. Indeed, the pCas used encodes both the Cas protein and the λ-Red components, giving the flexibility to toggle between the CRISPR and recombineering protocols using the same host strain.

DNA templates are constructed using overlap extension PCR (OE-PCR). Each template consists of: (i) a 25-100 bp upstream homology arm, (ii) the gene of interest, (iii) an antibiotic resistance cassette flanked by FLP recombinase target (FRT) “flip” sites, and (iv) a downstream homology arm. The final PCR products are purified and introduced into the pCas-bearing host through electroporation after arabinose induction, as described above. The recovery tie is typically longer (3-4 hours) before plating on appropriate antibiotic media. Integration was confirmed via diagnostic PCR. Once all genetic insertions are complete, a helper plasmid (pCP20) encoding the FLP recombinase is introduced in order to excise the resistance markers, leaving a single FRT site ("scar"). pCP20 is finally removed by cultivation at 42 °C.

4.1.2.3. DNA constructs

All plasmids and their functions are summarized in Table 2, Annex 2.

The first set of constructs was designed and built to improve the growth of *E. coli* SM strains in M9 methanol minimal medium, in line with Objective 1. Two disrupted genes identified in Section 2.1.3 were to be restored prior to initiating adaptive laboratory evolution (ALE):

- *recA*, plays an important role in homologous recombination and DNA repair and is essential for the ddp-BAC system to function (Nieh *et al.*, 2024), was interrupted by an insertion sequence (IS). Two CRISPR-Cas strategies were employed for restoration: excision of the IS element using **pAGT1** as the pTarget plasmid, or insertion of a full-length *recA* coding sequence at the SS9 locus using **pAGT2**. SS9 is a chromosomally neutral integration "safe harbor" characterized for stable gene insertion (Zheng *et al.*, 2025).

- *rpiA*, absent in the strain prior to auxotrophy engineering and later reintroduced on a plasmid (see Figure 1), was targeted for chromosomal reintegration to alleviate metabolic burden and recover an antibiotic marker. **pAGT3** is a pTarget designed to integrate a full-length *rpiA* coding sequence at the *maeA* locus.

The second set of constructs was designed and built to integrate recombinant L-Lactate in *E. coli*, ideally substituting the native D-Lactate Dehydrogenase, in line with Objective 2. To enable *E. coli* to produce L-lactate *in lieu* of D-lactate, the native *ldhA* gene had to be replaced with a recombinant L-lactate dehydrogenase (*L-Ldh*).

On grounds laid in Section 2.2.2.2, three candidates enzymes were bioprospected from heterologous expression: from *Bacillus coagulans*, *Streptococcus bovis*, and *Lactobacillus casei*. Coding sequences were sourced from NCBI and Uniprot databases and guided by primer designs from previous studies (see Table 1). All sequences were codon-optimized for *E. coli*, and ribosome binding sites (RBS) were designed using an RBS Calculator (Halper, Hossain and Salis, 2020) to achieve a target translation initiation rate of 100,000 arbitrary units. Synthesized RBS-ORF constructs were ordered from Integrated DNA Technologies (IDT) with flanking overhangs for Gibson cloning. Upon delivery, constructs were cloned into a pW87 backbone under the control of a *pLlacO1* promoter and a T1 terminator, yielding plasmids **pLY708, pLY709**, and **pLY710**. For **genome** editing, corresponding pTarget plasmids - **pAGT5, pAGT6, pAGT7** - were constructed to integrate each *L-ldh* at the chromosomal *ldhA* locus. These pTargets were further used to generate λ-Red templates serving the same purpose, incorporating a spectinomycin resistance cassette (SpecR): **LR5, LR6, LR7**. An outline of the afore-mentioned steps is shown in Table 2.

Table 2: DNA constructs to integrate a recombinant L-lactate dehydrogenase, either on plasmid or in the genome *in lieu* of native D-lactate dehydrogenase.

Source organism	Plasmid (Amp^R) to integrate the L-ldh extra-chromosomally	pTarget ($Spec^R$) for CRIPSR-Cas editing	Linear template ($Spec^R$) for λ-red edition
B. coagulans	pLY708	pAGT5	LR5
S. bovis	pLY709	pAGT6	LR6
L. casei	pLY710	pAGT7	LR7

The third set of constructs was designed and built to integrate the iLACCO biosensors in *E. coli*, ideally substituting the native D-Lactate Dehydrogenase, in line with Objectives 2 and 3. To avoid L-lac (re)-consumption, the lld gene had to be eliminated and the iLACCO biosensors had to be integrated. Like for ldhA and heterologous L-ldh, this knock out and knock in were attempted together. Three variants from the iLACCO series were provided by Dr. Nasu (Institute of Biological Chemistry, Academia Sinica, Taipei):

- iLACCO1.9 (high affinity, Kd = 14 µM)
- iLACCO1.9b (low affinity, Kd = 2.0 mM)
- and diLACCO1.9 (a non-responsive "dead" sensor which mimics the pH-dependence of the other two in both states; it serves as control to discriminate between a genuine response from a pH-induced artifact).

The plasmids on which the iLACCO proteins were provided were tailored for mammalian expression. So the first step was to subclone them into *E. coli*-compatible backbones under a constitutive prokaryotic promoter, featuring a custom ribosome binding site (RBS) each, a *Spec*^{R} marker, and a ColE1 origin of replication, yielding plasmids **pNasu9, pNasu9b, and pNasudi**. To integrate biosensors into the chromosome *lld* locus, corresponding pTargets **pAGT8, pAGT9, and pAGT10** were built.

To normalize for expression variability, *mCherry* , an RFP, was co-expressed along the cpGFP-based iLACCO sensors. Two combination strategies were attempted: fusion via a flexible (GGTGGS) linker, and bicistronic expression via the mCherry's RBS inserted downstream of the biosensor's stop codon. Given the foreseeable saturation of iLACCO1.9 (high affinity) at higher lactate titres, focus shifted to iLACCO1.9b and diLACCO1.9. Therefore, four λ-Red templates with chloramphenicol resistance (CM^R) were generated to integrate the double-fluorescence constructs into the genome: **LR9-linker, LR9-RBS, LR10-linker, LR10-RBS**. These GFP-RFP sequences were also integrated onto a plasmid, **pAGT11**, to obtain preliminary results. An overview of these constructs is provided in Table 3. Moreover, a separate knockout-only pTarget (**pAGT4**) was constructed to delete *lld* without biosensor integration, serving as a negative control.

Table 3: DNA constructs to integrate intracellular L-lactate biosensors, either on plasmid or in the genome, *in lieu of* native fermentative L-lactate dehydrogenase.

cpGFP-based L-lactate biosensors	Received from Dr. Nasu	Plasmids (Spec^R)	pTarget (Spec^R) for CRIPSR-Cas	Linear λ-red template with mCherry (CM^R)	Plasmid with mCherry (CM^R)
High affinity iLACCO1.9	pcDNA-iLACCO 1.9	pNasu9	pAGT8	-	
Low affinity iLACCO1.9b	pcDNA-iLACCO 1.9b	pNasu9b	pAGT9	LR9-linker LR9-RBS	pAGT11_LR9-linker pAGT11_LR9-RBS
pH-responsive (+) ctrl biosensor diLACCO	pcDNA-diLACCO 1.9	pNasudi	pAGT10	LR10-linker LR10-RBS	pAGT11_LR10-linker pAGT11_LR10-RBS

It is important to emphasize that the design and assembly of the DNA constructs detailed above accounted for the majority of the experimental effort during this study, spanning approximately four out of the five months of the research period before thesis submission. The plasmids, pTargets and λ-red templates were successfully constructed, purified and verified, which represents a considerable outcome in its own right. Regrettably, after transformation(s), effective genome editing using these constructs faced substantial technical challenges (see Discussion)— ultimately limiting the progression through even a single complete pTarget iteration. Although not further discussed in the Results section, these efforts in foundational molecular biology formed the backbone of the project and reflect the primary investment of time and resources throughout the internship.

4.2. ADAPTIVE LABORATORY EVOLUTION (ALE)

In the context of this study, ALE was performed as part of Objective 1, which aimed to improve the growth of synthetic methylotrophic *E. coli* strains in M9 methanol-minimal medium. Initially, strains SM7 and SM8 were selected for parallel evolution. SM7 and SM8 differ in genomic stability: SM7 carries a *mutS* deletion (hypermutator phenotype), whereas SM8 is has been stabilised (*mutS* restored) (see Figure 1). While both strains were intended to undergo pre-ALE genome restoration of disrupted genes (detailed in Section 4.1.2.3.), these edits could not be successfully completed. As a result, ALE was instead initiated using SM1, a precursor strain from the same lineage with recA undisrupted (described in the same section and visible in Figure 1). SM1 preceded the transformation of the ddp-BAC system, which is proved essential to supports continuous evolutionary adaptation, therefore it was introduced in the strain. SM1 with ddp-BAC and without ddp-BAC were evolved in parallel, in MOPS and in M9 methanol-minimal medium. The precise composition of these media can be found in Annex 3.

ALE experiments were performed in triplicate using an RTS-8 Plus bioreactor system (Biosan), which provides automated shaking and in-line optical density monitoring. Cultures were maintained in 25 mL volumes in 50 mL membrane-capped polypropylene tubes, at 37 °C and 2700 rpm agitation, reverse spin every second. OD_{600} was logged every 10 minutes. Each passage corresponded to one liquid transfer cycle, typically conducted at the end of the exponential growth phase to avoid DPC. Cultures were reinoculated at an initial OD_{600} of around 0.2. Under this setup, each passage represents approximately 3–4 generations of growth.

4.3. BIOSENSOR SIGNAL DETECTION AND VERIFICATION

4.3.1. Microplate-Based Fluorescence and Absorbance Measurements

Fluorescence, absorbance, and optical density (OD) measurements of liquid cultures were performed using a Synergy H1 Hybrid Multi-Mode Microplate Reader (BioTek Instruments). Cultures were loaded into black (fluorescence) or clear (absorbance) 96-well plates. OD600 was recorded to monitor cell growth. Fluorescence was measured at the wavelength specified in the fluorescent protein characterization, e.g. Hario et al. (2024) for the iLACCO series. Data acquisition and visualisation were conducted using Gen5™ software and Microsoft Excel.

4.3.2. Fluorescence Imaging of Colonies on Agar Plates

Fluorescent colony imaging was performed using a UVP ChemStudio Plus system (Analytik Jena) equipped with VisionWorks® software. Colonies grown on agar plates were imaged using the “Colony Count” mode. For each plate, two images were acquired (5 ms exposure time for each): on the one hand, a standard white light image, on the other hand, a fluorescence image using the FITC channel (excitation/emission ~488/520 nm). The two images were subsequently merged to visualize spatial fluorescence intensity across colonies. It is important to note that this imaging setup provides relative fluorescence intensity rather than absolute quantification (commented on in Discussion).

4.3.3. Flow cytometry

Flow cytometric analysis was carried out using a CytoFLEX S flow cytometer (Beckman Coulter), equipped with a 488 nm blue laser operating at 51 mW output. Both forward scatter (FSC) and side scatter (SSC) were recorded to assess cell size and granularity, respectively. Fluorescence signals were simultaneously detected through the appropriate emission filters. Bacterial samples were prepared by diluting cultures in sterile, autoclaved 1× phosphate-buffered saline (PBS) and adjusted to a final concentration of approximately 1.5×10^6 cells/mL. Data acquisition was performed at a rate exceeding 1000 events per second (corresponding to an approximate sample flow rate of 30 µL/s), maintaining an abort rate below 10%. Fluorescence distribution histograms and quantitative analyses were performed using FCS Express 7 software (De Novo Software).

4.3.4. L-lactate quantification

Lactate concentrations were determined using a commercial Lactate Assay Kit (MAK064, Sigma-Aldrich), following the manufacturer's protocol. This enzymatic assay quantifies L(+)-Lactate and results in an endpoint colorimetric (570 nm) output. For extracellular lactate analysis, culture supernatants were clarified by centrifugation at 12000 rpm for 5min and deproteinized using 10 kDa molecular weight cut-off (MWCO) spin filters. For intracellular lactate measurements, cells were lysed using BugBuster Master Mix (Merck). Lysates were centrifuged, and the supernatant was processed directly. A standard curve (0–10 nmol/well) was prepared for each assay, and sample concentrations were interpolated from the standard curve. Samples were diluted as necessary to fall within the linear detection range.

5. Results and Discussion

5.1. Experiment(s) for Objective 1: Growth improvement of SM strains in M9 medium

5.1.1. ALE of SM7 and SM8

5.1.1.1. Presentation and discussion of successive generations

While CRISPR-Cas–based restoration of the *recA* gene was underway, preliminary ALE experiments were conducted using the unmodified SM7 and SM8 strains to serve as negative controls. ALE was performed over approximately 6-7 generations in parallel under two conditions M9 methanol minimal medium, with MOPS methanol minimal medium as control (quantitative in Table 1, Annex 5). In brief, no improvement in growth rate was observed under either condition.

Figure 5: ALE of SM7 (above) and SM8 (below) in M9 methanol minimal medium, with MOPS methanol minimal medium as control.

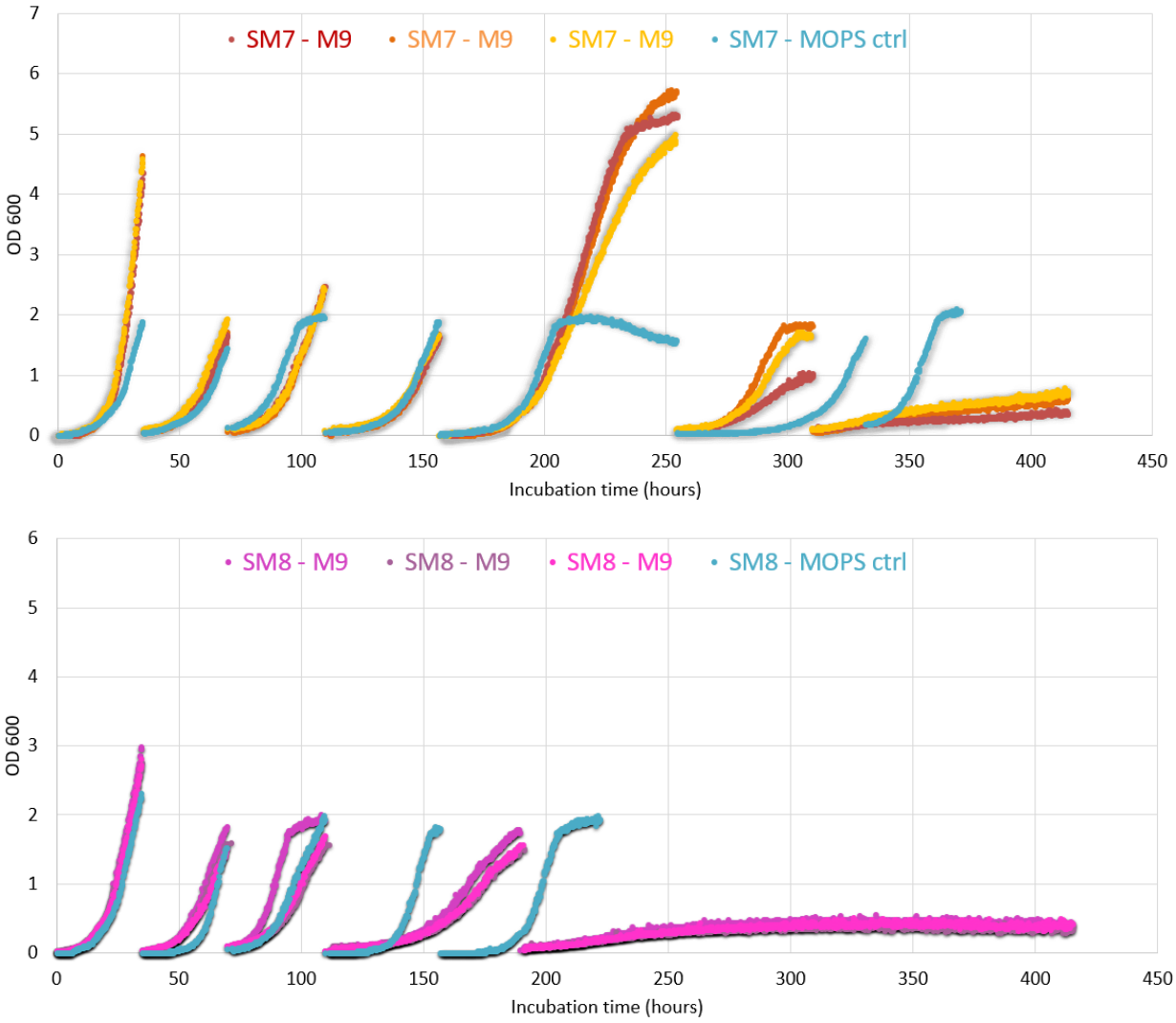

During the first passage (P1) of ALE, both SM7 and SM8 strains exhibited robust growth in M9, likely supported by residual nutrients from the LB pre-culture. However, from the third passage (P3) onward, both strains began to show prolonged lag phases. SM8 exhibited a more pronounced decline in

performance. Between P3 and P4, SM8's growth rate dropped substantially, and by P5, it ceased to grow altogether in M9 medium, though it continued to proliferate in MOPS medium. SM7, in contrast, could still reach high optical densities (OD_{600} of 5–6) at P5. However, at P5 the cultures were let to approach stationary phase, and subsequent passages began to show deteriorating growth. By the seventh passage, SM7 had also ceased to grow in M9, though it continued to grow steadily in MOPS throughout all passages. It is worth noticing that when the MOPS control for SM7 was subjected to an extended stationary phase (P5), the following passage exhibited a pronounced lag phase —an observation consistent with prior work by Nieh et al. (2024), who observed that stationary phase persistence worsened DPC and delayed recovery.

Both SM7 and SM8 are visibly less viable in M9-based methanol medium than in in MOPS-based methanol medium. A hypothesis is that this gradual decline in growth performance for both strains is due to the lack of recA and therefore of a functional ddp-BAC adaptative system. This system allows to alleviate DNA–protein crosslinks (DPCs) arising during methanol metabolism. Its absence limits the cell's capacity to tolerate methanol-induced DNA damage, reducing the effectiveness of ALE by hindering the accumulation of beneficial mutations. Although SM7 was previously reported to have accumulated compensatory mutations that partially mitigate the need for recA in MOPS medium, full recA function remains advantageous for evolving the strains for fast growth in M9 medium.

As a next step, a new ALE experiment was initiated using SM1, a precursor strain from the same lineage with recA intact. SM1 preceded the transformation of the ddp-BAC system (see Figure 1), which proved essential to supports continuous evolutionary adaptation, therefore it was introduced in the strain. SM1 with ddp-BAC and without ddpBAC were evolved in parallel, in MOPS and in M9 methanol-minimal medium. Too few passages have elapsed to report definitive results yet, but there are already promising trends. SM1 demonstrates markedly improved growth with ddp-BAC than without, and in M9 than in MOPS. The fact that M9 medium appears more favourable than in MOPS, paving the way toward engineering a strain with industrial relevance. In all likelihoods, the evolutionary trajectory of SM1 optimisation in M9 will differ from the progression of SM1 to SM7 (optimisation in MOPS). Comparative genomic analysis of these lineages will provide valuable insights into environment-specific adaptive mechanisms.

5.1.1.2. Challenges with CRIPSR-Cas editing

Although the CRISPR-Cas9 system has been successfully implemented in *E. coli* BW25113 (and other Keio-derived strains) , multiple attempts at genomic editing using this method failed in restoring recA. One plausible explanation is the persistence of Cas9 expression after recombination, which can lead to re-cutting of the genome. Such double-strand breaks (DSBs) are lethal if not rapidly repaired, resulting in the loss of edited cells. This resonates with some observations: in some cases, genome editing appeared successful initially, evidenced by mixed colonies with partial edits (two bands on gel). But after restreaking, no edited cells could be recovered. Perhaps unprotected edited genomes were repeatedly cleaved, ultimately eliminating the desired variants from the population.

Additionally, suboptimal design of either the gRNA or the homology arms of the repair template can sharply reduce editing efficiency (Shukal *et al.*, 2022; Chai *et al.*, 2024). In Keio strains, local sequence variations or the presence of FRT scars may respectively complicate gRNA binding and alter local chromatin structure, thereby reducing editing efficiency (Swings *et al.*, 2018). Moreover, multicomponent systems (like the two-plasmid pCas + pTarget setup used here) may suffer from plasmid instability, leaky expression, or induction imprecision—especially under selective pressure. These factors collectively create a stressful cellular environment. SM7 and SM8 are already genetically burdened, CRISPR-Cas9 introduces double-strand DNA breaks (DSBs), activates DNA repair mechanisms, and adds plasmid-related metabolic load (Cas9 and gRNA expression, selection markers which further stresses the cells. Electroporating such stressed cells with more plasmids or donor DNA can reduce their survival, since their repair, replication, and metabolic machinery are already heavily taxed. One way to

move forward is to restore recA function in SM7n strain using CRISPR or lambda-Red, SM7n lacks ddp-BAC therefore suffers less metabolic burden, and then re-transform ddp-BAC in; this is in progress.

5.1.1.3. Comments on M9 and MOPS methanol minimal media

One of the primary objectives of this ALE experiment was to adapt the synthetic methylotrophic strains SM7 and SM8—originally optimized for growth in MOPS minimal medium—to grow more efficiently in M9 methanol-minimal medium (see Objectives). M9 minimal medium is preferred to MOPS due to its lower cost and widespread adoption in industrial microbial cultivation. As evidenced by the growth curves (see Figure 5), both strains consistently exhibited more sustainable growth in MOPS compared to M9.

An avenue forward lies in optimizing the composition of the M9-based growth medium. In that regard, the series of papers by Zhou et al. on production of D-lactic acid is particularly informative. In 2003, they constructed an *E. coli* W3110 derivative capable of producing optically pure D-lactic acid in mineral salts medium (Zhou *et al.*, 2003). By 2005, they achieved the complete fermentation of 10% (w/v) glucose to D-lactate. (Zhou *et al.*, 2005). In 2006, they reported a production titer of 1.2 M D-lactate from 12% glucose using mineral salts medium (Zhou *et al.*, 2006b). The successive papers investigate the effects of different media (complex vs. mineral salts), additives, and environmental conditions (e.g. pH, aeration) on cell growth, productivity, and lactate yield, aiming to reduce costs and improve the economic viability of bioproduction.

Initially engineered *E. coli* K12-based strains for lactate production were unable to ferment 10% (w/v) glucose completely neither in minimal nor in complex rich medium. The authors turned to *E. coli* B-based strains derived from an ethanologenic *E. coli* KO11 which they had developed. They eliminated the *Z. mobilis* genes (*pdc* and *adhB*) which they had heterologously expressed for pyruvate conversion to and the strain was virtually similar to the K12 strains. The key difference remained that B-strains are natively able to ferment sucrose, which is an advantage for culture in high sugar concentrations. D-lactic acid production. SZ132 rapidly fermented 10% (w/v) sugars to completion, albeit LB was still required.

They investigated the barriers causing the poor bioproduction performance in mineral salts medium with glucose and found that osmotic stress from both the substrate and product limited productivity in mineral salts medium. They added betaine (1 mM), a protective osmolyte, in the medium: the yield doubled, volumetric productivity tripled, and enantiospecificity and glycolytic flux improved by 50%, exceeding that in Luria broth. However, betaine increase the levels of succinate and acetate (unwanted co-products). To solve this issue, the authors drew inspiration from their previous experience with earlier K-12 strains: acetate accumulated in the broth during the initial 96 hours of incubation, part of which was subsequently consumed during cell growth. They supplemented fermentations with sodium acetate (10 mM) eliminated the long lag and stimulated lactate production, increasing both the maximum volumetric and specific productivity.

In terms of environmental parameters, the authors identified pH 7.5 as optimal. Indeed, the toxicity of weak organic acids such as lactate increases at lower pH due to the membrane-permeable neutral form, which acts as an uncoupling agent, so higher pH is preferable. Moreover, the iLACCO biosensors employed in this work are themselves pH-sensitive, which justifies the necessity of pNasudi as control. Finally, oxygenation strategies also played a key role. For strain SZ58, an initial aerobic phase of 8 hours in M9 with 5% glucose significantly reduced growth lag, increased biomass yield tenfold within the first 24 hours, and accelerated lactate production—although sometimes at the expense of final yields. These findings suggest that early oxygen supply can prime cellular metabolism for more efficient production.

Taken together, the strategies outlined by Zhou et al. provide a valuable blueprint for optimizing the growth environment - namely M9 methanol minimal medium - of synthetic methylotrophs. They may enhance the adaptation and productivity of strains during ALE experiments and later guide scale-up.

5.2. Experiment(s) for Objective 2: Rational engineering for L-lactate Production

5.2.1. Heterologous expression of L-ldh and resulting L-lactate production

This experiment aimed to evaluate and compare the performance of three recombinant L-lactate dehydrogenases (*L-ldh*)—from *B. coagulans*, *S. bovis*, and *L. casei*—in order to prioritize the most effective enzyme for genome integration. The rationale was twofold: (a) to benchmark their relative efficiency against findings from the literature, particularly the comparative analysis reported by (Niu et al. (2014), and (b) to reduce experimental complexity. Initially, a full factorial design was envisioned, involving the integration of each of the 3 *L-ldh* with each of the 3 different iLACCO biosensors across 4 strain backgrounds using both techniques, CRISPR-Cas9 and λ-Red recombineering. However, the technical challenges arising from genome editing and the vast screening load led to prioritization of constructs for feasibility.

5.2.1.1. Comparison of the performance of the three candidate recombinant L-ldh

As shown in Figure 6, the three *L-ldh* genes were cloned onto plasmids (see Table 2) and expressed in *E. coli* strains incubated anaerobically for minimum four hours (experimental triplicates). Supernatants were submitted to the colorimetric L-lactate assay. The *L-ldh* from *B. coagulans* seem to yield the highest L-lactate levels, followed by *S. bovis* and *L. casei*. This order mirrors what Niu et al., (2014) reported; they attributed this superior performance to thermostability, cofactor preference, and pH tolerance. In brief, this experiment validated the selection of *B. coagulans L-ldh* for subsequent genomic integration.

Figure 6 : Extracellular L-Lactate production in WT *E. coli* by 3 recombinant L-ldh on plasmids

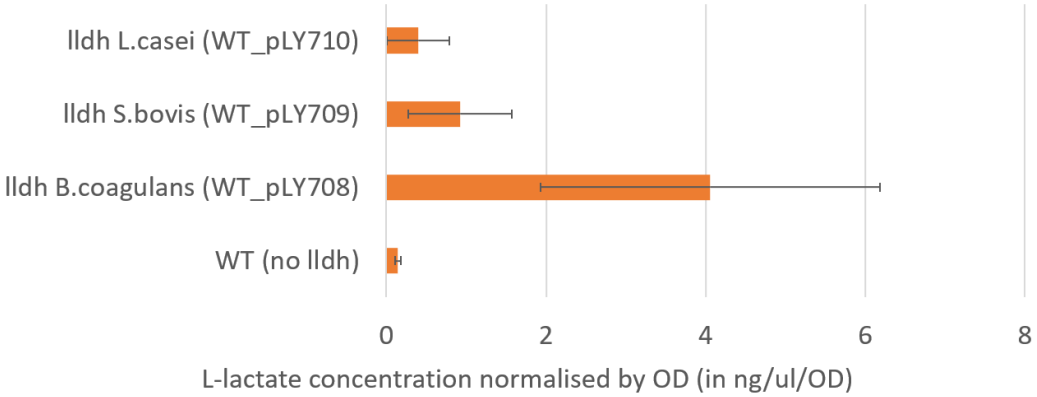

5.2.1.2. Comparison of integration of L-ldh on plasmid versus in genome

Following the prioritization of L-ldh from *B. coagulans*, we pursued genome integration of it in tandem with deletion of the native *ldhA* gene. Two approaches were used: CRISPR-Cas editing via pAGT5 and λ-Red via the LR5 template (Table 2). The latter proved successful, generating a strain capable of producing exclusively L-lactate, as D-lactate production was abolished via *ldhA* knockout. λ-Red recombineering proved more robust and ultimately successful for genomic integration in this study than CRIPSR-Cas. The λ-Red system is generally less dependent on precise timing and offers more flexibility in donor design. Unlike CRISPR-Cas9, it does not generate toxic DSBs, making it less stressful for the host and more forgiving to incomplete edits or variable expression levels (Sharan *et al.*, 2009). The use of particularly long homology arms (>100bp, inherited from pTarget plasmids, see Table 2) and very clean PCR products (gel extraction at each step of the SOE PCR building process) probably enhanced the integration efficiency.

Figure 7 : Extracellular L-lactate production by recombinant L-ldh from *B. coagulans* on plasmid or on genome

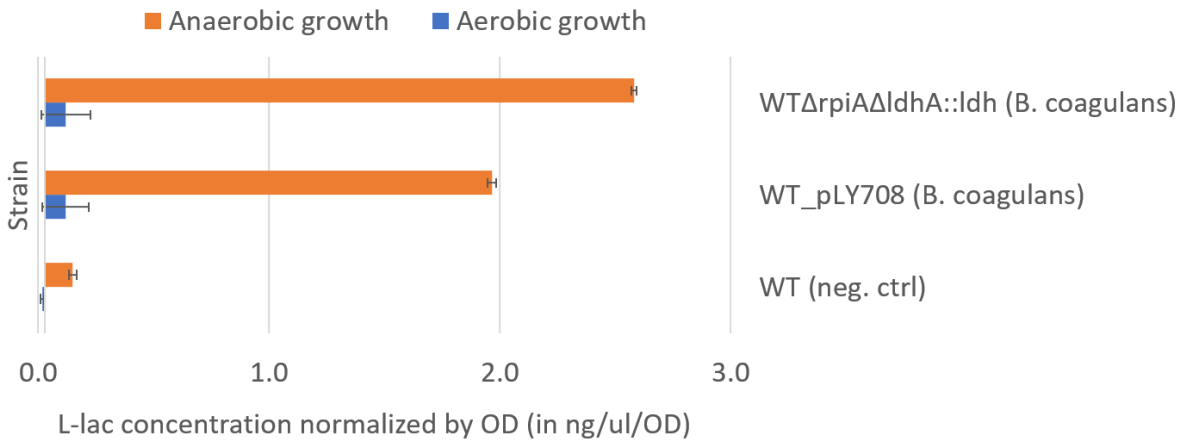

In Figure 7, the engineered strain *WT-ΔrpiAΔldhA::L-ldh(B. coagulans)* is compared to a control strain expressing the same enzyme under the same promoter from a plasmid (pLY708). The *rpiA* deletion is not expected to impact L-lactate production under the tested conditions. Notably, the strain with the *L-ldh* on the chromosome exhibited improved L-lactate production. This advantage over the strain with the L-ldh on plasmid may be attributed to two factors: on the one hand, improved expression stability due to genomic context, on the other hand, the elimination of D-lactate production as a competing route.

To verify the effect of oxygen availability, the same strains (Figure 7) were incubated in parallel under aerobic conditions. As expected, L-lactate accumulation was minimal, first because redox balance was ensured via glycolysis and the electron transport chain, and second because in the presence of oxygen, L-lactate can be re-utilized as a carbon source. Nonetheless, small amounts of L-lactate were still detected in strains harbouring the *L-ldh*, probably not due to suboptimal oxygenation but rather the abundance of nutrients in rich LB medium did not pressure the cell to rely on lactate (the *lldPRD* operon is repressed under glucose presence (Aguilera *et al.*, 2008).

5.2.1.3. Implications for SM strains

Although small, measurable levels of lactate were still detected in strains grown aerobically. This observation is encouraging for future applications, as synthetic methylotrophic (SM) strains such as SM7 and SM8 are unable to grow anaerobically. Consequently, an L-lactate cell factory based on SM genotypes would have to produce under aerobic conditions — an advantage in terms of scalability and process control in bioreactor environments. Indeed, from an industrial standpoint aerobic fermentation eliminates the need for a strict anoxic containment and reduces risks associated with anaerobic culture such as incomplete substrate utilization or pH instability (Papini, Salazar and Nielsen, 2010).

Nevertheless, improving L-lactate yields in aerobic systems will likely require rational metabolic engineering to redirect carbon flux away from respiration and toward fermentative pathways. One possibility involves disrupting the TCA cycle, refraining the cells to fully oxidize pyruvate and compelling them rely on alternatives to respiration to regenerate NAD^+, typically lactate fermentation. Zhou et al. (2016) and Zhao et al. (2016) are examples of such strategies. Zhou et al. (2016) inactivated *sucA*. This gene encodes a subunit of the 2-oxoglutarate dehydrogenase complex, which converts 2-oxoglutarate (α-ketoglutarate) to succinyl-CoA, keeping the latter from reacting with pyruvate and fuelling the Krebs cycle Zhao et al. (2016) inactivated *sdhABCD*. Deleting the succinate dehydrogenase complex halts the conversion of succinate to fumarate and interrupts the respiratory chain's connection to the TCA cycle. Such modifications could be envisaged in the current project.

5.3. EXPERIMENT(S) FOR OBJECTIVE 3: EXPRESSING AND TESTING THE ILACCO BIOSENSORS

5.3.1. Confirmation of biosensor functionality in E. coli through extracellular L-lactate titration

Upon cloning, the biosensors plasmids (pNasu series) were transformed in DH5α before being introduced into WT strain(see Methods). The biosensors successfully expressed in DH5α. A titration experiment was conducted to confirm the functionality of iLACCO biosensor in E. coli. Biosensor-expressing DH5α strains were incubated in glucose MOPS minimal medium supplemented with a range of L-lactate concentrations. The fluorescence response was measured after 3 hours (Figure 8). The results demonstrate that the low-affinity biosensor (iLACCO1.9b) responds to L-lactate concentrations ranging from 12.5 mM to 100 mM. The pH-sensitive positive control (diLACCO1.9) shows no significant response, which also aligns with expectations. However, the high affinity biosensor (iLACCO1.9) was expected to emit a steeper response than its low affinity equivalent. Plasmidic DNA extraction from the DH5α strains betrayed that several versions of the iLACCO plasmids co-existed in colonies or even in cells (all retaining Spec resistance). In particular, a 4bp deletion at the start of the iLACCO ORF (30% occurrence in pNasu9) most likely disabled the protein, hence its low signal.

Figure 8: Fluorescence response of biosensor expressed in DH5a grown 3 hours in glucose MOPS minimal medium with L-lactate concentrations ranging from 12.5 mM to 100 mM

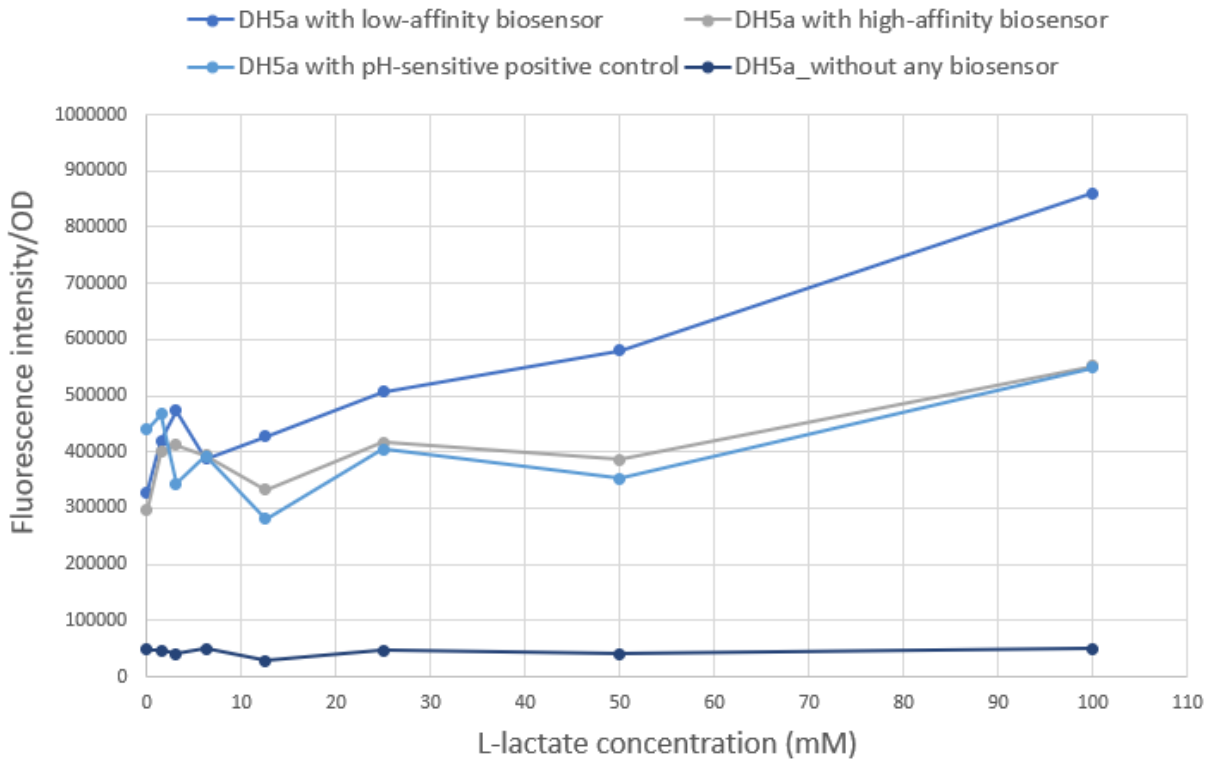

5.3.2. Relationship between fluorescence and L-lactate production

These experiments aimed to qualitatively demonstrate that the intracellular L-lactate biosensors responded to L-lactate produced by heterologously expressed L-ldh genes. The ideal outcome would be a discernible correlation between biosensor fluorescence intensity and L-lactate production levels, thereby confirming the sensor's functionality in vivo. Beyond confirming iLACCO sensitivity, the experiment would also reveal potential issues related to saturation dynamics, plasmid compatibility, expression burden, or interference between the metabolic and sensing components.

5.3.2.1. Co-expression of L-ldhs and biosensors

A wild-type *E. coli* strain was co-transformed with two plasmids (see Table 2 and 3 respectively): one encoding an L-ldh, the other encoding an iLACCO biosensor, and then spread on plates. Each transformation was accompanied by appropriate negative controls, resulting in a 4 × 4 experimental matrix (see Figure 10). Because both constructs were introduced via plasmids, neither the native *ldhA* (D-lactate dehydrogenase) nor *lldD* (L-lactate oxidase) genes were knocked out. In consequence the cells retained the ability to produce D-lactate and potentially consume L-lactate via aerobic metabolism (unlikely on LB medium).

The first results were encouraging. Figure 9 shows that for a given L-ldh, the diLACCO was brightest (pH-sensitive positive control), then iLACCO1.9 (high affinity) then iLACCO1.9b (low affinity). Vice versa, for a given biosensor, the L-ldh from *B. coagulans* was brighter than the one from *S. bovis*, itself brighter than the one from *L. casei*. This is perfectly consistent with the assay presented in Figure 6.

The brightest fluorescent colonies among the biosensor–L-ldh co-transformants were selected and restreaked over five successive passages, always in duplicate. However, as passages progressed, divergence increased between duplicates, indicating phenotypic drift. The biosensor-only control strains had to be replated daily to match the growth stage of the experimental plates at each imaging timepoint, and their reliability was compromised as well. Repeated subculturing likely permitted adaptive changes even in these controls, undermining their interpretability over time.

Figure 9: Green fluorescence imaging of *E. coli* double-plasmid transformants expressing biosensors and L-LDHs, along with negative controls for each construct.

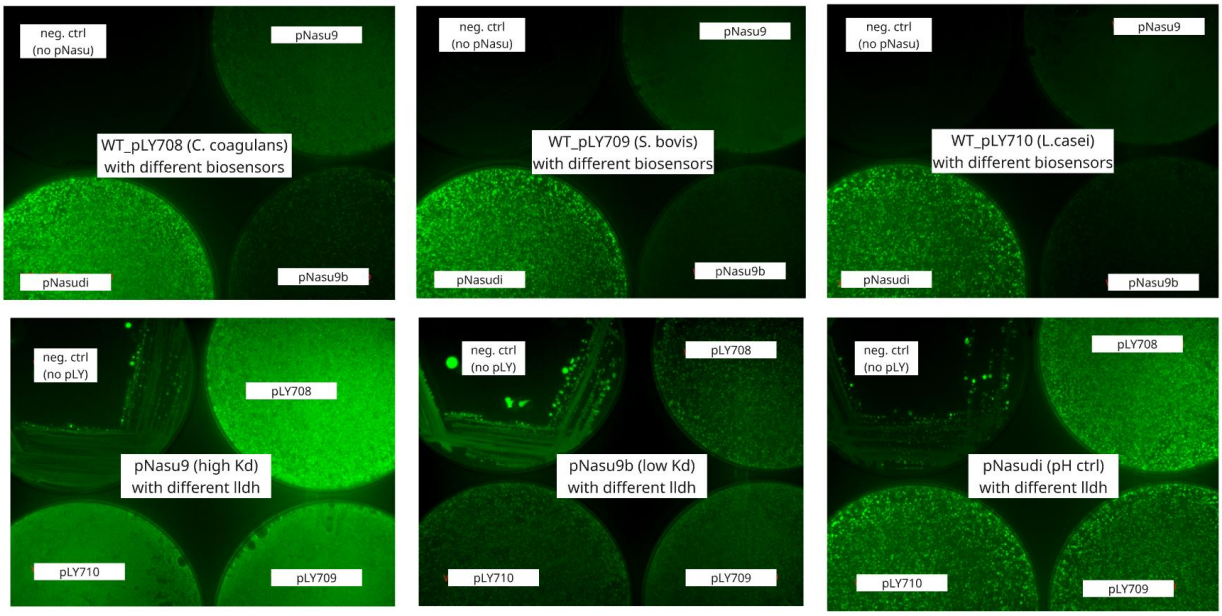

5.3.2.2. Investigation of cofounding factors in fluorescence response

A similar experiment was conducted some months later, again every combination L-ldh-expressing plasmid (pLY series) and biosensor plasmid (pNasu series) plated separately (Figure 10). Even within a single plate—where all colonies should be genetically identical—marked variation in fluorescence intensity was visible. Moreover, control colonies expressing only the biosensor but no L-ldh still exhibited detectable fluorescent colonies under aerobic conditions, in other words false positives.

Two "bright" and two "dark" colonies from each agar plate were selected. On the one hand, these colonies were restreaked under the same conditions (LB Agar with Spec and Amp) to test phenotypic stability. After overnight incubation, brightness levels remained consistent—bright colonies retained higher fluorescence, while dark colonies remained dim—suggesting that the observed differences were

heritable or at least stable over short generational spans. On the other hand, colonies were also restreaked on plates supplemented with IPTG to boost expression of the *L-ldh* gene, driven by the IPTG-inducible *pLlac01* promoter. If the biosensors were faithfully reporting intracellular L-lactate levels, we expected increased fluorescence in IPTG-induced conditions. However, IPTG induction had no discernible impact on fluorescence intensity. This suggest that the sensor signal does not reflect the L-lactate concentration in the cell, but rather the copy number of the pNasu (sensor) plasmid.

Figure 10: Schematic representation of the experimental workflow used to assess intra-plate heterogeneity across co-transformed *E. coli* colonies.

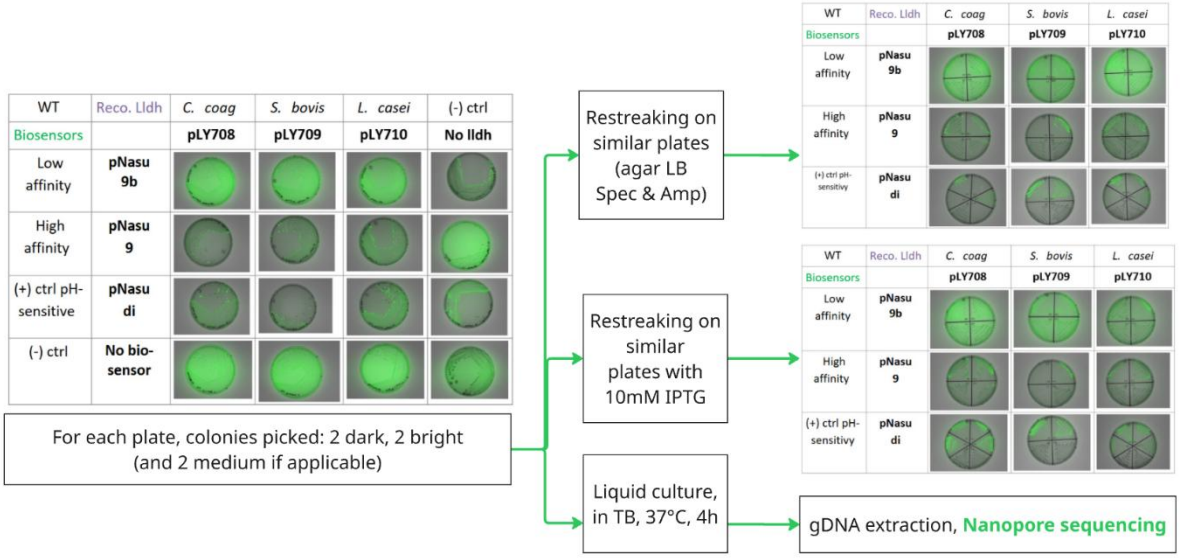

To explore this hypothesis, the whole-genome of the selected bright and dark colonies were sequenced. The sequencing data revealed striking differences in plasmid copy number: as anticipated, brighter colonies contained higher copies of the pNasu biosensor plasmid. pNasu plasmids carry a ColE1 origin of replication (high-copy-number), which generally confers consistent plasmid abundance among cells. Further examination of the sequences revealed that some plasmids had created tandem repeats of the iLACCO protein (as part of a longer fragment). No definite explanation can be given for the moment, but further investigation is under way. These structural variants suggest that the differential fluorescence intensities variations stem from variability in plasmid copy number, but also CNV of the *iLACCO* cassette within individual plasmids.

Although this experiment provided valuable insights, it is limited by several factors. An improvement would have been to grow the plates anaerobically, but prior internal work with these strains (not reported here) entail that the overall conclusions would remain unchanged. A major impediment is that fluorescence imaging on agar plates is inherently semi-quantitative. Parameters such as colony morphology, spatial positioning, and localized background fluorescence can introduce artifacts. More critically, the VisionWorks® software applies automatic contrast scaling based on the brightest signal in each image. Consequently, fluorescence intensity is represented relatively rather than absolutely, which can result in uniform green tinting across the plate in cases of low signal variation. This relative scaling should be considered when interpreting fluorescence intensity differences between samples.

In conclusion, these findings indicate that biosensor signal strength was confounded by plasmid copy number, intra-plasmid CNVs of the sensor gene, and differential expression levels. To address this challenge, a dual-reporter system was designed. A revised dual-reporter design was constructed, from pNasu plasmids without CNV, in which the GFP-based iLACCO biosensor is co-expressed with a RFP (mCherry) to normalize for expression levels (see Table 3).

Preliminary results with pAGT11_9R show little success in mitigating signal variability by that approach. Even if effective, this approach undermines the premise of single-protein intensiometric biosensors. Adding a second fluorescent protein (e.g., mCherry) for ratiometric normalization contradicts the core appeal of single-FP biosensors: their simplicity, genetic compactness, and low cellular burden compared traditional ratiometric FRET-based systems. FRET biosensors, although prevailing in physiology studies in mammalian systems, are not as easy to use in high-throughput sorting (e.g., FACS) as intensity-based sensors like GFP (Mahr, 2016). This is due to their complexity, low signal amplitude, and lack of direct selection. As a matter of fact, they require two fluorescent proteins and precise energy transfer, making them harder to clone, express, and tune (Wang *et al.*, 2023). Moreover, signal-to-noise is often low in bacterial cytosol, especially under evolutionary pressure.

Single-FP sensors are often favoured in bacterial systems precisely because they avoid the complexities and stoichiometric constraints of dual-fluorophore constructs (Greenwald, Mehta and Zhang, 2018) . By introducing a second FP, the system begins to resemble FRET-style architectures in both design and limitations, re-introducing issues such as increased cellular load, competition for transcriptional/translational machinery, and optical channel overlap, that is to say factors that single-FP biosensors have been specifically invented to minimize (Miyawaki *et al.*, 1997). Ultimately, while ratiometric correction is conceptually sound, its implementation in this project must be carefully balanced against the core goals of biosensor-guided ALE simplicity, scalability, and compatibility with high-throughput workflows.

6. CONTINUATION AND PERSPECTIVES

A number of avenues for future research and refinement of the L-lactate cell factory have been proposed throughout the discussion already. These include both genetic and environmental interventions aimed at optimizing production efficiency, sensor reliability, and strain robustness:

- Global-level rational metabolic engineering at the global cell level to impede respiration and favour fermentation even under aerobic conditions
- Optimisation of media and growth conditions targeting osmotic balance, pH buffering, and early aeration
- Sensor signal normalization through co-expression a spectrally distinct protein to calibrate the iLACCO response
- Genomic integration of biosensor constructs to knock-out lld, improve signal consistency, reduce metabolic burden, and eliminate copy number variation (CNV) artifacts
- Improved fluorescence imaging protocols, including fixed exposure scaling and anaerobic plate incubation.

6.1. FURTHER EXPERIMENTAL STEPS

6.1.1. Quantifying intracellular lactate levels

Previous experiments using a colorimetric enzymatic assay measured L-lactate concentrations in the extracellular medium. From a bioprocessing standpoint, this approach is pragmatic, as downstream purification is considerably more straightforward when the product is secreted into the supernatant rather than retained intracellularly. However, the iLACCO biosensors were developed to detect intracellular L-lactate dynamics. Consequently, efforts to correlate biosensor fluorescence with lactate titres must directly account for intracellular concentrations. Indeed, it is inaccurate to assume that intracellular and extracellular levels are at equilibrium.

This disconnect arises because wild-type *E. coli* lacks a native L-lactate export system. WT *E. coli* does not produce L-lactate, however, when engineered to produce L-lactate, some does appear in the medium (Wieschalka *et al.*, 2013), but transport is a bottleneck. Secretion may occur via unspecific transport, leakage, or indirect efflux mechanisms. This is also what is observed in our experiments (Figures 6 and 7). *E. coli* has general monocarboxylate transporters (e.g., YhjX, AtoE, or multidrug efflux pumps) that might allow export of small anions like lactate, especially under stress or high concentrations. No direct evidence confirms this for L-lactate in particular, but functional redundancy and leakiness of transporters is common in bacteria. Passive diffusion across membranes, although limited, could occur at low pH, when lactate is predominantly under lactic acid form.

As the cells are evolved, production levels by the recombinant L-lactate dehydrogenase might exceed export capacity. As lactate builds up, intracellular concentrations may transiently spike. Variations in pH gradients, membrane potential, or transport capacity can exacerbate this effect. In extreme cases, intracellular accumulation may result in metabolic overflow, stress, or even membrane damage, leading to leakage or partial lysis—further complicating interpretation of extracellular titres as well as downstream processing at greater scale. A study by Tsuge et al. 2019 in *Corynebacterium glutamicum* similarly found that intracellular lactate accumulation constrained both growth and yield in the absence of efficient export mechanisms.

Moreover, as underscored in the State-of the-art, another critical confounding factor may be intracellular re-consumption. Indeed, if lactate concentrations reach high levels inside the cells; *E. coli* may re-oxidize it via LldD (especially under aerobic conditions), reducing net yields. In the reported results, the biosensors are plasmid-based and *lldD* remains intact. The integration of iLACCO constructs into the genome (replacing *lldD*) is therefore capital. Furthermore, these intracellular-extracellular

dynamics are especially problematic in the context of iLACCO-like sensors, which are known to be pH-sensitive (Hario *et al.*, 2024). L-lactate, being a weak acid, can affect intracellular pH during accumulation, and the resulting pH shifts may lead to artifactual fluorescence changes. The use of pH-insensitive control variants like diLACCO partially mitigates this issue but underscores the need for tighter control of proton fluxes and buffering conditions during fluorescence-based measurements.

A future direction therefore involves the heterologous expression of specialized L-lactate transporters to alleviate intracellular bottlenecks. For instance, the lactate permease gene *lldP* from *Corynebacterium glutamicum* characterized by Wieschalka et al. (2013), or more broader-scope transporters. A study by Tsuge et al. (2019) also demonstrated that heterologous expression of monocarboxylate transporters improved lactic acid secretion in engineered yeast. By incorporating such transporters into the strain design, one could potentially improve both production yields and the interpretability of biosensor signals.

6.1.2. Monitoring and characterizing inputs and outputs

Comprehensive monitoring of substrate consumption and product formation is essential for evaluating and optimizing the metabolic performance of a cell factory. In the present context, this will include both quantifying methanol uptake and profiling key fermentation byproducts such as acetate, formate, ethanol, succinate, and self-evidently the target metabolite, L-lactate.

To this end, gas chromatography–mass spectrometry (GC–MS) and liquid chromatography–mass spectrometry (LC–MS) provide powerful analytical techniques. Volatile compounds such as methanol, ethanol, formate, and acetate can be analyzed using a GC–MS system equipped with a non-polar capillary column and a mass-selective detector. A common setup involves helium as the carrier gas under constant pressure, with a thermal program starting at 40 °C (held for 2 minutes), ramping at 10 °C/min to 60 °C, then rapidly to 220 °C at 40 °C/min, with a final hold (Chen et al. 2020). For non-volatile or polar fermentation products such as L-lactate and succinate, triple quadrupole LC–MS systems are typically used, in conjunction with a reversed-phase C18 column or ion-exclusion column, depending on the compound's properties. For instance, one method employs a sulfuric acid-based mobile phase (e.g., 30 mM H_2SO_4) at a flow rate of 0.6 mL/min over 30 minutes for organic acid quantification. Methanol consumption can also be monitored using gas chromatography coupled with flame ionization detection (GC–FID), using a polar FFAP column designed for alcohols and organic acids (Nieh *et al.*, 2024).

Critically, a determinant step will be to validate the origin of carbon in fermentation products, in other words to prove that in the L-lactate by the cell factory is originates from methanol. Isotope labeling can be used for that verification. In their study, Chen et al. (2020) passaged their engineered strain for six generations in minimal medium with uniformly labelled ^{13}C-methanol until isotopic steady-state was reached. Their results confirmed that acetate was double-labelled and formate was single-labelled, verifying that methanol was the exclusive carbon source supporting both growth and product synthesis. This strategy could be replicated to confirm that lactate produced in the present system originates entirely from methanol metabolism. In such case, it should appear triple-labelled. M+2, M+1, or unlabelled (M+0) peaks would suggest contamination, incomplete labelling, or parallel carbon flux from other sources.

6.2. PROPOSITIONS FOR THE WIDER BIOPRODUCTION OR SUPPLY CHAIN LEVEL

6.2.1. Sourcing methanol sustainably

The economic viability of a methanol-to-lactate bioproduction system is intrinsically linked to the availability and affordability of methanol—particularly from renewable sources. As of 2025, fossil-derived methanol remains the significantly cheaper, with prices typically ranging from $400–500 per tonne in global markets (Methanex, 2025). In contrast, bio-methanol—produced from biomass, waste, or black liquor—and e-methanol—synthesized from renewable hydrogen and captured CO_2—command prices upwards of $900–1,200 per tonne, depending on production scale and region (Mandegari *et al.*, 2023; Raouf, 2024).

This price gap is rooted in high capital and operational costs associated with renewable electricity, electrolytic hydrogen, and carbon capture technologies, compounded by limited economies of scale (Dell'Aversano *et al.*, 2024). However, techno-economic projections suggest that renewable methanol could reach cost parity with fossil methanol by the late 2020s or early 2030s, especially in hard-to-decarbonize sectors like marine shipping and aviation (Cordero-Lanzac *et al.*, 2022; Deka *et al.*, 2022; Sollai *et al.*, 2023).

These projections hinge on ongoing declines in electrolyzer and renewable electricity costs, coupled with the scaling of integrated CO_2-to-methanol plants. Large-scale projects confirm this trajectory. The world's first commercial-scale e-methanol facility, with an initial capacity of 42 ktonnes/year, began operations in in Denmark one month ago (May 2025)—using CO_2 from biogas and waste incineration paired with renewable power (European Energy, 2025). Policy support (carbon taxes, green mandates, fuel standards) is also decisive. Policies such as FuelEU Maritime, carbon pricing, and green fuel mandates are also pivotal drivers expected to shift market dynamics (Mandegari *et al.*, 2023).

6.2.2. Utilizing biosensors (TF-based and iLACCO-like) differently

Sandberg et al., (2019) underline that the evolutionary success of ALE heavily depends on the selective pressure used. Improving stress tolerance or growth rate is often more straightforward, as these traits directly impact cell fitness, fitter cells dominate the culture and can be naturally selected over time. In contrast, enhancing production phenotypes—such as increasing the titre of a desired metabolite—poses a greater challenge. Indeed, L-lactate production do not confer a direct growth advantage and may even impose a metabolic burden, thus reducing the evolutionary benefit for producer cells. In other words, there is no evolutionary incentive to produce more unless production is somehow tied to survival or reproductive success.

Consequently, selection for production traits typically requires coupled selection strategies, such as biosensor-assisted screening or growth-coupled production systems, to link product formation to cellular fitness (Dragosits and Mattanovich, 2013; Godara and Kao, 2020; Hirasawa and Maeda, 2023). A very common strategy used with TF-based fluorescent biosensors is to directly integrate bioproduction with selection. In other words, the TF binds to the target metabolite and expresses not a fluorescence reporter, but a gene directly tied to cell survival or growth rate. TF-based sensors can be easily wired to antibiotic resistance genes, toxin-antitoxin systems, or auxotrophy complementation/ rescue. Biosensor-driven survival reflect intracellular product levels, which is ideal for adaptive laboratory evolution (ALE). A notable example is the production of 3-hydroxypropanoic acid (3-HP) in *E. coli* by Seok et al.(2021). Their biosensor linked 3-HP levels to antibiotic resistance (e.g., *tetA*). During ALE progressively increasing tetracycline concentrations, strains producing more 3-HP survived, outcompeted others, and redistributed carbon flux toward 3-HP, achieving 93% of the theoretical maximum yield. Such strategies have also been deployed for malonyl-CoA, fatty acids, and aromatic compounds, transforming biosensors from passive reporters into active regulators of cellular fitness (Raman *et al.*, 2014; Rogers and Church, 2016; Rogers, Taylor and Church, 2016).

In contrast, iLACCO-type biosensors—based on circularly permuted GFP fusions—do not regulate gene expression. They function purely as real-time reporters of intracellular metabolite levels, making them ill-suited for growth-coupled ALE by themselves. Their strength resides elsewhere: iLACCO biosensors allow for imaging-based selection on solid media, enabling high-throughput visual screening of metabolite levels across colonies. Nasu et al. (2021) emphasized their quantitative capacity, where sensor variants with different affinities can be used to approximate metabolite concentrations within cells based on fluorescence intensity distributions. However, this screening approach does not account for growth rate or population fitness, and - as witnessed in experiments discussed earlier - is prone to confounding by plasmid copy number variations, protein expression noise, or image normalization artifacts.

The final recommendation is that to fully harness the capabilities of iLACCO-like sensors, their role could shift from mere end-product detectors to real-time monitors of intracellular metabolic routing. Their modular nature across host organisms (e.g., *E. coli*, yeast, mammalian cells) and their capacity for real-time, non-invasive metabolic monitoring underscores their strategic value. Instead of using these sensors solely for selecting the best lactate producers on plates, they could be integrated strategically downstream of key metabolic branch points to report the direction and magnitude of carbon flux. In this vision, the biosensor signal would serve as a “metabolic traffic light”, indicating whether the host cell is naturally channelling resources toward a target pathway or diverting them elsewhere. Different host strains could then be benchmarked or pre-screened based on these intracellular signals before any production module is installed. Over time, this would yield a library of chassis strains — each pre-optimized for metabolic flow into distinct product pathways (e.g., lactate, succinate, itaconate). These pre-adapted platforms could then serve as foundations for modular cell factories, dramatically accelerating synthetic biology pipelines.

7. CONCLUSION

One of the key challenges in microbial metabolic engineering is the lack of efficient evolution platforms for optimizing bioproduction. In this project, we aim to develop a biosensor-guided evolutionary strategy to enhance the production of L-lactate by E. coli using methanol as the sole carbon source. This serves as a proof-of-concept to derive a methodological pipeline for building robust, high-performing microbial cell factories.

The project emerged at the convergence of prior research efforts at the Institute of Biological Chemistry, Academia Sinica. On one hand, Dr. James Liao's laboratory engineered synthetic E. coli strains capable of methanol assimilation. On the other, Dr. Nasu's laboratory developed genetically encoded, intensiometric L-lactate biosensors. Together, these advancements provide a unique ground to build an E. coli cell factory coupling methanol utilization with L-lactate biosynthesis.

The State-of-the-Art chapter highlighted the relevance of methanol as substrate, of *E. coli* as a versatile microbial chassis, and of L-lactate as a high-value bioproduct. While natural methylotrophy is well understood, synthetic methylotrophy—particularly in industrial hosts like *E. coli*—remains nascent. To date, only a single study has demonstrated methanol-to-lactate conversion, yet its reported lactate titres fall well below industrial relevance. This motivates our effort to establish an efficient and scalable evolution platform for methanol-based bioproduction.

This work extended Dr. Liao's team's progress by further enhancing the growth of synthetic methylotrophic strains in M9 minimal medium, which is pertinent for industry. To this end, adaptive laboratory evolution (ALE) was employed, leveraging the strain's intrinsic evolutionary plasticity for self-rewiring to resolve metabolic bottlenecks, prevent pathway overflow, and optimize internal resource allocation—achievements that remain out of reach through rational design alone.

This work extended Dr. Nasu's team's progress by applying the biosensors in a novel way. Biosensors such as the iLACCO series: genetically encoded, single cpGFP-based, calcium-independent, and intensiometric, have never been as systematic tools for strain development. These biosensors embody the convergence of synthetic biology, protein engineering, and optical sensing. While traditionally used in physiological research to study intracellular dynamics, they hold untapped potential in microbial evolution for biomanufacturing.

To unite these two streams, synthetic methylotrophic strains were engineered to produce L-lactate, and enable detection thereof by the biosensor. This required a multi-faceted approach to metabolic engineering, including targeted gene knockouts, redox balancing, and heterologous gene expression. All in all, this project required extensive foundational work to bridge methanol assimilation, L-lactate production, and biosensor functionality within a single *E. coli* chassis, before the evolutionary framework can be implemented. Throughout the thesis, the genetic engineering and construct assembly represented the bulk of the work completed. The DNA constructs—including plasmids, pTargets, and λ-Red templates—were successfully designed, assembled, and validated, despite setbacks in achieving chromosomal editing. Hence, most experimental results were obtained using plasmid-based expression.

Several candidate L-lactate dehydrogenases were identified, expressed and compared. All three recombinant dehydrogenases enabled L-lactate production in *E. coli*, measurable extracellularly. The most effective candidate was successfully integrated into the genome, substituting the native D-lactate dehydrogenase gene, and yielded improved performance over plasmid-based expression. A titration experiment validated the functionality of the iLACCO biosensor in response to L-lactate, though complications such as genetic duplication and recombination introduced variability and warrant further investigation. Co-expression of *lldh* and iLACCO in *E. coli* provided real-time insights into intracellular production levels, though qualitative appreciation needs to be complemented by further quantitative methods.

While significant progress was achieved in each individual stream - enhanced growth on M9, reliable L-lactate production, precise biosensing - their full integration into one functional strain remains an ongoing objective. Nevertheless, the results already obtained inspired a number of future directions, including refining genetic constructs, planning further modifications to alternate with ALE periods, expanding assays (e.g., intracellular quantification, byproduct profiling, substrate uptake) to control biosensor accuracy, addressing compartmentalization and transport of L-lactate, changing growth conditions and medium composition, and optimizing scale-up logistics.

From a broader perspective, this thesis supports the feasibility of leveraging C1 feedstocks such as methanol to produce more complex molecules in scalable, sustainable processes. The platform developed here lays the groundwork for expanding iLACCO-like biosensor applications in biomanufacturing, especially in domains where conventional biosensors are ill-suited. Taking a step back to assess the broader utility of iLACCO-like sensors in strain developments, this type of sensor might be better utilized for dynamic pathway calibration and metabolic flux analysis. A proposed application would be to integrate such biosensors downstream of key branching points in central metabolism, enabling real-time visualization of flux distribution. In this context, ALE could then be used not to select for end-product levels per se, but for pathway architectures that naturally balance growth with metabolite flow toward a desired product.

8. REFERENCES

Adams, B.L. (2016) 'The Next Generation of Synthetic Biology Chassis: Moving Synthetic Biology from the Laboratory to the Field', *ACS Synthetic Biology*, 5(12), pp. 1328–1330. Available at: https://doi.org/10.1021/acssynbio.6b00256.

Aguilar, A., Twardowski, T. and Wohlgemuth, R. (2019) 'Bioeconomy for Sustainable Development', *Biotechnology Journal*. Wiley-VCH Verlag. Available at: https://doi.org/10.1002/biot.201800638.

Aguilera, L. *et al.* (2008) 'Dual role of LldR in regulation of the lldPRD operon, involved in L-lactate metabolism in Escherichia coli', *Journal of Bacteriology*, 190(8), pp. 2997–3005. Available at: https://doi.org/10.1128/JB.02013-07.

Baba, T. *et al.* (2006) 'Construction of Escherichia coli K-12 in-frame, single-gene knockout mutants: The Keio collection', *Molecular Systems Biology*, 2. Available at: https://doi.org/10.1038/msb4100050.

Béal, C. *et al.* (2023) 'Lactic acid microbial production and recovery: Review and recent advances in bioprocess integration', in *Lactic Acid Bacteria as Cell Factories*. Elsevier, pp. 77–108. Available at: https://doi.org/10.1016/B978-0-323-91930-2.00016-X.

Becker, J. *et al.* (2015) 'Top value platform chemicals: Bio-based production of organic acids', *Current Opinion in Biotechnology*. Elsevier Ltd, pp. 168–175. Available at: https://doi.org/10.1016/j.copbio.2015.08.022.

Bennett, R.K. *et al.* (2018) 'Engineering the bioconversion of methane and methanol to fuels and chemicals in native and synthetic methylotrophs', *Current Opinion in Biotechnology*. Elsevier Ltd, pp. 81–93. Available at: https://doi.org/10.1016/j.copbio.2017.11.010.

Bernard, N. *et al.* (1991) 'Cloning of the D-lactate dehydrogenase gene from *Lactobacillus delbrueckii* subsp. *bulgaricus* by complementation in *Escherichia coli*', *FEBS Letters*, 290(1–2), pp. 61–64. Available at: https://doi.org/10.1016/0014-5793(91)81226-X.

Bertau, M. *et al.* (no date) *Methanol: The Basic Chemical and Energy Feedstock of the Future*.

Bilal, M., Niu, D. and Wang, Z. (2024) 'Biotechnological Strategies and Perspectives for Food Waste Treatment: The Role of Lactic Acid and Microbial Biomass', *Waste and Biomass Valorization* [Preprint]. Springer Science and Business Media B.V. Available at: https://doi.org/10.1007/s12649-024-02705-y.

Bollella, P. and Katz, E. (2020) 'Biosensors—recent advances and future challenges', *Sensors (Switzerland)*. MDPI AG, pp. 1–5. Available at: https://doi.org/10.3390/s20226645.

Borgogna, A. *et al.* (2019) 'Methanol production from Refuse Derived Fuel: Influence of feedstock composition on process yield through gasification analysis', *Journal of Cleaner Production*, 235, pp. 1080–1089. Available at: https://doi.org/10.1016/j.jclepro.2019.06.185.

Carter, E. (2025) 'Sustainable Biomanufacturing: Leveraging Circular Economy Principles for Competitive Advantage', *Journal of Commercial Biotechnology*, 30(1), pp. 1–10. Available at: https://doi.org/10.5912/jcb2486.

Chai, F. *et al.* (2023) 'Maximizing the performance of protein-based fluorescent biosensors', *Biochemical Society Transactions*. Portland Press Ltd, pp. 1585–1595. Available at: https://doi.org/10.1042/BST20221413.

Chai, R. *et al.* (2024) 'The Influence of Homologous Arm Length on Homologous Recombination Gene Editing Efficiency Mediated by SSB/CRISPR-Cas9 in Escherichia coli', *Microorganisms*, 12(6), p. 1102. Available at: https://doi.org/10.3390/microorganisms12061102.

Chang, D.-E. *et al.* (1999) *Homofermentative Production of D-or L-Lactate in Metabolically Engineered Escherichia coli RR1*, *APPLIED AND ENVIRONMENTAL MICROBIOLOGY*. Available at: https://journals.asm.org/journal/aem.

Chen, C. and Wang, J. (2020) 'Optical biosensors: An exhaustive and comprehensive review', *Analyst*. Royal Society of Chemistry, pp. 1605–1628. Available at: https://doi.org/10.1039/c9an01998g.

Chen, F.Y.H. *et al.* (2020) 'Converting Escherichia coli to a Synthetic Methylotroph Growing Solely on Methanol', *Cell*, 182(4), pp. 933-946.e14. Available at: https://doi.org/10.1016/j.cell.2020.07.010.

Chen, W.H. and Lin, S.C. (2018) 'Biogas partial oxidation in a heat recirculation reactor for syngas production and CO2 utilization', *Applied Energy*, 217, pp. 113–125. Available at: https://doi.org/10.1016/j.apenergy.2018.02.123.

Cheng, F., Tang, X.L. and Kardashliev, T. (2018) 'Transcription Factor-Based Biosensors in High-Throughput Screening: Advances and Applications', *Biotechnology Journal*. Wiley-VCH Verlag. Available at: https://doi.org/10.1002/biot.201700648.

Chistoserdova, L., Kalyuzhnaya, M.G. and Lidstrom, M.E. (2009) 'The expanding world of methylotrophic metabolism', *Annual Review of Microbiology*, pp. 477–499. Available at: https://doi.org/10.1146/annurev.micro.091208.073600.

Chong, S.L. *et al.* (2024) 'Third-Generation L-Lactic Acid Biorefinery Approaches: Exploring the Viability of Macroalgae Detritus', *Bioenergy Research* [Preprint]. Available at: https://doi.org/10.1007/s12155-024-10801-z.

Collins, D.A. and Kalyuzhnaya, M.G. (2018) 'Navigating methane metabolism: Enzymes, compartments, and networks', in *Methods in Enzymology*. Academic Press Inc., pp. 349–383. Available at: https://doi.org/10.1016/bs.mie.2018.10.010.

Contag, P.R., Williams, M.G. and Rogers, P. (1990) *Cloning of a Lactate Dehydrogenase Gene from Clostridium acetobutylicum B643 and Expression in Escherichia coli*, *APPLIED AND ENVIRONMENTAL MICROBIOLOGY*. Available at: https://journals.asm.org/journal/aem.

Cook, A., Walterspiel, F. and Deo, C. (2023) 'HaloTag-Based Reporters for Fluorescence Imaging and Biosensing', *ChemBioChem*, 24(12). Available at: https://doi.org/10.1002/cbic.202300022.

Cordero-Lanzac, T. *et al.* (2022) 'A techno-economic and life cycle assessment for the production of green methanol from CO2: catalyst and process bottlenecks', *Journal of Energy Chemistry*, 68, pp. 255–266. Available at: https://doi.org/10.1016/j.jechem.2021.09.045.

Della Corte, D. *et al.* (2020) 'Engineering and application of a biosensor with focused ligand specificity', *Nature Communications*, 11(1). Available at: https://doi.org/10.1038/s41467-020-18400-0.

Cowan, A.E. *et al.* (2023) 'Microbial production of fuels, commodity chemicals, and materials from sustainable sources of carbon and energy', *Current Opinion in Systems Biology*. Elsevier Ltd. Available at: https://doi.org/10.1016/j.coisb.2023.100482.

Dalena, F. *et al.* (2018) 'Methanol Production and Applications: An Overview', in *Methanol: Science and Engineering*. Elsevier, pp. 3–28. Available at: https://doi.org/10.1016/B978-0-444-63903-5.00001-7.

Datsenko, K.A. and Wanner, B.L. (2000) 'One-step inactivation of chromosomal genes in Escherichia coli K-12 using PCR products', *PNAS*, 97(12). Available at: www.pnas.orgcgidoi10.1073pnas.120163297.

Davy, A.M., Kildegaard, H.F. and Andersen, M.R. (2017) 'Cell Factory Engineering', *Cell Systems*. Cell Press, pp. 262–275. Available at: https://doi.org/10.1016/j.cels.2017.02.010.

Dean, K.M. and Palmer, A.E. (2014) 'Advances in fluorescence labeling strategies for dynamic cellular imaging', *Nature Chemical Biology*, 10(7), pp. 512–523. Available at: https://doi.org/10.1038/nchembio.1556.

Deka, T.J. *et al.* (2022) 'Methanol fuel production, utilization, and techno-economy: a review', *Environmental Chemistry Letters*, 20(6), pp. 3525–3554. Available at: https://doi.org/10.1007/s10311-022-01485-y.

Dell'Aversano, S. *et al.* (2024) 'E-Fuels: A Comprehensive Review of the Most Promising Technological Alternatives towards an Energy Transition', *Energies*. Multidisciplinary Digital Publishing Institute (MDPI). Available at: https://doi.org/10.3390/en17163995.

Dien, B.S., Nichols, N.N. and Bothast, R.J. (2001) *Recombinant Escherichia coli engineered for production of L-lactic acid from hexose and pentose sugars*, *Journal of Industrial Microbiology & Biotechnology*. Available at: https://academic.oup.com/jimb/article/27/4/259/5990339.

Dien, B.S., Nichols, N.N. and Bothast, R.J. (2002) 'Fermentation of sugar mixtures using Escherichia coli catabolite repression mutants engineered for production of L-lactic acid', *Journal of Industrial Microbiology and Biotechnology*, 29(5), pp. 221–227. Available at: https://doi.org/10.1038/sj.jim.7000299.

Ding, N., Zhou, S. and Deng, Y. (2021) 'Transcription-Factor-based Biosensor Engineering for Applications in Synthetic Biology', *ACS Synthetic Biology*. American Chemical Society, pp. 911–922. Available at: https://doi.org/10.1021/acssynbio.0c00252.

Dong, X. *et al.* (2021) 'Broad-Spectrum Polymeric Nanoquencher as an Efficient Fluorescence Sensing Platform for Biomolecular Detection', *ACS Sensors*, 6(8), pp. 3102–3111. Available at: https://doi.org/10.1021/acssensors.1c01277.

Dragosits, M. and Mattanovich, D. (2013) 'Adaptive laboratory evolution – principles and applications for biotechnology', *Microbial Cell Factories*, 12(1), p. 64. Available at: https://doi.org/10.1186/1475-2859-12-64.

E. Bjorck, C., D. Dobson, P. and Pandhal, J. (2018) 'Biotechnological conversion of methane to methanol: evaluation of progress and potential', *AIMS Bioengineering*, 5(1), pp. 1–38. Available at: https://doi.org/10.3934/bioeng.2018.1.1.

Eason, M.G. *et al.* (2020) 'Genetically Encoded Fluorescent Biosensor for Rapid Detection of Protein Expression', *ACS Synthetic Biology*, 9(11), pp. 2955–2963. Available at: https://doi.org/10.1021/acssynbio.0c00407.

Eisavi, B. *et al.* (2022) 'Low-carbon biomass-fueled integrated system for power, methane and methanol production', *Energy Conversion and Management*, 253. Available at: https://doi.org/10.1016/j.enconman.2021.115163.

Mulok, T. *et al.* (2009) 'Engineering of E. coli for increased production of L-lactic acid', *African Journal of Biotechnology*, 8(18), pp. 4597–4603. Available at: http://www.academicjournals.org/AJB.

Faber, K. (2018) *Biotransformations in Organic Chemistry*. 7th edn. Cham: Springer International Publishing. Available at: https://doi.org/10.1007/978-3-319-61590-5.

Fei, Q. *et al.* (2020) 'Biological valorization of natural gas for the production of lactic acid: Techno-economic analysis and life cycle assessment', *Biochemical Engineering Journal*, 158. Available at: https://doi.org/10.1016/j.bej.2020.107500.

Fu, R. *et al.* (2023) 'Application and progress of techno-economic analysis and life cycle assessment in biomanufacturing of fuels and chemicals', *Green Chemical Engineering*. KeAi Communications Co., pp. 189–198. Available at: https://doi.org/10.1016/j.gce.2022.09.002.

Garg, S. *et al.* (2018) 'Bioconversion of methane to C-4 carboxylic acids using carbon flux through acetyl-CoA in engineered Methylomicrobium buryatense 5GB1C', *Metabolic Engineering*, 48, pp. 175–183. Available at: https://doi.org/10.1016/j.ymben.2018.06.001.

Germond, A. *et al.* (2016) 'Design and development of genetically encoded fluorescent sensors to monitor intracellular chemical and physical parameters', *Biophysical Reviews*, 8(2), pp. 121–138. Available at: https://doi.org/10.1007/s12551-016-0195-9.

Gezae Daful, A. and Görgens, J.F. (2017) 'Techno-economic analysis and environmental impact assessment of lignocellulosic lactic acid production', *Chemical Engineering Science*, 162, pp. 53–65. Available at: https://doi.org/10.1016/j.ces.2016.12.054.

Godara, A. and Kao, K.C. (2020) 'Adaptive laboratory evolution for growth coupled microbial production', *World Journal of Microbiology and Biotechnology*. Springer Science and Business Media B.V. Available at: https://doi.org/10.1007/s11274-020-02946-8.

Goto, S. *et al.* (2018) 'Cloning and heterologous expression of lactate dehydrogenase genes from acid-tolerant lactobacillus acetotolerans HT', *Food Science and Technology Research*, 24(5), pp. 861–868. Available at: https://doi.org/10.3136/fstr.24.861.

Grasa, E.T. *et al.* (2021) 'Commodity chemical production from third-generation biomass: a techno-economic assessment of lactic acid production', *Biofuels, Bioproducts and Biorefining*, 15(1), pp. 257–281. Available at: https://doi.org/10.1002/bbb.2160.

Greenwald, E.C., Mehta, S. and Zhang, J. (2018) 'Genetically Encoded Fluorescent Biosensors Illuminate the Spatiotemporal Regulation of Signaling Networks', *Chemical Reviews*, 118(24), pp. 11707–11794. Available at: https://doi.org/10.1021/acs.chemrev.8b00333.

Halper, S.M., Hossain, A. and Salis, H.M. (2020) 'Synthesis Success Calculator: Predicting the Rapid Synthesis of DNA Fragments with Machine Learning', *ACS Synthetic Biology*, 9(7), pp. 1563–1571. Available at: https://doi.org/10.1021/acssynbio.9b00460.

Hanahan, D., Jessee, J. and Bloom, F.R. (1995) 'Techniques for transformation of *E. coli*', in *DNA Cloning 1*. Oxford University PressOxford, pp. 1–36. Available at: https://doi.org/10.1093/oso/9780199634774.003.0001.

Hario, S. *et al.* (2024) 'High-Performance Genetically Encoded Green Fluorescent Biosensors for Intracellular l-Lactate', *ACS Central Science*, 10(2), pp. 402–416. Available at: https://doi.org/10.1021/acscentsci.3c01250.

Hellweg, L. *et al.* (2023) 'A general method for the development of multicolor biosensors with large dynamic ranges', *Nature Chemical Biology*, 19(9), pp. 1147–1157. Available at: https://doi.org/10.1038/s41589-023-01350-1.

Hirasawa, T. and Maeda, T. (2023) 'Adaptive Laboratory Evolution of Microorganisms: Methodology and Application for Bioproduction', *Microorganisms*. MDPI. Available at: https://doi.org/10.3390/microorganisms11010092.

Hosseinpour, A., Shayesteh, K. and Es'haghi, P. (2025) 'A Review of the Importance, Production, Economics, and Future of Methanol in Iran and the World', *Chem. Res. Tech*, 2, pp. 1–11. Available at: https://doi.org/10.22034/CHEMRESTEC.2025.493857.1032.

Ibraheem, A. and Campbell, R.E. (2010) 'Designs and applications of fluorescent protein-based biosensors', *Current Opinion in Chemical Biology*, pp. 30–36. Available at: https://doi.org/10.1016/j.cbpa.2009.09.033.

Ioannidou, S.M. *et al.* (2022) 'Techno-economic risk assessment, life cycle analysis and life cycle costing for poly(butylene succinate) and poly(lactic acid) production using renewable resources', *Science of the Total Environment*, 806. Available at: https://doi.org/10.1016/j.scitotenv.2021.150594.

Irla, M. and Wendisch, V.F. (2022) 'Efficient cell factories for the production of N-methylated amino acids and for methanol-based amino acid production', *Microbial Biotechnology*. John Wiley and Sons Ltd, pp. 2145–2159. Available at: https://doi.org/10.1111/1751-7915.14067.

Jiang, S. *et al.* (2023) 'Metabolic reprogramming and biosensor-assisted mutagenesis screening for high-level production of L-arginine in Escherichia coli', *Metabolic Engineering*, 76, pp. 146–157. Available at: https://doi.org/10.1016/j.ymben.2023.02.003.

Jin, Z. *et al.* (2024) 'Colorimetric sensing for translational applications: from colorants to mechanisms', *Chemical Society Reviews*. Royal Society of Chemistry, pp. 7681–7741. Available at: https://doi.org/10.1039/d4cs00328d.

Juodeikiene, G. *et al.* (2015) 'Green metrics for sustainability of biobased lactic acid from starchy biomass vs chemical synthesis', *Catalysis Today*, 239, pp. 11–16. Available at: https://doi.org/10.1016/j.cattod.2014.05.039.

Karimi-Maleh, H. *et al.* (2021) 'A critical review on the use of potentiometric based biosensors for biomarkers detection', *Biosensors and Bioelectronics*. Elsevier Ltd. Available at: https://doi.org/10.1016/j.bios.2021.113252.

Kelso, P.A. *et al.* (2022) 'Toward Methanol-Based Biomanufacturing: Emerging Strategies for Engineering Synthetic Methylotrophy in Saccharomyces cerevisiae', *ACS Synthetic Biology*. American Chemical Society, pp. 2548–2563. Available at: https://doi.org/10.1021/acssynbio.2c00110.

Khoshbin, Z. *et al.* (2021) 'Recent advances in computational methods for biosensor design', *Biotechnology and Bioengineering*. John Wiley and Sons Inc, pp. 555–578. Available at: https://doi.org/10.1002/bit.27618.

Kim, H. *et al.* (2021) 'Genetically encoded biosensors based on fluorescent proteins', *Sensors (Switzerland)*. MDPI AG, pp. 1–18. Available at: https://doi.org/10.3390/s21030795.

Kim, H.J. *et al.* (2013) 'Genome-wide analysis of redox reactions reveals metabolic engineering targets for d-lactate overproduction in Escherichia coli', *Metabolic Engineering*, 18, pp. 44–52. Available at: https://doi.org/10.1016/j.ymben.2013.03.004.

Koberstein, J.N. *et al.* (2021) 'A Sort-Seq Approach to the Development of Single Fluorescent Protein Biosensors', *ACS Chemical Biology*, 16(9), pp. 1709–1720. Available at: https://doi.org/10.1021/acschembio.1c00423.

Kostyuk, A.I. *et al.* (2018) 'Redox biosensors in a context of multiparameter imaging', *Free Radical Biology and Medicine*, 128, pp. 23–39. Available at: https://doi.org/10.1016/j.freeradbiomed.2018.04.004.

LaCroix, R.A., Palsson, B.O. and Feist, A.M. (2017) 'A model for designing adaptive laboratory evolution experiments', *Applied and Environmental Microbiology*, 83(8). Available at: https://doi.org/10.1128/AEM.03115-16.

Lee, Y., Lafontaine Rivera, J.G. and Liao, J.C. (2014) 'Ensemble Modeling for Robustness Analysis in engineering non-native metabolic pathways', *Metabolic Engineering*, 25, pp. 63–71. Available at: https://doi.org/10.1016/j.ymben.2014.06.006.

Li, C. *et al.* (2022) 'Advances and prospects of transcription-factor-based biosensors in high-throughput screening for cell factories construction', *Food Bioengineering*. John Wiley and Sons Inc, pp. 135–147. Available at: https://doi.org/10.1002/fbe2.12019.

Li, J.-W. *et al.* (2020) 'Transcription Factor Engineering for High-Throughput Strain Evolution and Organic Acid Bioproduction: A Review', *Frontiers in Bioengineering and Biotechnology*, 8. Available at: https://doi.org/10.3389/fbioe.2020.00098.

Li, M., Chen, Z. and Huo, Y.-X. (2024) 'Application Evaluation and Performance-Directed Improvement of the Native and Engineered Biosensors', *ACS Sensors*, 9(10), pp. 5002–5024. Available at: https://doi.org/10.1021/acssensors.4c01072.

Li, S.-A. *et al.* (2024) 'Progress in pH-Sensitive sensors: essential tools for organelle pH detection, spotlighting mitochondrion and diverse applications', *Frontiers in Pharmacology*, 14. Available at: https://doi.org/10.3389/fphar.2023.1339518.

Li, Z., Zhang, J. and Ai, H. (2021) 'Genetically Encoded Green Fluorescent Biosensors for Monitoring UDP-GlcNAc in Live Cells', *ACS Central Science*, 7(10), pp. 1763–1770. Available at: https://doi.org/10.1021/acscentsci.1c00745.

Liang, G.T. *et al.* (2022) 'Enhanced small green fluorescent proteins as a multisensing platform for biosensor development', *Frontiers in Bioengineering and Biotechnology*, 10. Available at: https://doi.org/10.3389/fbioe.2022.1039317.

Lin, Y.-C. *et al.* (2018) 'The Pseudomonas aeruginosa Complement of Lactate Dehydrogenases Enables Use of D- and L-Lactate and Metabolic Cross-Feeding', *mBio*, 9(5). Available at: https://doi.org/10.1128/mBio.00961-18.

Liu, T. *et al.* (2022) 'Engineered Microbial Cell Factories for Sustainable Production of L-Lactic Acid: A Critical Review', *Fermentation*. MDPI. Available at: https://doi.org/10.3390/fermentation8060279.

Liu, Yang, Liu, Ye and Wang, M. (2017) 'Design, optimization and application of small molecule biosensor in metabolic engineering', *Frontiers in Microbiology*. Frontiers Media S.A. Available at: https://doi.org/10.3389/fmicb.2017.02012.

Di Lorenzo, R.D. *et al.* (2022) 'State of the Art on the Microbial Production of Industrially Relevant Organic Acids', *Catalysts*. MDPI. Available at: https://doi.org/10.3390/catal12020234.

Mahr, R. (2016) *Development and application of single cell biosensors for the improvement of amino acid production in Escherichia coli and Corynebacterium glutamicum*. Heinrich-Heine-Universität Düsseldorf.

Manandhar, A. and Shah, A. (2023) 'Techno-Economic Analysis of the Production of Lactic Acid from Lignocellulosic Biomass', *Fermentation*, 9(7). Available at: https://doi.org/10.3390/fermentation9070641.

Mandegari, M. *et al.* (2023) 'Decarbonizing British Columbia's (<scp>BC</scp> 's) marine sector by using low carbon intensive (<scp>CI</scp>) biofuels', *Biofuels, Bioproducts and Biorefining*, 17(4), pp. 1101–1114. Available at: https://doi.org/10.1002/bbb.2495.

Mao, Y. *et al.* (2023) 'Genetically Encoded Biosensor Engineering for Application in Directed Evolution', *Journal of Microbiology and Biotechnology*, 33(10), pp. 1257–1267. Available at: https://doi.org/10.4014/jmb.2304.04031.

Marx, V. (2017) 'Cell biology: Tracking a cell's cycle', *Nature Methods*, 14(3), pp. 233–236. Available at: https://doi.org/10.1038/nmeth.4186.

Matsuo, M. *et al.* (2024) *Challenges in Advancing Biomanufacturing Toward Bioeconomy and Framework for Key Considerations in Policy Discussions*. Available at: https://www.whitehouse.gov/briefing-room/statements-releases/2022/09/12/fact-sheet-president-biden-to-launch-a-national-biotechnology-and-.

Mazumdar, S. *et al.* (2013) 'Efficient synthesis of L-lactic acid from glycerol by metabolically engineered Escherichia coli', *Microbial Cell Factories*, 12(1). Available at: https://doi.org/10.1186/1475-2859-12-7.

Methanex (2025) *Pricing*, *https://www.methanex.com/about-methanol/pricing/*. Available at: https://www.methanex.com/about-methanol/pricing/ (Accessed: 11 May 2025).

Meyer, F. *et al.* (2018) 'Methanol-essential growth of Escherichia coli', *Nature Communications*, 9(1). Available at: https://doi.org/10.1038/s41467-018-03937-y.

Mishra, S. *et al.* (2022) 'Green synthesis of biomethanol—managing food waste for carbon footprint and bioeconomy', *Biomass Conversion and Biorefinery*. Springer Science and Business Media Deutschland GmbH, pp. 1889–1909. Available at: https://doi.org/10.1007/s13399-021-02188-0.

Miyawaki, A. *et al.* (1997) 'Fluorescent indicators for Ca2+based on green fluorescent proteins and calmodulin', *Nature*, 388(6645), pp. 882–887. Available at: https://doi.org/10.1038/42264.

Mordor Intelligence (2025) *Lactic acid Market*. Available at: https://www.mordorintelligence.com/industry-reports/lactic-acid-market (Accessed: 10 April 2025).

Mostufa, S. *et al.* (2024) 'Advancements and Perspectives in Optical Biosensors', *ACS Omega*. American Chemical Society, pp. 24181–24202. Available at: https://doi.org/10.1021/acsomega.4c01872.

Nasu, Y. *et al.* (2021) 'Structure- and mechanism-guided design of single fluorescent protein-based biosensors', *Nature Chemical Biology*. Nature Research, pp. 509–518. Available at: https://doi.org/10.1038/s41589-020-00718-x.

Nieh, L.-Y. *et al.* (2024) 'Evolutionary engineering of methylotrophic E. coli enables fast growth on methanol', *Nature Communications*, 15(1), p. 8840. Available at: https://doi.org/10.1038/s41467-024-53206-4.

Nielsen, J. and Keasling, J.D. (2016) 'Engineering Cellular Metabolism', *Cell*. Cell Press, pp. 1185–1197. Available at: https://doi.org/10.1016/j.cell.2016.02.004.

Niu, D. *et al.* (2014) 'Highly efficient L-lactate production using engineered Escherichia coli with dissimilar temperature optima for L-lactate formation and cell growth', *Microbial Cell Factories*, 13(1). Available at: https://doi.org/10.1186/1475-2859-13-78.

Núñez, M.F. *et al.* (2002) 'Transport of L-lactate, D-lactate, and glycolate by the LldP and GlcA membrane carriers of Escherichia coli', *Biochemical and Biophysical Research Communications*, 290(2), pp. 824–829. Available at: https://doi.org/10.1006/bbrc.2001.6255.

Ovechkina, V.S. *et al.* (2021) 'Genetically encoded fluorescent biosensors for biomedical applications', *Biomedicines*. MDPI. Available at: https://doi.org/10.3390/biomedicines9111528.

Pandey, K. *et al.* (2024) 'Bioprocessing 4.0 in biomanufacturing: paving the way for sustainable bioeconomy', *Systems Microbiology and Biomanufacturing*. Springer Nature, pp. 407–424. Available at: https://doi.org/10.1007/s43393-023-00206-y.

Papadimitriou, K. *et al.* (2016) 'Stress Physiology of Lactic Acid Bacteria', *Microbiology and Molecular Biology Reviews*, 80(3), pp. 837–890. Available at: https://doi.org/10.1128/mmbr.00076-15.

Papini, M., Salazar, M. and Nielsen, J. (2010) 'Systems Biology of Industrial Microorganisms', in *Biosystems Engineering I*. Berlin, Heidelberg: Springer Berlin Heidelberg, pp. 51–99. Available at: https://doi.org/10.1007/10_2009_59.

Park, W., Cha, S. and Hahn, J.S. (2024) 'Advancements in Biological Conversion of C1 Feedstocks: Sustainable Bioproduction and Environmental Solutions', *ACS Synthetic Biology*. American Chemical Society, pp. 3788–3798. Available at: https://doi.org/10.1021/acssynbio.4c00519.

Penchovsky, R. (2013) 'Computational design and biosensor applications of small molecule-sensing allosteric ribozymes', *Biomacromolecules*, 14(4), pp. 1240–1249. Available at: https://doi.org/10.1021/bm400299a.

Peng, B. *et al.* (2021) 'Optically Modulated and Optically Activated Delayed Fluorescent Proteins through Dark State Engineering', *Journal of Physical Chemistry B*, 125(20), pp. 5200–5209. Available at: https://doi.org/10.1021/acs.jpcb.1c00649.

Pessione, E. (2012) 'Lactic acid bacteria contribution to gut microbiota complexity: lights and shadows.', *Frontiers in cellular and infection microbiology*, p. 86. Available at: https://doi.org/10.3389/fcimb.2012.00086.

Pham, C. *et al.* (2022) 'Advances in engineering and optimization of transcription factor-based biosensors for plug-and-play small molecule detection', *Current Opinion in Biotechnology*. Elsevier Ltd. Available at: https://doi.org/10.1016/j.copbio.2022.102753.

Qin, L. *et al.* (2022) 'Mining and design of biosensors for engineering microbial cell factory', *Current Opinion in Biotechnology*. Elsevier Ltd. Available at: https://doi.org/10.1016/j.copbio.2022.102694.

Raman, S. *et al.* (2014) 'Evolution-guided optimization of biosynthetic pathways', *Proceedings of the National Academy of Sciences of the United States of America*, 111(50), pp. 17803–17808. Available at: https://doi.org/10.1073/pnas.1409523111.

Raouf, A.A. (2024) *Economic and Environmental Benefits of CO2 conversion to value-added products in Oman*. Master of Science in Chemical and Process Engineering. Sultan Qaboos University. Available at: https://www.proquest.com/docview/3195708688?pq-origsite=gscholar&fromopenview=true&sourcetype=Dissertations%20&%20Theses (Accessed: 11 April 2025).

Reiter, M.A. *et al.* (2024) 'A synthetic methylotrophic Escherichia coli as a chassis for bioproduction from methanol', *Nature Catalysis*, 7(5), pp. 560–573. Available at: https://doi.org/10.1038/s41929-024-01137-0.

Ren, Y. *et al.* (2025) 'Combing Directed Enzyme Evolution with Metabolic Engineering to Develop Efficient Microbial Cell Factories', *Chem and Bio Engineering* [Preprint]. American Chemical Society. Available at: https://doi.org/10.1021/cbe.5c00002.

Rogers, J.K. and Church, G.M. (2016) 'Genetically encoded sensors enable real-time observation of metabolite production', *Proceedings of the National Academy of Sciences of the United States of America*, 113(9), pp. 2388–2393. Available at: https://doi.org/10.1073/pnas.1600375113.

Rogers, J.K., Taylor, N.D. and Church, G.M. (2016) 'Biosensor-based engineering of biosynthetic pathways', *Current Opinion in Biotechnology*. Elsevier Ltd, pp. 84–91. Available at: https://doi.org/10.1016/j.copbio.2016.03.005.

Ruales-Salcedo, A. V. *et al.* (2022) 'Production of high-added value compounds from biomass', in *Biofuels and Biorefining*. Elsevier, pp. 381–445. Available at: https://doi.org/10.1016/B978-0-12-824116-5.00001-5.

Sandberg, T.E. *et al.* (2019) 'The emergence of adaptive laboratory evolution as an efficient tool for biological discovery and industrial biotechnology', *Metabolic Engineering*, 56, pp. 1–16. Available at: https://doi.org/10.1016/j.ymben.2019.08.004.

Santos, C.N.S. and Stephanopoulos, G. (2008) 'Melanin-based high-throughput screen for L-tyrosine production in Escherichia coli', *Applied and Environmental Microbiology*, 74(4), pp. 1190–1197. Available at: https://doi.org/10.1128/AEM.02448-07.

Seok, J.Y. *et al.* (2021) 'Synthetic biosensor accelerates evolution by rewiring carbon metabolism toward a specific metabolite', *Cell Reports*, 36(8). Available at: https://doi.org/10.1016/j.celrep.2021.109589.

Shaner, N.C. *et al.* (2013) 'A bright monomeric green fluorescent protein derived from Branchiostoma lanceolatum', *Nature Methods*, 10(5), pp. 407–409. Available at: https://doi.org/10.1038/nmeth.2413.

Sharan, S.K. *et al.* (2009) 'Recombineering: a homologous recombination-based method of genetic engineering', *Nature Protocols*, 4(2), pp. 206–223. Available at: https://doi.org/10.1038/nprot.2008.227.

Shepelin, D. *et al.* (2018) 'Selecting the best: Evolutionary engineering of chemical production in microbes', *Genes*. MDPI AG. Available at: https://doi.org/10.3390/genes9050249.

Shi, S. *et al.* (2022) 'Metabolite-based biosensors for natural product discovery and overproduction', *Current Opinion in Biotechnology*. Elsevier Ltd. Available at: https://doi.org/10.1016/j.copbio.2022.102699.

Shukal, S. *et al.* (2022) 'Metabolic engineering of Escherichia coli BL21 strain using simplified CRISPR-Cas9 and asymmetric homology arms recombineering', *Microbial Cell Factories*, 21(1), p. 19. Available at: https://doi.org/10.1186/s12934-022-01746-z.

Singh, A. *et al.* (2021) 'Recent advances in electrochemical biosensors: Applications, challenges, and future scope', *Biosensors*. MDPI. Available at: https://doi.org/10.3390/bios11090336.

Singh, H.B. *et al.* (2022) 'Developing methylotrophic microbial platforms for a methanol-based bioindustry', *Frontiers in Bioengineering and Biotechnology*. Frontiers Media S.A. Available at: https://doi.org/10.3389/fbioe.2022.1050740.

Skládal, P. (2024) 'Piezoelectric biosensors: shedding light on principles and applications', *Microchimica Acta*. Springer. Available at: https://doi.org/10.1007/s00604-024-06257-9.

Sollai, S. *et al.* (2023) 'Renewable methanol production from green hydrogen and captured CO2: A techno-economic assessment', *Journal of CO2 Utilization*, 68, p. 102345. Available at: https://doi.org/10.1016/j.jcou.2022.102345.

Srirangan, K. *et al.* (2012) 'Towards sustainable production of clean energy carriers from biomass resources', *Applied Energy*, 100, pp. 172–186. Available at: https://doi.org/10.1016/j.apenergy.2012.05.012.

Stingele, J., Bellelli, R. and Boulton, S.J. (2017) 'Mechanisms of DNA-protein crosslink repair', *Nature Reviews Molecular Cell Biology*. Nature Publishing Group, pp. 563–573. Available at: https://doi.org/10.1038/nrm.2017.56.

Suma, B.P. and Adarakatti, P.S. (2024) 'Brief Overview of Different Biosensors: Properties, Applications, and Their Role in Chemistry', in *Biosensing Technology for Human Health*. Royal Society of Chemistry, pp. 1–32. Available at: https://doi.org/10.1039/9781837676323-00001.

Sun, Y. and Tang, Y. (2023) 'Municipal solid waste gasification integrated with water electrolysis technology for fuel production: A comparative analysis', *Chemical Engineering Research and Design*, 191, pp. 14–26. Available at: https://doi.org/10.1016/j.cherd.2023.01.023.

Swings, T. *et al.* (2018) 'CRISPR-FRT targets shared sites in a knock-out collection for off-the-shelf genome editing', *Nature Communications*, 9(1), p. 2231. Available at: https://doi.org/10.1038/s41467-018-04651-5.

Tabibian, S.S. and Sharifzadeh, M. (2023) 'Statistical and analytical investigation of methanol applications, production technologies, value-chain and economy with a special focus on renewable methanol', *Renewable and Sustainable Energy Reviews*, 179. Available at: https://doi.org/10.1016/j.rser.2023.113281.

Taguchi, H. and Ohta, T. (1991) 'D-lactate dehydrogenase is a member of the D-isomer-specific 2-hydroxyacid dehydrogenase family. Cloning, sequencing, and expression in Escherichia coli of the D-lactate dehydrogenase gene of Lactobacillus plantarum', *Journal of Biological Chemistry*, 266(19), pp. 12588–12594. Available at: https://doi.org/10.1016/S0021-9258(18)98939-8.

Tamura, T. and Hamachi, I. (2014) 'Recent progress in design of protein-based fluorescent biosensors and their cellular applications', *ACS Chemical Biology*. American Chemical Society, pp. 2708–2717. Available at: https://doi.org/10.1021/cb500661v.

Tellechea-Luzardo, J., Stiebritz, M.T. and Carbonell, P. (2023) 'Transcription factor-based biosensors for screening and dynamic regulation', *Frontiers in Bioengineering and Biotechnology*. Frontiers Media S.A. Available at: https://doi.org/10.3389/fbioe.2023.1118702.

Teng, Y. *et al.* (2022) 'Biosensor-enabled pathway optimization in metabolic engineering', *Current Opinion in Biotechnology*. Elsevier Ltd. Available at: https://doi.org/10.1016/j.copbio.2022.102696.

Teusink, B., Bachmann, H. and Molenaar, D. (2011) 'Systems biology of lactic acid bacteria: A critical review', *Microbial Cell Factories*, 10(SUPPL. 1). Available at: https://doi.org/10.1186/1475-2859-10-S1-S11.

Thorn, K. (2017) 'Genetically encoded fluorescent tags', *Molecular Biology of the Cell*, 28(7), pp. 848–857. Available at: https://doi.org/10.1091/mbc.e16-07-0504.

Tian, L. *et al.* (2009) 'Imaging neural activity in worms, flies and mice with improved GCaMP calcium indicators', *Nature Methods*, 6(12), pp. 875–881. Available at: https://doi.org/10.1038/nmeth.1398.

Tsuge, Y. *et al.* (2019) 'Metabolic engineering of Corynebacterium glutamicum for hyperproduction of polymer-grade l- and d-lactic acid', *Applied Microbiology and Biotechnology*, 103(8), pp. 3381–3391. Available at: https://doi.org/10.1007/s00253-019-09737-8.

Turner, A. (2013) 'Biosensors: then and now', *Trends in Biotechnology*, 31(3), pp. 119–120. Available at: https://doi.org/10.1016/j.tibtech.2012.10.002.

Tuyishime, P. and Sinumvayo, J.P. (2020) 'Novel outlook in engineering synthetic methylotrophs and formatotrophs: a course for advancing C1-based chemicals production', *World Journal of Microbiology and Biotechnology*. Springer. Available at: https://doi.org/10.1007/s11274-020-02899-y.

Unden, G., Steinmetz, P.A. and Degreif-Dünnwald, P. (2014) 'The Aerobic and Anaerobic Respiratory Chain of *Escherichia coli* and *Salmonella enterica* : Enzymes and Energetics', *EcoSal Plus*, 6(1). Available at: https://doi.org/10.1128/ecosalplus.esp-0005-2013.

Unser, S. *et al.* (2015) 'Localized surface plasmon resonance biosensing: Current challenges and approaches', *Sensors (Switzerland)*. MDPI AG, pp. 15684–15716. Available at: https://doi.org/10.3390/s150715684.

Vanapalli, K.R. *et al.* (2023) 'Life cycle assessment of fermentative production of lactic acid from bread waste based on process modelling using pinch technology', *Science of the Total Environment*, 905. Available at: https://doi.org/10.1016/j.scitotenv.2023.167051.

Vigneshvar, S. *et al.* (2016) 'Recent advances in biosensor technology for potential applications - an overview', *Frontiers in Bioengineering and Biotechnology*. Frontiers Media S.A. Available at: https://doi.org/10.3389/fbioe.2016.00011.

Wang, S. *et al.* (2023) 'Genetically encoded ATP and NAD(P)H biosensors: potential tools in metabolic engineering', *Critical Reviews in Biotechnology*. Taylor and Francis Ltd., pp. 1211–1225. Available at: https://doi.org/10.1080/07388551.2022.2103394.

Wang, Y. *et al.* (2020) 'Synthetic Methylotrophy: A Practical Solution for Methanol-Based Biomanufacturing', *Trends in Biotechnology*. Elsevier Ltd, pp. 650–666. Available at: https://doi.org/10.1016/j.tibtech.2019.12.013.

Wang, Y. *et al.* (2021) 'Directed Evolution: Methodologies and Applications', *Chemical Reviews*, 121(20), pp. 12384–12444. Available at: https://doi.org/10.1021/acs.chemrev.1c00260.

Wang, Y., Zhang, B. and Bao, J. (2025) 'Rigorous Calculation of Greenhouse Gases (GHG) in Sustainable l-lactic Acid Production from Lignocellulosic Biomass based on Advanced Biorefinery Processing Technology', *ACS Sustainable Chemistry and Engineering* [Preprint]. Available at: https://doi.org/10.1021/acssuschemeng.4c10527.

Wegat, V., Fabarius, J.T. and Sieber, V. (2022) 'Synthetic methylotrophic yeasts for the sustainable fuel and chemical production', *Biotechnology for Biofuels and Bioproducts*. BioMed Central Ltd. Available at: https://doi.org/10.1186/s13068-022-02210-1.

Whitaker, W.B. *et al.* (2015) 'Synthetic methylotrophy: Engineering the production of biofuels and chemicals based on the biology of aerobic methanol utilization', *Current Opinion in Biotechnology*. Elsevier Ltd, pp. 165–175. Available at: https://doi.org/10.1016/j.copbio.2015.01.007.

Wieschalka, S. *et al.* (2013) 'Bio-based production of organic acids with Corynebacterium glutamicum', *Microbial Biotechnology*, pp. 87–102. Available at: https://doi.org/10.1111/1751-7915.12013.

Williams, T.C., Pretorius, I.S. and Paulsen, I.T. (2016) 'Synthetic Evolution of Metabolic Productivity Using Biosensors', *Trends in Biotechnology*. Elsevier Ltd, pp. 371–381. Available at: https://doi.org/10.1016/j.tibtech.2016.02.002.

Wu, Y. *et al.* (2022) 'Advanced strategies and tools to facilitate and streamline microbial adaptive laboratory evolution', *Trends in Biotechnology*. Elsevier Ltd, pp. 38–59. Available at: https://doi.org/10.1016/j.tibtech.2021.04.002.

Yan, X. *et al.* (2024) 'Microbial Cell Factories in the Bioeconomy Era: From Discovery to Creation', *BioDesign Research*. American Association for the Advancement of Science. Available at: https://doi.org/10.34133/bdr.0052.

Yuan, L. *et al.* (2005) 'Laboratory-Directed Protein Evolution', *Microbiology and Molecular Biology Reviews*, 69(3), pp. 373–392. Available at: https://doi.org/10.1128/MMBR.69.3.373-392.2005.

Zhang, J. *et al.* (2023) 'Genetically Encoded Boronolectin as a Specific Red Fluorescent UDP-GlcNAc Biosensor', *ACS Sensors*, 8(8), pp. 2996–3003. Available at: https://doi.org/10.1021/acssensors.3c00409.

Zhang, Xiaomei *et al.* (2022) 'Rational Metabolic Engineering Combined with Biosensor-Mediated Adaptive Laboratory Evolution for L-Cysteine Overproduction from Glycerol in Escherichia coli', *Fermentation*, 8(7). Available at: https://doi.org/10.3390/fermentation8070299.

Zhao, C. *et al.* (2019) 'Discovery of potential genes contributing to the biosynthesis of short-chain fatty acids and lactate in gut microbiota from systematic investigation in E. coli', *npj Biofilms and Microbiomes*, 5(1). Available at: https://doi.org/10.1038/s41522-019-0092-7.

Zhao, Y. *et al.* (2016) 'Targeted optimization of central carbon metabolism for engineering succinate production in Escherichia coli', *BMC Biotechnology*, 16(1). Available at: https://doi.org/10.1186/s12896-016-0284-7.

Zheng, G. *et al.* (2025) 'iCASRED, a scarless DNA editing tool in E. coli for high-efficiency engineering of natural product biosynthetic gene clusters', *Synthetic and Systems Biotechnology*, 10(3), pp. 751–763. Available at: https://doi.org/10.1016/j.synbio.2025.03.008.

Zhou, L. *et al.* (2016) 'Metabolic engineering strategies for D-lactate over production in Escherichia coli', *Journal of Chemical Technology and Biotechnology*. John Wiley and Sons Ltd, pp. 576–584. Available at: https://doi.org/10.1002/jctb.4856.

Zhou, S. *et al.* (2003) 'Production of optically pure D-lactic acid in mineral salts medium by metabolically engineered Escherichia coli W3110', *Applied and Environmental Microbiology*, 69(1), pp. 399–407. Available at: https://doi.org/10.1128/AEM.69.1.399-407.2003.

Zhou, S. *et al.* (2005) 'Fermentation of 10% (w/v) sugar to D(-)-lactate by engineered Escherichia coli B', *Biotechnology Letters*, 27(23–24), pp. 1891–1896. Available at: https://doi.org/10.1007/s10529-005-3899-7.

Zhou, S. *et al.* (2006a) 'Fermentation of 12% (w/v) glucose to 1.2 M lactate by Escherichia coli strain SZ194 using mineral salts medium', *Biotechnology Letters*, 28(9), pp. 663–670. Available at: https://doi.org/10.1007/s10529-006-0032-5.

Zhou, S. *et al.* (2006b) 'Fermentation of 12% (w/v) glucose to 1.2 M lactate by Escherichia coli strain SZ194 using mineral salts medium', *Biotechnology Letters*, 28(9), pp. 663–670. Available at: https://doi.org/10.1007/s10529-006-0032-5.

Zhu, T. *et al.* (2020) 'Engineering unnatural methylotrophic cell factories for methanol-based biomanufacturing: Challenges and opportunities', *Biotechnology Advances*. Elsevier Inc. Available at: https://doi.org/10.1016/j.biotechadv.2019.107467.

9. APPENDICES

9.1. ANNEX : ABBREVIATIONS GLOSSARY

Table 1: List of abbreviations and their meaning

Abbreviations for genes, enzymes and pathways in Figure 2 are described in the caption thereof.

Abbreviation	Definition
ALE	Adaptative laboratory Evolution
Amp	Ampicillin
BAC	Bacterial Artificial Chromosome
BLAST	Basic Local Alignment Search Tool
B. coag	Bacillus coagulans
Carb	Carbenicillin
CDS	Coding sequence
CM	Chloramphenicol
CNV	Copy Number Variation
cp	Circularly permuted
CRISPR	Clustered regularly interspaced short palindromic repeats
DPC	DNA-protein crosslinking
EMRA	Ensemble Modelling Robustness Analysis
FACS	Fluorescent Assorted Cell Sorting
FP (GFP, RFP,YFP)	Fluorescent protein (green, red, yellow)
FRET	Fluorescence resonance energy transfer
L. casei	Lactobacillus casei
LB	Luria Broth
LCA	Life-cycle Assessment
Met. min. med	Methanol minimal medium
OD	Optical density
PBS	Phosphate buffered saline
RBS	Ribosome binding site
S. bovis	Streptococcus bovis
SM	Synthetic methylotroph
Spec	Spectinomycin
TB	Terrific Broth
TEA	Techno-economic assessment
WT	Wild-type

9.2. ANNEX : DNA CONSTRUCTS DETAILS

Table 1: *Escherichia coli* strains used in this study

Name	Description	Reference
BW25113	Wild-type used for establishing synthetic SM strains and parental strain for Keio collection	(Baba *et al.*, 2006)
Δpta BW25113	From the Keio collection	(Baba *et al.*, 2006)
ΔrpiA BW25113	From the Keio collection	(Baba *et al.*, 2006)
SM1	Strain evolved to grow on methanol as sole C-source	(Chen *et al.*, 2020)
SM7	Evolved from SM1 for fast growth on MOPS met.min.med	(Nieh *et al.*, 2024)
SM8	Repaired mutS in SM7 and evolved for 15 passages	(Nieh *et al.*, 2024)
DH5α	Wild-type used for plasmid construction	(Hanahan, Jessee and Bloom, 1995)

Table 2: Plasmids used in this study

Name	Description	Source
pAGT1	pTarget::gRNA to restore disrupted *recA* in SM strains; SpecR	This study
pAGT2	pTarget::gRNA to integrate *recA* at neutral SS9 locus; SpecR	This study
pAGT3	pTarget::gRNA to insert *rpiA* at *maeA* locus; SpecR	This study
pAGT4	pTarget::gRNA to knock out *lldD* (L-lactate oxidizer); SpecR	This study
pNasu9	pcDNA::iLACCO1.9 (GFP biosensor, high affinity, Kd = 14 µM); AmpR	This study, adapted from (Hario *et al.*, 2024)
pNasu9b	pcDNA::iLACCO1.9b (GFP biosensor, low affinity, Kd = 2.0 mM); AmpR	This study, adapted from (Hario *et al.*, 2024)
pNasudi	pcDNA::diLACCO1.9 (GFP control biosensor, non-responsive); AmpR	This study, adapted from (Hario *et al.*, 2024)
pLY708	pUC::L-*ldh* from *B. coagulans* under constitutive promoter; AmpR	Synthesized gene
pLY709	pUC:: L-*ldh* from *S. bovis*; AmpR	Synthesized gene
pLY710	pUC::L-*ldh* from *L. casei*; AmpR	Synthesized gene
pAGT5	pTarget::gRNA to replace *ldhA* with L-*ldh* (*B. coagulans*); SpecR	This study
pAGT6	pTarget::gRNA to replace *ldhA* with L-*ldh* (*S. bovis*); SpecR	This study
pAGT7	pTarget::gRNA to replace *ldhA* with L-*ldh* (*L. casei*); SpecR	This study
pAGT8	pTarget::Replace *lldD* with high-affinity biosensor (*iLACCO1.9*); SpecR	This study
pAGT9	pTarget::Replace *lldD* with low-affinity biosensor (*iLACCO1.9b*); SpecR	This study
pAGT10	pTarget::Replace *lldD* with control biosensor (*diLACCO1.9*); SpecR	This study
pAGT11	pSC101::iLACCO + mCherry reporter cassette; low-copy; CmR	This study

9.3. ANNEX : MEDIA COMPOSITION

MOPS-based methanol minimal medium was composed of:	M9-based methanol minimal medium was composed of:
- 400 mM methanol, - 50mg/mL chloramphenicol, - 1 mM IPTG, - MOPS EZ buffer (Teknova; 40mM MOPS, 3.02 nM CoCl2, 0.962 nM CuSO4, 50mM NaCl, 9.5mM NH4Cl, 0.525mM MgCl2, 4mM tricine, 1.32mM K2HPO4,0.276mM K2SO4,0.01 mM FeSO4, 0.5mM CaCl2,40 nMH3BO3, 8.08 nM MnCl2, 0.974 nM ZnSO4, and 0.292 nM (NH4)2MoO4.). - Trace vitamin mix, prepared and added so as to reach the following concentrations in the medium: 8.19 µM biotin, 10.49 µM calcium pantothenate, 4.53 µM folic acid, 40.94 µM nicotinamide, 13.29 µMriboflavin, 14.82 µM thiamine hydrochloride, and 0.07 µM vitamin B12.	- M9 salts (3 g/L KH2PO4, 0.5 g/L NaCl, 6.8 g/L Na2HPO4 and 1.0 g/L NH4Cl), - 400mM methanol, - 1 mM MgSO4, - 0.1 mM CaCl2, - 50mg/mL chloramphenicol, - 1 mM IPTG, - trace elements, with final concentrations as follows: 13.4mM Na2EDTA, 13.1 mM FeCl3-6H2O, 0.62mM ZnCl2,76 µM CuCl2-2H2O, 62 µMCoCl2-2H2O, 162 µMH3BO3 and 8.1 µMMnCl2-4H2O. - trace vitamin mix as for MOPS medium.

MOPS-based glucose minimal medium contained the same components as MOPS-based methanol minimal medium, except that methanol and CM were omitted, and 1% glucose was added.

9.4. ANNEX : DETAILED COMMENTS OF FIGURE 5, BIOSENSOR TYPES AND CHARACTERISTICS

To ensure reliability and utility of biosensors, research is undertaken to improve their detection limit, sensitivity, specificity, non-toxicity, small molecule detection and cost-effectiveness (Vigneshvar *et al.*, 2016). In publications, biochemists report on critical performance parameters, which allow to compare biosensors and choose the most appropriate ones for a given application. Listed and explained with a heavier focus on optical sensors, since such are used in this study, these metrics are:

- Dynamic range, i.e. the ratio fluorescence signal in the saturated (analyte-bound) vs. basal (analyte-free) state. A larger dynamic range improves signal-to-noise ratio.
- Affinity, as Kd or EC50, i.e. the metabolite concentration at which the sensor is 50% saturated. A higher affinity, in other words lower detection limit, is desirable for low-abundance analytes, and vice versa. Significant efforts in developing and using biosensors is spent in matching physiological analyte concentrations to avoid saturation or insensitivity (Hellweg *et al.*, 2023).
- Response time, usually given as the time to reach 90% signal change after analyte (un)binding. Fast kinetics (ms range) are crucial to monitor rapid processes (e.g., neuronal firing).
- Strength, for visual indicators often brightness, described relative to relative to EGFP (e.g., mNeonGreen is 2× brighter than EGFP (Shaner *et al.*, 2013). If brighter, lower-light is needed for imaging, or the signal can be perceived from deeper in the tissues.
- Stability, e.g. photostability, the resistance to photobleaching under sustained illumination (measured as half-life of fluorescence), is critical for long-term monitoring, or for subsequent analysis by FACS for instance (Marx, 2017).
- Specificity, as well as environmental sensitivity. Cross-Reactivity is tested via competition assays with structural analogs (e.g., Ca^{2+} vs. Mg^{2+}). Robustness to pH/temperature/ionic strength changes is also crucial (unless this is what is measured) to ensure that the signal reflects analyte variation, not artifacts (Ding, Zhou and Deng, 2021).

The biosensor landscape is rapidly transforming, driven by innovations in materials science, computational design, and multimodal transduction strategies. Advanced materials such as nanostructures, 3D-printed scaffolds, and smart polymers are increasingly employed to enhance biosensors, notably their portability for diagnostic and environmental monitoring applications (Bollella and Katz, 2020). Hybrid biosensors are emerging, combining multiple transduction modalities, for instance as optoelectrochemical or electro-optical systems (Qin *et al.*, 2022; Shi *et al.*, 2022). Significant progress is also occurring in photonic biosensors. Red and near-infrared fluorescent proteins like miRFP enable deeper tissue imaging with reduced autofluorescence (Shcherbakova *et al.*, 2020). Additionally, dark fluorescent proteins (FPs)—which become fluorescent only upon analyte binding—such as engineered dark YFP mutants for Zn^{2+} detection, improve signal-to-noise ratios in complex environments (Peng *et al.*, 2021). Lanthanide-based time-resolved FRET (TR-FRET) systems further advance this field by minimizing background fluorescence using long-lifetime donors like Tb^{3+} paired with GFP acceptors (Pham *et al.*, 2022). Addressing the same noise issue, nanoquencher-based sensors utilize gold nanoparticles conjugated with fluorescent dyes which activate when the analyte displaces the former (Dong *et al.*, 2021). Last but not least, biosensor development is increasingly guided by computational tools. Platforms such as AlphaFold for protein structure prediction and RNA secondary structure models are being used to design riboswitches, aptamers, and protein-based sensors with improved dynamic ranges and binding specificity (Penchovsky, 2013; Khoshbin *et al.*, 2021).

Table 1: Main classes, engineering principles, advantages and disadvantages of biosensors.

Type	Sub-types	Mechanism	Advantages	Disadvantages	References
Optical	Colorimetric Fluorescent Surface Plasmon Resonance (SPR)	Measures light-matter interactions (absorbance, fluorescence, refractive index shifts, etc.).	- Real-time, continuous, in vivo, label-free for SPR - High spatial resolution (sub-cellular) - Multiplexing capability - Compactable/ miniaturizable - insensitive to in electrical noise e.g. ionic environments - minimal instrumentation (except SPR) and simple protocols (colorimetric)	- Photobleaching (fluorescence) - Scattering in turbid samples - Some colorimetric sensors are only semi-quantitative - Expensive instrumentation (SPR)	(Unser et al., 2015; Chen and Wang, 2020; Ovechkina et al., 2021; Jin et al., 2024; Mostufa et al., 2024)
Electrochemical	Amperometric Potentiometric Impendimetric	Measures electrical signals (current, potential, impedance, or concentration changes) from redox reactions, resistance changes from binding events)	- High sensitivity (and specificity, especially when combined biological recognition elements like enzymes or antibodies) - Portable & low-cost (adapted to consumer market, cheaper than optical methods) - Quantitative (e.g., glucose monitoring) - Rapid response - Low power consumption (battery-powered, wirelss	- Cross-sensitivity and interference from electroactive compounds - Limited temperature range - Shelf Life and Stability (exposure may shorten lifespan) - dynamic range limitations - Limited multiplexing - Electrode fouling issues	(Karimi-Maleh *et al.*, 2021; Singh *et al.*, 2021)
Piezoelectric and others	**Piezoelectric** (e.g., quartz crystal micro-balance, QCM) **Thermal** (e.g. calorimetric)	Measures mass changes (e.g., QCM) or enthalpy changes.	- Label-free, no need for additional markers or labels - Gas-phase detection - Robust for industrial use - Relatively simple setups	- Low specificity and low sensitivity in liquids - Difficult calibration - Limited dynamic range - Low technological maturity	(Skládal, 2024; Suma and Adarakatti, 2024)

9.5. ANNEX: GROWTH RATE CHANGES DURING SM7 AND SM8 ALE EXPERIMENT

Table 1: Growth rate variations and comparison
over 7 ALE passages for SM7 and 5 ALE passages for SM8

Strain	SM7				SM8			
Medium	SM9			MOPS	SM9			MOPS
RTS	1	2	3	4	5	6	7	8
P1 GR (OD	0.356	0.400	0.373	0.143	0.175	0.154	0.156	0.133
P2 GR (OD	0.101	0.107	0.106	0.097	0.087	0.072	0.068	0.116
Up P(n-1)	-72%	-73%	-72%	-32%	-50%	-53%	-56%	-13%
Up P1	-72%	-73%	-72%	-32%	-50%	-53%	-56%	-13%
P3 GR (OD	0.112	0.117	0.111	0.037	0.100	0.061	0.066	0.075
Up P(n-1)	10%	10%	4%	-62%	15%	-15%	-3%	-36%
Up P1	-69%	-71%	-70%	-74%	-43%	-60%	-57%	-44%
P4 GR (OD	0.094	0.096	0.085	0.112	0.038	0.039	0.036	0.108
Up P(n-1)	-16%	-19%	-23%	207%	-62%	-36%	-46%	44%
Up P1	-74%	-76%	-77%	-21%	-78%	-75%	-77%	-19%
P5 GR (OD	0.107	0.108	0.063	0.097	0.005	0.004	0.004	0.107
Up P(n-1)	15%	13%	-26%	-14%	-87%	-91%	-88%	-1%
Up P1	-70%	-73%	-83%	-32%	-97%	-98%	-97%	-20%
P6 GR (OD	0.026	0.077	0.057	0.063				
Up P(n-1)	-76%	-29%	-9%	-35%				
Up P1	-93%	-81%	-85%	-56%				
P7 GR (OD	0.002	0.005	0.004	0.118				
Up P(n-1)	-92%	-94%	-93%	88%				
Up P1	-99%	-99%	-99%	-17%				